METHYLMERCURY PHOTODEMETHYLATION IN KEJIMKUJIK LAKES

by

© Sara Jane Klapstein

A Thesis submitted to the

School of Graduate Studies

In partial fulfillment of the requirements for the degree of

Doctor of Philosophy

Department of Environmental Science

Memorial University of Newfoundland

April 2017

St. John's, Newfoundland and Labrador

Abstract

Methylmercury (MeHg) concentration in surface waters is a key variable regulating mercury availability to food webs. Few studies have quantified the seasonal importance of photodemethylation reactions and the influence of chromophoric dissolved organic matter (DOM) properties on these relationships. To address this research gap we have used numerous controlled experiments that focused primarily on the quantification of the relationships between solar radiation exposures, DOM, and MeHg within six freshwater lakes in Kejimkujik National Park and National Historic Site in Nova Scotia. The concentration of DOM was found to strongly control the photoreactivity of DOM in these study lakes across sampling seasons (R^2=0.94). The effect of DOM photoreactivity on MeHg photodemethylation was directly tested using photochemically manipulated water from one lake collected in three different months. Photodemethylation rate constants and efficiencies tended to be higher in water collected during June, when *in-situ* DOM concentration was lower, than in water collected in August and October. Experiments that included water from all six lakes in summer and fall showed that DOM concentration could explain 76% of variation in photodemethylation rate constants. The outcomes from this combination of studies and experiments provide insight for prediction of photodemethylation potential in our study system and for comparison with MeHg concentrations in corresponding food webs. Methylmercury is associated with DOM (DOM-MeHg) in complexes, however in high DOM waters the proportion of DOM that is associated with MeHg (DOM-MeHg) will decrease and this MeHg-free DOM may be critical in regulating photodemethylation reactions. Photodemethylation will still occur in

high DOM waters but at a limited rate because a smaller proportion of the photoreactions will involve DOM-MeHg complexes. This is the first study to test and quantify a competitive interaction between MeHg photodemethylation and DOM phototransformations (both photomineralization and photobleaching) to support the conceptual idea that higher dissolved organic carbon systems will have slower rates of photodemethylation. Overall, this compiled body of work yielded a method for predicting seasonal and spatial changes to MeHg concentrations in surface waters depending on environmental and physicochemical factors.

Acknowledgments

A big thank you to the many funding agencies that made this research and all of the wonderful experiences I have had over the past 4 years possible. NSERC CREATE, PGS, and Discovery programs, the Canada Research Chairs Program, the Canada Foundation for Innovation, and Memorial University of Newfoundland. Additional funding thanks to both St. Francis Xavier University (Flux Lab!) and Acadia University (Environmental Biogeochemistry Lab & CARE Labs).

I would like to thank my supervisors; you are the tripod on which I am supported. Dr. Susan Ziegler (Memorial University of Newfoundland), you never cease to amaze me with your power to sift through my scramble and force me to see the big picture implications of our research. I am grateful we had the opportunity to work together. Dr. Nelson O'Driscoll (Acadia University), this project would have never been possible without you taking a chance on a climate junkie looking to immerse herself in Atlantic Canada research. You taught me to push myself, never give up, and see things through in a (usually) calm manner. You have provided me with a great diversity of opportunities and experiences for growth as a scientist and manager of research. Dr. Dave Risk (St. Francis Xavier University), the third advisor because in science 3 is better than 2 (3 is the magic number I like to tell budding scientists). You have continually kept me grounded throughout my entire academic endeavour and have been consistently confident in my abilities. I would also like to thank Dr. Erin Mann for being a smooth lab ninja, for teaching me some of her analytical chemist ways, and reiterating the "be prepared" motto (re: sandwiches and snacks, always!). On a more inclusive note, I thank all of the people I

have discussed research with (conferences, meetings, and informal avenues); these discussions have been integral to my development of this thesis and its interpretations.

A special thanks to all of the people who have made every field collection and study possible. Without you I would probably still be trying to paddle up Big Dam West in gale force winds, would have eaten far too many field chips on my own, and would be missing a lot of really cool data. Field assistants include: Erin Mann (MUN/Acadia), Hillary MacDonell (StFX), Leslie Klapstein, Paul Bunyan, Laura Graham (StFX), Jocelyn Egan (Dalhousie), Amanda Loder (Acadia), and Thora Christensen (Acadia). Logistical support from Parks Canada (particularly Chris McCarthy, Blaine Mailman, Dan Pouliot, and Matthew Smith), the Mersey Tobeatic Research Institute, and Environment and Climate Change Canada (particularly Rob Tordon and Rob Keenan). Special thanks to the wonderful K.C. Irving Centre Staff who have assisted with some pretty weird tasks over the years without too much questioning.

Finally, I would like to thank those family and friends who have shown me great patience and commitment on this adventure. Infinite thank yous to: my partner (for all of the things such as willingly coming to collect “water” samples with me in -22°C, letting me take over every surface with science and sticky note lists, and feeding me), my parents, (for picking up the phone, my love of the great outdoors, and reminding me just how amazing chemistry really is), and finally my friends (for providing me with unwavering inspiration, sounding boards, the ladies outdoors club, cheese, and matcha lattés).

TABLE OF CONTENTS

List of Tables

List of Figures

List of Symbols and Acronyms

A_{350} = absorbance at 350 nm

A_{350f} = final absorbance at 350 nm

A_{350i} = initial absorbance at 350 nm

ANCOVA = analysis of covariance

BAF = bioaccumulation factor

BAFA = branched chain fatty acids

BDE = Big Dam East

BDW = Big Dam West

BMF = biomagnification factor

BrCl = bromine monochloride

C = carbon

CARE = Centre for Analytical Research on the Environment

CRC = Canada Research Chair

CREATE = Collaborative Research and Training Experience

CVAFS = cold vapour atomic fluorescence spectrometer/spectrometry

D-MCM = Dynamic Mercury Cycling Model

DIC = dissolved inorganic carbon

DOC = dissolved organic carbon

DOM = dissolved organic matter

$^3DOM^*$ = excited triplet state dissolved organic matter

DOM_f = final dissolved organic matter concentration

DOM_i = initial dissolved organic matter concentration

DOM_p = photoreactive dissolved organic matter

DOM-MeHg/CH_3Hg-DOM = methylmercury associated with DOM complexes

DOM-Fe = iron bound to dissolved organic matter

E = Einstein; a mole of photons

EPA = Environmental Protection Agency

Fe = iron

Fe(II) = Ferrous iron; Fe^{2+} ion

Fe(III) = Ferric iron; Fe^{3+} ion

H^+ = hydrogen ions

HDPE = high density polyethylene

Hg-cysteine = mercury bound with cysteine

HCl = hydrochloric acid

Hg^0 = gaseous/dissolved elemental mercury

Hg(II) = divalent mercury, also referred to as inorganic mercury; the Hg^{2+} ion

$HgCl_2$ = mercuric chloride

HgS = mercury sulfide

HMW = high molecular weight

HNO_3 = nitric acid

K_d = attenuation coefficient

KOH = potassium hydroxide

k_{PB} = photobleaching rate constant

k_{PD} = photodemethylation rate constant

k_{PM} = photomineralization rate constant

LMW = low molecular weight

MeHg = methylmercury; monomethylmercury

MeHg(I) = bound methylmercury; monomethylmercury

MeHg(II)OH = monomethylmercury hydroxide

%MeHg = percent methylmercury

NCR; NC = North Cranberry

NIST = National Institute for Standards and Technology

NS = Nova Scotia

NSERC = National Science and Engineering Council of Canada

$^1O_2$ = singlet state oxygen

•OH = hydroxyl radical

OM = organic matter

PAR = photosynthetically active radiation

PDE = photodemethylation efficiency

PEB = Pebbleloggitch

PES = Peskawa

POM = particular organic matter

ppm = parts per million

PPRI = photochemically produced reactive intermediates

PTFE = polytetrafluoroethylene

PUFA = polyunsaturated fatty acids

PUZ = Puzzle

r = Pearson product-moment correlation coefficient

RS^- = thiols; sulfur groups

S = sulfur

$S_{275-295}$ = spectral slope from log transformed absorbance at 275 – 295 nm

$S_{290-350}$ = spectral slope from log transformed absorbance at 290 – 350 nm

SRB = sulfate reducing bacteria

$SUVA_{254}$ = specific ultraviolet absorbance at 254 nm

t = time

t_{24} = time at 24 hours

t_{48} = time at 48 hours

THg = total mercury

TOC-V CPH/TOC-CPN = total organic carbon – V CPH / total organic carbon -CPN

US = United States of America

UV = ultraviolet

UV-VIS; UV/Vis = ultraviolet and visible

UV S_R = ultraviolet spectral slope ratio

UV-A = ultraviolet-A; 320-400 nm

UV-B = ultraviolet-B; 280-320 nm

UV-C = ultraviolet-C; 200-280 nm

Zn(II) = divalent zinc

List of Appendices

Chapter 1 : INTRODUCTION AND OVERVIEW

Abstract

Mercury contamination is a growing concern for freshwater food webs even in ecosystems without direct point sources of mercury pollution. The methylmercury (MeHg) species of mercury is of particular interest, as this is the form of mercury that is bioaccumulative, can cross the blood-brain barrier, and has neurotoxic effects on organisms. The methylation of mercury occurs primarily through activity of sulfate reducing bacteria in areas that have high organic content and lack oxygen availability such as wetlands and benthic sediments. Biological uptake of MeHg is controlled by physicochemical characteristics such as pH, thiol groups, and dissolved organic matter (DOM) as well as biological attributes of food webs including structure and species interactions. The degradation of MeHg through photochemical reactions is thought to be one of the most effective destruction mechanisms in freshwater lakes, however, there remains large uncertainty around the relationships between these photoreactions and the role of DOM. A comprehensive investigation into the controls DOM imposes on photodemethylation is needed, in particular the photoreactive nature of DOM and the potential for photoreactions with MeHg leading to photodemethylation.

1 THESIS RATIONALE

Mercury is a heavy metal and ubiquitous environmental contaminant that can have severe effects on organisms due to its neurotoxic properties. Methylmercury contamination is a growing concern in aquatic food webs far from point sources of pollution (Evers et al. 2007; Wyn et al. 2010; Kidd et al. 2011; Lehnherr 2014). Common loons in the Maritimes, and particularly Kejimkujik National Park and National Historic Site in Nova Scotia, have the highest blood mercury concentration in all of North America (Evers et al. 1998) and these concentrations are thought to be partially responsible for declined loon productivity (Burgess and Meyer 2007). This region also has documented high concentrations of mercury in bats (Little et al. 2015) and prey species (Depew et al. 2013b) such as yellow perch (Wyn et al. 2010). The rationale behind these high mercury burdens is unclear but likely due to the physicochemical attributes of these ecosystems (Clayden et al. 2013). The mercury sensitivity of the Kejimkujik National Park ecosystem is also linked to high DOM concentrations (commonly quantified as dissolved organic carbon (DOC)) throughout the park. Naturally occurring DOM is well correlated with total mercury concentrations in the park (Meng et al. 2005) and affects photochemical reactions involving mercury, such as photoreduction of divalent mercury to elemental (Haverstock et al. 2012).

Incoming solar radiation can facilitate the demethylation of toxic MeHg through a process called photodemethylation and this pathway can be a significant sink for MeHg in freshwater lakes (Sellers et al. 1996, 2001; Hammerschmidt and Fitzgerald 2006; Lehnherr and St Louis 2009; Li et al. 2010; Black et al. 2012). Dissolved MeHg in freshwater is bound to dissolved organic matter (DOM) and it is thought to be the

photoreactive DOM that primarily absorbs the ultraviolet (UV) solar radiation and is responsible for initiating these photoreactions (Tai et al. 2014; Qian et al. 2014; Jeremiason et al. 2015). The speciation of mercury in aquatic ecosystems along with water chemistry characteristics controls the efficiency of mercury retention and biomagnification in food webs. While many studies have focused on mercury speciation and mercury methylation processes, few have examined rates of toxic MeHg removal from natural freshwaters. Additionally, there are very few studies examining temporal and spatial trends in MeHg photodemethylation rate constants (Poste et al. 2015), and fewer still addressing the direct role of DOM to this process in natural freshwaters (Fleck et al. 2014). This thesis provides fundamental kinetics of MeHg photodemethylation reactions and investigates the influence of DOM on these photoreactions.

The overall objective of this thesis was to determine how DOM concentration and its photoreactivity (i.e. chromophoric properties), in combination with ultraviolet (UV) radiation exposure, controls photodemethylation rate constants within freshwater lakes. We chose to quantify DOM concentration as DOC concentration because DOC is a well-documented variable in many ecosystems and is a useful proxy for DOM. We also chose to focus on the dissolved organic matter and filter out particulate matter because previous studies have identified that MeHg bound with DOM is more likely to photodemethylate, but also that POM would likely introduce much more error into our experimental analysis. Both DOM and MeHg concentrations are variable in time and space, and under certain conditions, this variation may lead to increased risk of MeHg exposure to the base of the food web. Rate kinetics and thresholds for MeHg removal mechanisms that limit this exposure must be quantified. For this work, water was collected for monitoring and

experimentation repeatedly from the same six lakes in Kejimkujik National Park in 2013, 2014, and 2015. Study lakes were specifically chosen to represent a range of naturally occurring DOM concentration across seasons. In 2013, controlled laboratory experiments that focused on characterizing photoreactive DOM in these six lakes took place at the Mersey Tobeatic Research Institute in Caledonia, Nova Scotia in June (summer), August (late-summer), and September (fall). In 2014, controlled laboratory experiments were used to address the relationship between photoreactive DOM and MeHg in one of the six lakes (a high carbon lake; Big Dam West). These laboratory experiments took place at Acadia University in June (summer), August (late-summer), and October (fall). In 2015, experiments were used to compare photodemethylation rate constants between the six lakes in two seasons, during May (spring), July (summer), and October (fall). The pairing of lab and field methods provides advantages, in that analytical chemistry and ecosystem processes can both be quantified, to provide a unique understanding of photodemethylation rate constants in these mercury sensitive environments.

2 THESIS ORGANIZATION

This thesis consists of five chapters. Chapter 1 includes a brief overview of thesis rational and structure, then a literature review that focuses on the significance of photodemethylation in the context of freshwater mercury cycling and examines uncertainties in MeHg sources, sinks, and the implications for MeHg bioavailability to food webs. Chapter 5 is a summary of the major conclusions and the significance and implications of the thesis findings. Chapters 2, 3, and 4 are research papers and correspond with specific research themes for each year of experiments: 2013, 2014, &

2015, respectively. Therefore, each data chapter has its own inclusive introduction and conclusions. The main objectives and hypotheses from the data chapters are provided below.

2.1 Thesis objectives and hypotheses

Chapter 2 examines the photochemical characteristics of DOM from lake waters in Kejimkujik National Park and discusses possible implications for MeHg photoreactions. I hypothesized that if there was a reduction of UV radiation entering lakes from summer through to fall that lead to a decrease of associated losses of chromophoric structures from *in-situ* DOM, then I predicted that UV-A photoreactivity of lake water would increase over the sampling season (summer through fall; Figure 1.1). I also predicted that higher concentrations of photoreactive DOM would facilitate an increased rate of photoreactions involving DOM, and that these reactions could interact with MeHg in the lakes (Figure 1.1). Results showed that DOM concentrations and photoreactivity were related, and that water samples with higher DOM concentration were more susceptible to photobleaching and loss of absorbance. Photoreactions involving mercury (MeHg in particular) may be inhibited because DOM can dominate photoreactions.

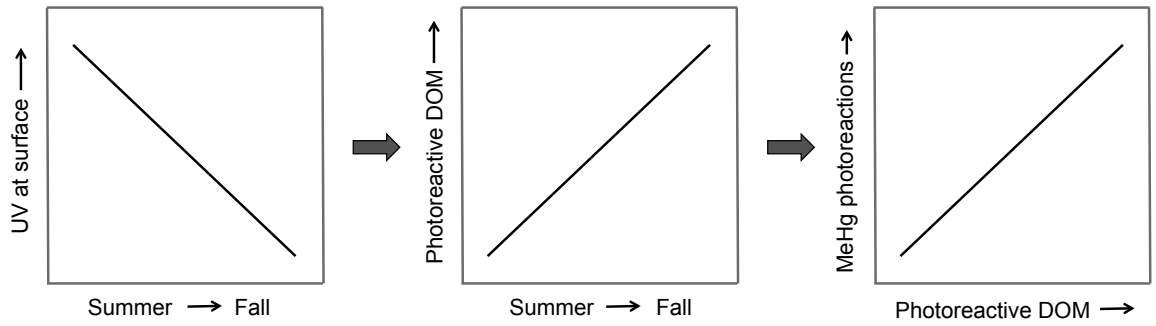

Figure 1.1 Initial predictions for Chapter 3 – photoreactive dissolved organic matter (DOM) will increase over sampling seasons (summer, late-summer, fall), which corresponds with photoreactive DOM likely influencing photoreactions involving methylmercury (MeHg).

The next chapter, Chapter 3, building on the results from Chapter 2 examines if variability in photoreactive DOM (defined as A_{350}) could explain MeHg photodemethylation reaction rates. I hypothesized that if intramolecular photodemethylation reactions involving charge transfer within the DOM to DOM-bound MeHg were occurring (Tai et al. 2014; Jeremiason et al. 2015), then the rate of MeHg photodemethylation and photoreactive DOM would be positively related (Figure 1.2). I also predicted that DOM previously exposed to photochemical processing would yield lower rates of photodemethylation and that there would be a seasonal difference in photodemethylation rate constants because photoreactive DOM would be different at each of the June, August, and October sampling points - mirroring shifts in DOM concentration that are controlled by inputs and photoprocessing (Figure 1.2). Results from these laboratory experiments showed that pre-processed DOM had no effect on photodemethylation rate constants from month to month. However, photodemethylation efficiencies were higher in the lower photoreactive DOM (more photobleached) treatments. All treatments in June had higher photodemethylation rate constants

compared to the other sampling months suggesting a potential seasonal effect. These results suggested that waters with less photoreactive DOM offer greater potential for photodemethylation, the opposite of initial predictions.

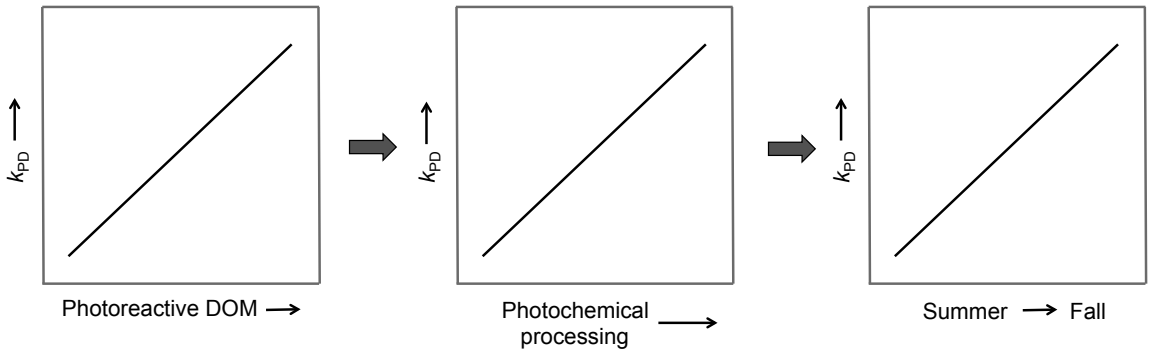

Figure 1.2 Initial predictions for Chapter 3 – increased photoreactive dissolved organic matter (DOM) will increase MeHg photodemethylation rate constants (k_{PD}), which means that photochemical processing of DOM will also increase k_{PD}, which will also correspond with sampling seasons (summer, late-summer, fall).

In order to focus on research gaps identified in Chapter 3 and test MeHg photoreactions in water from more than one lake, Chapter 4 examines how MeHg photodemethylation rate constants varied across six lakes in response to DOM (concentration and photoreactivity) and sampling season. Controlled experiments described previously were laboratory-based, whereas this set of experiments took place outside to replicate many of the physical conditions present within the surface of natural lakes. This change in experimental design helped further validate the controls on photodemethylation under natural conditions, including irradiance (diurnal cycles) and temperatures. I hypothesized that if an increase in the competition for incoming photons

had occurred between DOM and DOM-MeHg complexes, then rates of photodemethylation would decrease with increasing DOM concentration (Figure 1.3). I predicted that at low DOM concentrations, a larger proportion of the photoreactive DOM-MeHg complexes would be involved in photodemethylation reactions, whereas at higher DOM concentrations competition for photons by DOM would result in comparatively less photodemethylation of MeHg (Figure 1.3). Results from Chapter 4 clearly demonstrate that DOM concentration is a dominant control on photodemethylation in Kejimkujik National Park lakes. As DOM became progressively more photobleached and photomineralized, less MeHg photodemethylation occurred. The clear consequence is that photodemethylation is less likely to reduce toxic MeHg in high carbon lakes, as compared with transparent low-DOM lakes. Additionally, because lake hydrology controls lake transparency and DOM concentration, the potential for photodemethylation is driven by characteristic hydrologic regimes and events that cause shifts in DOM concentration and photoreactivity over time.

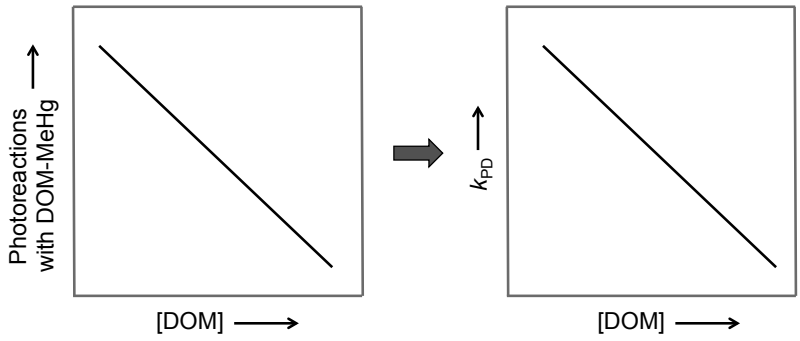

Figure 1.3 Initial predictions for Chapter 4 – increased dissolved organic matter (DOM) concentrations will result in decreased photoreactions with DOM-MeHg, which will result in decreased MeHg photodemethylation rate constants (k_{PD}).

3 LITERATURE REVIEW: REVIEW OF FACTORS AFFECTING METHYLMERCURY PRODUCTION, BIOAVAILABILITY, AND DEGRADATION IN REMOTE FRESHWATER LAKES

3.1 Mercury ecotoxicity in remote freshwaters

Ecosystem sensitivity to mercury contamination has been defined as the ability of a particular ecosystem to methylate inorganic mercury (Hg(II)) into methylmercury (MeHg) and transfer that MeHg into biota (Munthe et al. 2007). Furthermore, there are three principal hypotheses discussed iteratively in scientific literature (Kidd et al. 2011; Clements et al. 2012) that may in conjunction address this phenomenon from a fresh angle to rationalize this phenomenon (Figure 1.4). First and foremost, there must be MeHg present in the environment for uptake by organisms. A better understanding of MeHg availability within freshwater ecosystems is warranted because concentrations are governed by the balance between methylation and demethylation processes (Figure 1.5) (Xun et al. 1987; Miskimmin et al. 1992; Sellers et al. 2001; French et al. 2014). Methylation rates are typically used for assessing risk of mercury contamination (Schartup et al. 2015; Calder et al. 2016) but it is critical to include demethylation rates and food web uptake pathways in these assessments. Second, the species composition of the food web can affect the mechanisms of MeHg transport and consequently the biomagnification rates in each ecosystem. Third, the position of an organism within the food web and the length of the food web will affect the MeHg burdens because higher trophic level organisms have greater MeHg concentrations (Bloom 1992). The main purpose of this review is to highlight the importance of demethylation relative to methylation and bioaccumulation of MeHg.

The toxicity of mercury, specifically the organic form MeHg, is of great concern to wildlife and human populations due to its neurotoxic and endocrine disrupting capabilities (Mergler et al. 2007; Burgess and Meyer 2007; Batchelar et al. 2013). Anthropogenic activity has increased atmospheric deposition of mercury by 3-fold in some areas due to industrial emissions (Lindberg et al. 2007). This increased flux has altered the amount of mercury that is actively cycling between the lithosphere, atmosphere, terrestrial, and aquatic environments (Nriagu 1993). Mercury can undergo both biomagnification through food webs as MeHg (Morel et al. 1998; Walters et al. 2016) and long range transport as gaseous elemental mercury (Hg^0) to be deposited in remote regions far from point sources of pollution (Fitzgerald et al. 1998). Food webs in many remote environments show increasing concentrations of mercury and this trend is particularly pronounced in fish and fish-eating organisms (Evers et al. 2007; Kidd et al. 2011; Lehnherr 2014). Determining the potential for mercury contamination across ecosystems is complex given the many physical, biological, and chemical factors that can affect mercury speciation and in combination have different predictability for mercury fate in freshwaters.

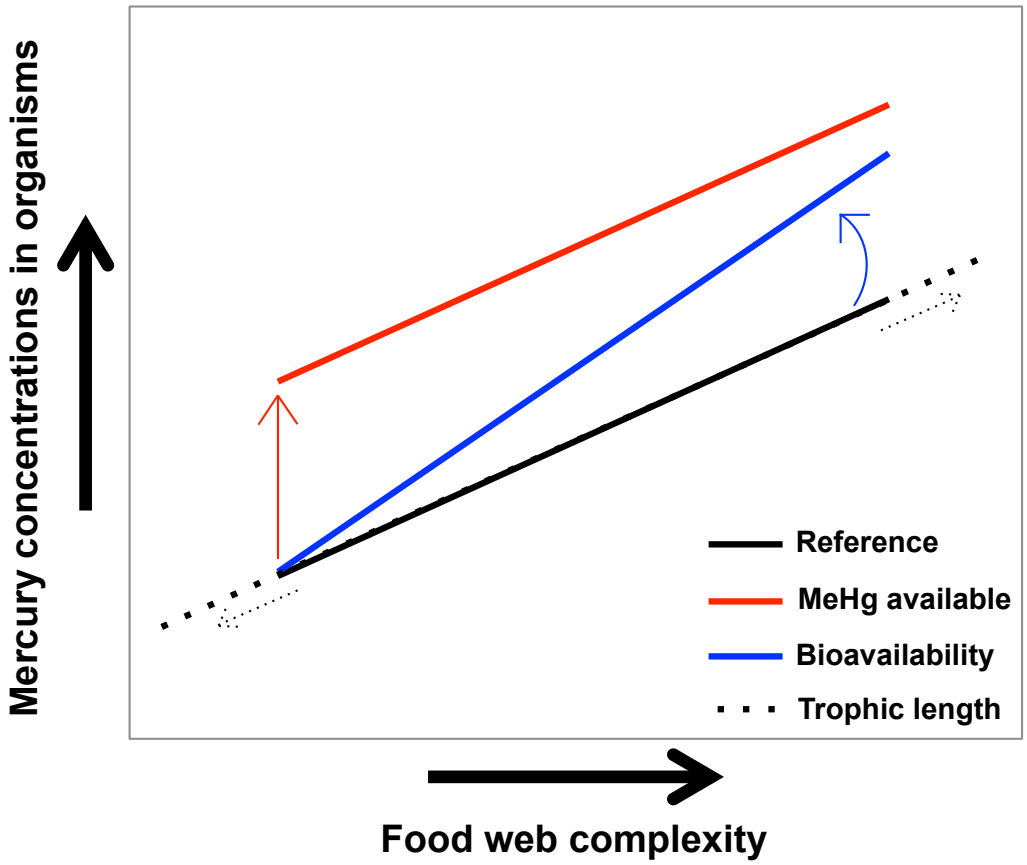

Figure 1.4 Variation in methylmercury (MeHg) contamination across organisms and sites can be explained through the use of several well studied mechanisms in freshwaters: the amount of MeHg at the base of the food web by quantifying the net outcome of methylation and demethylation pathways, bioavailability of that MeHg to organisms and how the structure of food webs will alter the rate in which MeHg is retained, and the trophic length or complexity of food webs. This figure is modified from Kidd et al. (2011).

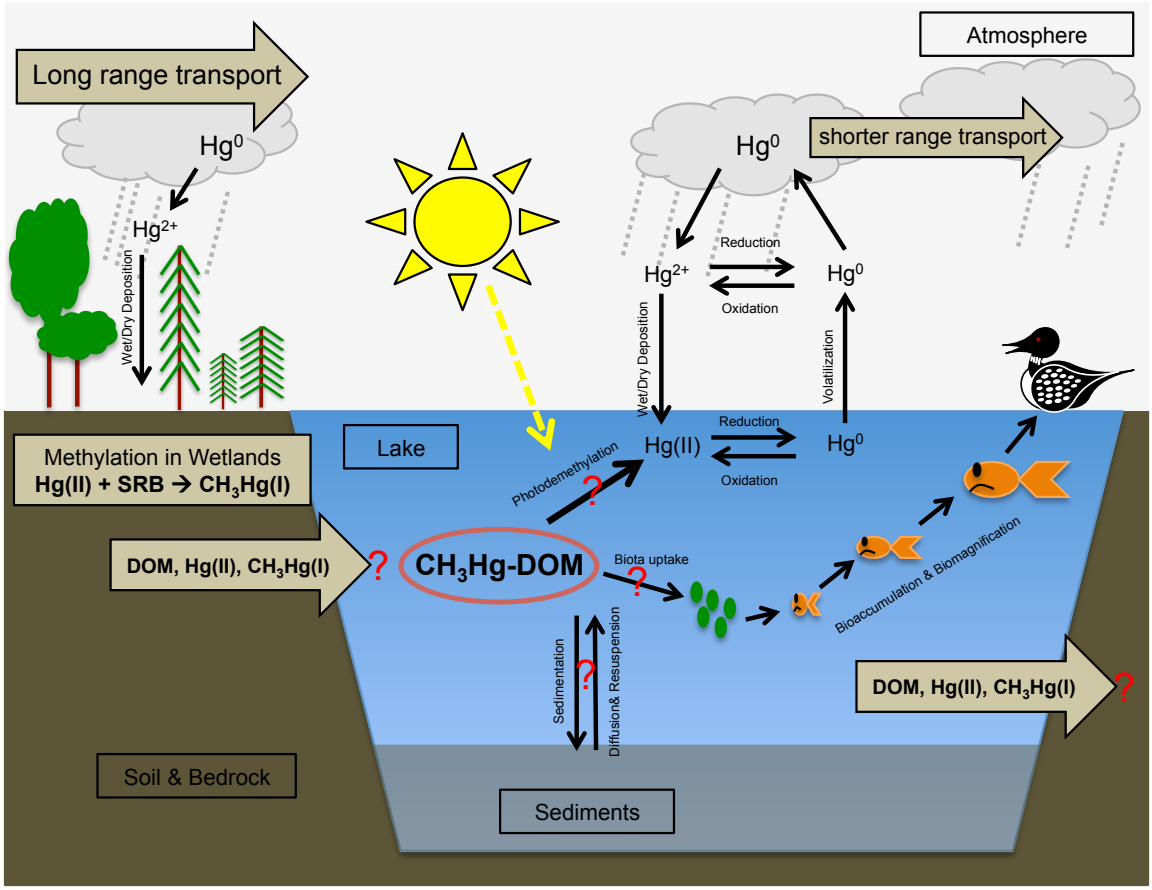

Figure 1.5 Mercury cycling and speciation in freshwater lakes are governed by external inputs and outputs to the system (brown arrows) and internal processes (black arrows). The magnitude of each of these sources and sinks is of great importance to quantifying risk of mercury uptake to biota in remote mercury sensitive lake ecosystems.

3.2 Production of methylmercury in freshwaters

3.2.1 Biological production of methylmercury by bacteria

Methylation of Hg(II) in natural environments is a biological process mediated primarily by anaerobic sulfate reducing bacteria (SRB) (Compeau and Bartha 1985; Gilmour et al. 1992, 1998, Benoit et al. 1999, 2003), likely iron reducing bacteria (Kerin et al. 2006), and any organism that contains the two genes responsible for methylation (Parks et al. 2013). Sulfate reducing bacteria are obligate anaerobes that use sulfate as a terminal electron acceptor in order to gain energy through the oxidation of organic matter (Compeau and Bartha 1985). Methylation is stimulated by sulfate additions and stopped through the inhibition SRB activity (Gilmour et al. 1992). The deposition of sulfate in acid rain is hypothesized to be partially responsible for high concentrations of MeHg in some remote regions (Branfireun et al. 1999). Neutral mercury-sulfide (HgS) complexes have been suggested to be the dominant speciation of Hg(II) uptake by methylating bacteria (Benoit et al. 1999) because of the strong affinity between Hg(II) and reduced sulfur (Dyrssen and Wedborg 1991) and the ability for HgS to passively diffuse through cell membranes (Benoit et al. 2001). Uptake of Hg(II) in green algae (*Selenastrum capriconutum*) does not differ between live and dead cells (Filip and Lynn 1972) further supporting that passive transport of mercury across lipid layers occurs (Morel et al. 1998). Additionally, Hg(II) forms complexes with the amino acid cysteine, which promotes bacteria cell uptake (shown with *Geobacter sulfurreducens*) and methylation of mercury (Schaefer and Morel 2009). Experiments also suggest that uptake of Hg(II) by bacteria is an active transport mechanism facilitated by low molecular weight thiol complexes that use divalent metal ion (such as zinc (Zn(II)) cell wall channels (Schaefer and Morel 2009;

Schaefer et al. 2014). Both charged (Hg-cysteine) and neutral species ($HgCl_2$) can actively enter cells in the absence of Zn(II) but uptake is inhibited with increasing Zn(II) concentrations (Schaefer et al. 2014). This strong relationship between sulfur and Hg(II) is key for increasing Hg(II) bioavailability to SRB which then methylate this species of mercury and produce MeHg.

Labile carbon as an energy source to microbial communities is also very important for methylation. Methylmercury concentrations in sediments have been shown to correlate with organic content (Mason and Lawrence 1999) and complexation of Hg(II) by dissolved organic matter (DOM) can facilitate bacterial uptake by stimulating mercury methylating bacteria (Mazrui et al. 2016). Concentrations of dissolved MeHg in lakes tend to be positively correlated with DOM concentrations (Krabbenhoft et al. 2002; Meng et al. 2005) and methylation rates increase with increasing DOM concentrations (Miskimmin 1991). More than 90% of Hg(II) (Lindqvist et al. 1991; Gherini et al. 1994) and 40-90% of MeHg (Gherini et al. 1994; Hill et al. 2009) in lake waters will be associated with DOM. High concentrations of DOM may however inhibit methylation possibly through the binding of Hg(II) with DOM that cannot be transported into cells (Miskimmin et al. 1992) and uptake or bioavailability of Hg(II) could exhibit a threshold effect (Driscoll et al. 1995; French et al. 2014; Isidorova et al. 2016). Low pH environments will result in more MeHg association with reduced sulfur groups further stimulating methylation and uptake (Ullrich et al. 2001). The effect of carbon is not straightforward, however the effect of pH is quite clear with higher methylation rates in more acidic conditions (Miskimmin et al. 1992; Rudd 1995; Chen et al. 2005).

3.2.2 Physicochemical characteristics affecting potential for sites of mercury methylation

Bacteria-mediated methylation occurs in environments with low redox potential including wetlands (Rudd 1995), sediments (Gilmour et al. 1992), and anoxic portions of the water column (Eckley et al. 2005; Eckley and Hintelmann 2006). Specifically, it is aquatic environments with low pH and high organic matter that favour formation and high solubility of MeHg (Watras et al. 1998; Ullrich et al. 2001). Methylation occurs rapidly at the sediment surface and within the top few centimeters of the sediment-water boundary (Gilmour et al. 1998). Hot spots for methylation occur along ecosystem boundaries (McClain et al. 2003) such as the transition from terrestrial to aquatic (streams and littoral), sediment to aquatic (benthic), and oxic to anoxic (water column) where the influx of new solutes to a system occurs. River flood-plain corridors are also likely hot spots for mercury methylation principally during periods of fluctuating inundation (Singer et al. 2016). Hot spots for MeHg production in peatlands exist immediately adjacent to the boundary of upland forest and peatland initiation (Mitchell et al. 2008). Similarly, in a mining reservoir the river-reservoir interface had 68% more food web MeHg than farther into the reservoir near the dam wall (Stewart et al. 2008). Natural (through seasonal or climate change induced hydrological regimes) (Isidorova et al. 2016; de Wit et al. 2016) and anthropogenic (land use change) landscape disturbances (O'Driscoll et al. 2006; de Wit et al. 2014) alter the flux of organic matter and mercury into aquatic systems and the balance of MeHg production and bioavailability to biota.

3.2.3 Emergent methylmercury production

Quantifying the potential for methylation to occur is a critical component of the mercury contamination story and this potential may be altered through shifts in organisms, land use, and climate. Methylation occurs through the expression of two genes, *hgc*A and *hgc*B (Parks et al. 2013). A recent study by Podar et al. (2015) has identified that organisms with these genes exist in many places on Earth and therefore that the potential for methylation also exists in many places previously not considered (Figure 1.6). These methylation environments not only include dynamic landscapes such as thawing permafrost, coastal zones, and extreme environments but also the digestive tract of some invertebrate organisms (Podar et al. 2015). Given changing hydrology with climate change, the export of more organic matter in Scandinavian boreal rivers and lakes (Isidorova et al. 2016; de Wit et al. 2016) as well as northeastern United States (Strock et al. 2016) is predicted and this shift will likely coincide with increased inputs of mercury and promotion of methylation.

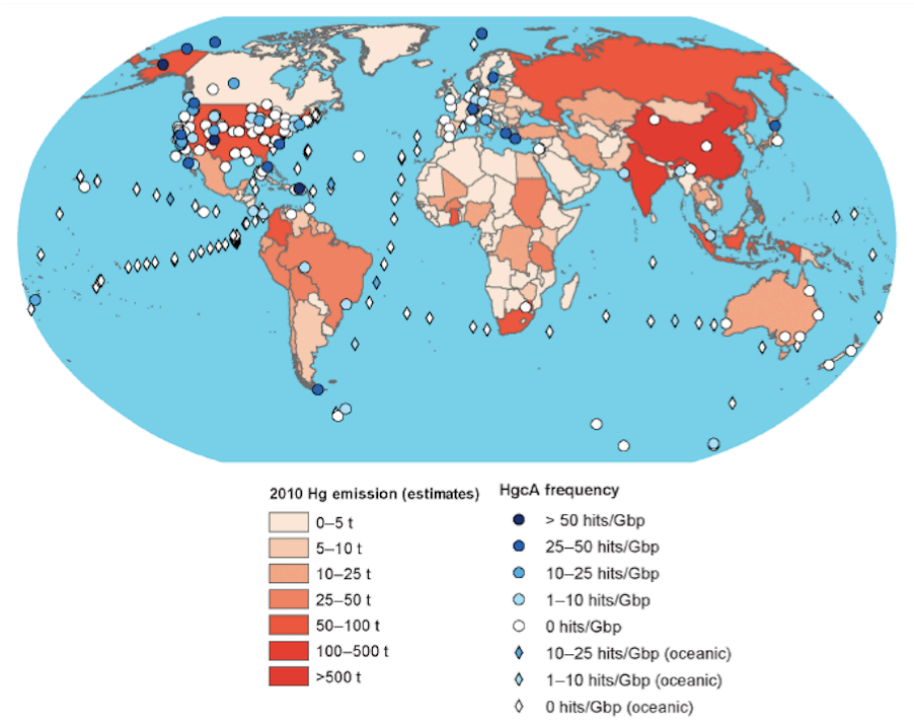

Figure 1.6 Global locations and frequency of *hgc*AB genes that have the potential to methylate mercury. This figure is from a study by Podar et al. (2015) and also contains 2010 mercury emission estimates.

3.3 Removal of methylmercury from water columns

3.3.1 Physicochemical processes act as a methylmercury sink

There are a number of physical constraints on MeHg availability within water columns of freshwater lakes. Methylmercury bound with large organic matter particles that are too large to cross cell membranes is inaccessible (Miskimmin et al. 1992). Just like MeHg produced in sediments and released to the water column, MeHg physically removed from the water column and incorporated into sediments can be re-suspended or dissolved into the water column due to physical disturbance to the sediments or dramatic decreases in pH that increase the solubility of MeHg (Watras et al. 1998; Ullrich et al. 2001). Browning of boreal lake waters due to increased rainfall predictions from climate

change may enhance organic matter burial and therefore MeHg bound with particulate organic matter and flocculates (Isidorova et al. 2016) although there is still great uncertainty regarding the net outcomes of these processes.

3.3.2 Biological processes that demethylate methylmercury

There are not many studies that focus on the demethylation of MeHg by microorganisms. Anaerobic microorganisms like SRB that methylate Hg(II) can also demethylate MeHg (Bridou et al. 2011) through oxidative demethylation resulting in Hg(II) (Oremland et al. 1991; Barkay and Wagner-Döbler 2005). Microbial demethylation can also occur by reductive demethylation resulting in Hg^0 (Oremland et al. 1991) but oxidative demethylation is thought to be the dominant pathway in natural environments (Lin et al. 2011). Biological speciation of mercury, both methylation and demethylation occurs primarily in substrates with high organic content, such as sediments (Gilmour et al. 1992; Marvin-DiPasquale and Oremland 1998; Benoit et al. 1999). To date there has been no measurable biological removal mechanism of MeHg in aerobic lake water (Hammerschmidt and Fitzgerald 2010; Klapstein et al. 2016).

3.3.3 Photochemical processes are methylmercury sink in freshwaters

Demethylation of MeHg can also occur through photochemical reactions, a mechanism called photodemethylation (Sellers et al. 1996). Photodemethylation is the primary sink (up to 80%) for MeHg in some freshwater surfaces (Sellers et al. 2001; Hines and Brezonik 2004; Hammerschmidt and Fitzgerald 2006; Lehnherr and St Louis 2009; Poste et al. 2015) and is less effective at depth in water columns due to attenuation of radiation by DOM (Krabbenhoft et al. 2002; Lehnherr and St Louis 2009; Zhang and

Hsu-Kim 2010; Poste et al. 2015). The controls and rates of photodemethylation need to be better quantified across broad ecosystems, particularly those sensitive to mercury contamination and that contain high concentrations of photoreactive dissolved species such as DOM.

3.3.3.1 Well quantified factors controlling methylmercury photodemethylation

Several studies have identified that photodemethylation will proceed at different rates depending on the radiation wavebands present (Lehnherr and St Louis 2009; Black et al. 2012; Fernández-Gómez et al. 2013). Screens of different material have been used to remove radiation wavebands and thereby test the effects of those specific wavebands on photodemethylation rate constants. In temperate lake water samples exposed only to visible light (400-700 nm; UV was screened out using Lee film) photodemethylation rate constants were about 10-fold less than in samples exposed to full spectrum radiation (Lehnherr and St Louis 2009). Black et al. (2012) found that photodemethylation rate constants were 400-fold greater for UV-B (280-320 nm) and 37-fold greater for UV-A (320-400 nm) radiation as compared to visible radiation in water from temperate wetlands. In many freshwaters DOM readily absorbs shorter wavelengths of UV radiation (Scully and Lean 1994; Morris et al. 1995; Haverstock et al. 2012; Poulin et al. 2014) and much of the visible light is absorbed in surface waters of high carbon systems resulting in brown waters (Bertilsson and Tranvik 2000; Osburn et al. 2009) and thereby reduces the available energy at those shorter wavelengths for photoreactions involving MeHg. UV-A is the portion of UV that is the most relevant for MeHg photoreactions in natural freshwaters due to the fast attenuation of shorter wavelengths (Lehnherr and St Louis

2009) and therefore research that focuses on this portion of UV radiation and its interactions with DOM is key to quantifying the effect of DOM on MeHg photochemistry in freshwaters (Kim and Zoh 2013).

Photodemethylation occurs in a photochemically active layer within water columns. The thickness of this layer will depend on the attenuation of solar radiation wavelengths that are capable of facilitating photodemethylation (Sellers et al. 1996). Therefore, the depth of potential photodemethylation reactions is dependent on the DOM concentration. Lakes with higher concentrations of DOM generally attenuate these wavelengths more effectively than lower DOM lakes (Scully and Lean 1994; Morris et al. 1995; Poste et al. 2015). A lake with a DOM concentration of 12.8 mg C L^{-1}, for example, can be predicted to have photodemethylation occurring in the top 30 cm of the water column (Lehnherr and St Louis 2009). Whereas a nearby lake with a concentration of 5.3 mg C L^{-1} could in theory have photodemethylation to a depth of 2.5 m using the same DOM-based attenuation relationship (Lehnherr and St Louis 2009). Consequently, high DOM lakes in Nova Scotia (9.2-12.3 mg C L^{-1}) also have limited depths (19-17 cm) at which UV photoreactions with DOM will occur (Haverstock et al. 2012).

Loss of MeHg through photodemethylation can appear linear within short timeframes and when there is no limiting reactant (Fleck et al. 2014; Klapstein et al. 2016). Subsequently, quantification of this process is best determined based on cumulative radiation energy received using first-order rate constants instead of being a time-based parameter (Lehnherr and St Louis 2009; Black et al. 2012; Li et al. 2012; Fleck et al. 2014; Klapstein et al. 2016). Early studies focusing on photodegradation of MeHg have reported MeHg losses as a function of time (days typically) (Sellers et al.

1996; Krabbenhoft et al. 2002); however, the amount of radiation is highly variable from day to day and it is the energy provided by photons that actually drives the reaction. Cumulative energy received is typically presented as cumulative photosynthetically active radiation (PAR; 400-700 nm) likely for two reasons: consistency, as this is the way that the first photodemethylation study presented the calculation (Sellers et al. 1996), and instrumentation, as it is simpler methodologically to quantify PAR than specific wavebands of UV and therefore measured more often globally. The need for more global UV irradiance measurements is imperative moving forward so that such work can be coupled with ongoing mechanistic research addressing photoreactive DOM and photodemethylation rate constants.

3.3.3.2 Effects of dissolved organic matter on methylmercury photodemethylation

Direct photolysis of MeHg can in theory happen (Tossell 1998) but this is not very likely at Earth's surface because the necessary short radiation wavelengths are depleted due to ozone absorption. Photodemethylation of MeHg will not occur in natural environments without a photosensitizer present (Zhang and Hsu-Kim 2010; Tai et al. 2014; Qian et al. 2014; Jeremiason et al. 2015; Zhang et al. 2016). Consequently, MeHg will not photodegrade in pure water and the rate of photodemethylation will increase as low doses of DOM are added to water (Qian et al. 2014; Jeremiason et al. 2015). Photoreactive dissolved constituents such as DOM (Zhang and Hsu-Kim 2010; Tai et al. 2014; Qian et al. 2014; Jeremiason et al. 2015; Zhang et al. 2016) and Fe (Hammerschmidt and Fitzgerald 2010; Zhang et al. 2016) can facilitate photodemethylation by first absorbing available wavelengths of radiation and then

through photochemically produced reactive intermediates (PPRI) (Jeremiason et al. 2015). Initial mechanistic photodemethylation hypotheses predicted that the production and release of radicals from DOM such as reactive oxygen species ($^1O_2$/OH•) and excited triplet state (^{3}DOM*) (Zepp et al. 1985) might drive an intermolecular photodemethylation pathway (Zhang and Hsu-Kim 2010; Hammerschmidt and Fitzgerald 2010; Black et al. 2012; Fernández-Gómez et al. 2013). Laboratory experiments, however, have not been able to identify a specific radical responsible for driving photodemethylation using radical quenching techniques by scavenger addition for $^1O_2$, OH•, ^{3}NOM*, and hydrated electron (e^-_{aq}) (Tai et al. 2014). Photodemethylation has recently been proposed to be an intramolecular process (Tai et al. 2014; Qian et al. 2014; Jeremiason et al. 2015) stimulated by the absorption of photons by photoreactive DOM. It has recently been proposed that ^{3}DOM* may be responsible for the intramolecular charge transfer to break the carbon-mercury bond of the methyl group (Qian et al. 2014).

Methylmercury associated with reduced thiol functional groups (RS^-) will be more easily photodemethylated than MeHg associated with chloride species due to a weakening of the carbon-mercury bond in the methyl group (Ni et al. 2006; Zhang et al. 2016). Concentrations of DOM in freshwaters are likely high enough that MeHg will preferentially form complexes with DOM and not chloride and this has been shown in high carbon waters such as Everglades water (Zhang and Hsu-Kim 2010; Tai et al. 2014). The addition of thiol ligands not associated with DOM reduced photodemethylation rate constants in simulated waters that only contain photoreactive DOM likely through the thiols making the MeHg inaccessible to photodegradation (Jeremiason et al. 2015). Photoreactive DOM contains aromatic functional groups, commonly quantified by the

absorbance of radiation at 350 nm (A_{350}) (Baker and Spencer 2004) or the specific ultraviolet absorption at 254 nm ($SUVA_{254}$) (Weishaar et al. 2003). These structures are responsible for absorbing solar radiation in DOM-MeHg complexes which will then facilitate photodemethylation (Qian et al. 2014). The bond between the mercury and carbon atom in MeHg cannot be broken through direct photochemical cleavage in natural waters (Tossell 1998) and the RS-MeHg bond also does not absorb solar UV radiation (Jeremiason et al. 2015). Qian et al. (2014) found that DOM containing both thiolate and aromatic functional groups in the same molecule result in the highest rates of photodemethylation. MeHg can bind weakly with carboxylic groups but it will preferentially bind with reduced sulfur functional groups over relatively short time periods of 4-24 hours (Hintelmann et al. 1995; O'Driscoll and Evans 2000). The effect of DOM on photodemethylation can differ depending on the size of DOM, small molecular weight compounds (<3.5 kDa) have been shown to promote photodemethylation through a reactive effect whereas larger molecular weight compounds (>3.5 kDa) will inhibit methylation through radiation attenuation (Kim et al. 2017). The interaction between MeHg and DOM is key for photodemethylation to occur and thiols promote photodemethylation when another component of the DOM is photoreactive.

Due to the importance of MeHg binding with specific structural groups within DOM, the effect of pH on photodemethylation of MeHg is key. Photodemethylation is promoted in more alkaline solutions and rate constants increase with increases in pH (Kim et al. 2017). Increases of pH from 5.0 to 7.0 has been shown to increase the rate of photodemethylation but the same experiments also showed a decrease at a pH of 8.0 but then another increase in rate at 9.0 suggesting that the relationship between pH and

photodemethylation rate is complex (Zhang et al. 2016) but likely is linked to binding capacities and efficiencies of the MeHg with DOM.

Optical characterization of DOM can increase our knowledge about the influence of DOM structures on photodemethylation, while structural techniques are important for identifying where the MeHg is within a DOM complex, optical data can infer which structures are involved in photodemethylation. Absorbance and fluorescence spectroscopy have determined that MeHg photodemethylation can occur without the loss of DOM concentration (Fleck et al. 2014) and that the photoreactive components of the DOM will be transformed into less photoreactive structures (Cory et al. 2011). Absorbance spectral slopes and the ratio between these (S_R; $S_{275\text{-}290}/S_{350\text{-}400}$) can be associated with the molecular size of the chromophoric DOM molecules and changes in these slopes can signify internal structural changes caused by photochemical reactions through selective losses of higher molecular weight associated chromophores leading to a shift in the proportion of these chromophore groups (Helms et al. 2008). Increase of S_R corresponds with MeHg loss in wetland waters and a decline in the molecular size of chromophoric DOM due to photochemical reactions (Fleck et al. 2014). Additionally Fleck et al. (2014) suggest that there may be a pool of base refractory photoreactive DOM because fluorescence excitation-emission matrices across the wetland study sites became more similar following photochemical processing. Photodemethylation can be inhibited by high molecular weight DOM (Zhang et al. 2016) because this fraction of the DOM pool has a higher radiation attenuation capacity (Li et al. 2010; Fernández-Gómez et al. 2013) since it is composed of more humic aromatics (Weishaar et al. 2003). A significant portion (40-70%) of the MeHg in freshwater lakes and wetlands associates with low

molecular weight DOM (<5kDa) (Hill et al. 2009). These studies highlight the synergistic effects of reduced sulfur groups and photoreactive aromatics and the need for better understanding of the DOM composition of DOM-MeHg complexes to better predict photodemethylation rates in natural waters.

3.4 Mercury contamination in freshwater organisms

3.4.1 Mercury entry into the base of food webs

The uptake of mercury into organisms occurs via two pathways: direct water-to-organism transfer and through the consumption of organisms that already contain mercury. In freshwater environments dissolved mercury exists in several forms: Hg^0, Hg(II) and MeHg. Both Hg(II) and MeHg form lipid soluble hydrophobic complexes with chloride and phytoplankton receive mercury through uptake of these complexes (Mason et al. 1996). Phytoplankton species accumulate MeHg actively through cellular function and not passive diffusion like Hg(II) uptake, which was shown in experiments that compared MeHg and Hg(II) concentrations in live and dead cells (Pickhardt and Fisher 2007). Bacterial uptake of MeHg was ten times greater than algal uptake perhaps due to higher surface area-to-volume ratios and possibly more binding sites for reactive mercury compounds on bacterial than algal cells (Pickhardt and Fisher 2007). Additionally, the partitioning of mercury within algal cells is different for MeHg and Hg(II), with up to 64% of MeHg but only 9 - 16% of the Hg(II) in the cytoplasm (Pickhardt and Fisher 2007). This difference in distribution within the cells leads to more efficient retention of MeHg than Hg(II) during transfer from phytoplankton to zooplankton (Pickhardt and Fisher 2007). Reinfelder et al. (1991) and Mason et al. (1996) further suggest that the

cytoplasmic concentrations of trace metals like mercury are readily transferred and amassed in consumers.

Many chemical factors within an environment control the uptake of mercury into unicellular organisms. Environmental pH and dissolved organic matter (DOM) can alter the cellular membrane and thereby influence the transmembrane transport of MeHg. Lower pH will favour the formation of chloride complexes (Morel et al. 1998) and more free hydrogen ions (H^+) reduce available binding sites on DOM for MeHg, which means greater MeHg bioavailability in more acidic waters (Watras et al. 1998). The effect of DOM on MeHg uptake from water is complicated; increased DOM concentrations increase the cellular membrane's permeability to metals, causing more transfer into cells (Campbell et al. 1997) and increased DOM flushed from terrestrial and wetland landscapes into streams and lakes also carries more mercury to these systems, thus increasing the baseline concentrations of MeHg available in a system. A whole lake manipulation experiment with decreased pH and increased lake water DOM concentration led to higher MeHg in zooplankton (Watras et al. 1998) by affecting the MeHg available to the base of the food web (Watras and Bloom 1992). A DOM threshold for maximum bioavailability of MeHg of 8.5 mg C L^{-1} has been proposed with uptake declining as DOM concentrations decrease and increase from that maxima (French et al. 2014). However, this study used organisms from lakes with different physical features (permafrost thaw causing slumping at lake edges versus lakes with stable edges) and the invertebrate MeHg concentrations tended to group by lake type on opposite sides of the threshold (French et al. 2014), which could have influenced these results. Nevertheless, it

is an intriguing idea, that DOM may exert some threshold control on regulating MeHg availability to biota.

Ecosystem parameters such as forest cover, mercury deposition, and alkalinity can also explain regional differences in MeHg available to the base of the food web (Lavoie et al. 2013; Depew et al. 2013a; b) and ultimately variation in piscivore mercury concentrations (Chasar et al. 2009; Wyn et al. 2009). The concentrations of MeHg in lower trophic levels are an important predictor of mercury contamination within a food web and local environment. To determine the mercury in lower trophic levels we must recognize the influence of chemical factors such as complexation of mercury with sulfide and DOM, pH variability, and also the biological factors, such as food web structure and diet, on bioavailability of mercury from water and the method for available mercury uptake.

3.4.2 Organisms exposed to mercury through diet

Mercury is a nonessential element acquired by consumers as a consequence of food source. Regardless of mercury concentration, consumers tend to choose diet entities based on quality and quantity of resources available (Marcarelli et al. 2011). Primary producers are the base of aquatic food webs, and more specifically, a source of fixed carbon (organic matter) to consumers. Alternatively, sources of organic carbon to food chains can also come from detrital organic matter; consumers of this carbon source are known as detritivores. Detrital inputs can be fairly continuous or shift seasonally due to plant life cycles, migratory animal behaviour such as deposition of bird guano, fish reproduction and death (semelparous), and hydrological regimes (Blais et al. 2007).

Terrestrial detritus is a major source of organic matter to every aquatic ecosystem and encompasses a wide range of size classes including DOM and particulate organic matter (Wetzel 2001).

In the initial stages of food chains it is difficult to determine the energy (and therefore mercury) pathway into and between organisms. Perhaps the specific primary producer species is less important than the source of fixed carbon used to derive metabolic energy, since organic matter facilitates mercury transport through food chains. MeHg concentrations in consumers, for example, are predicted by the type of diet consumed (Kainz et al. 2003; Kainz and Mazumder 2005; de Wit et al. 2012). Mid-trophic level macrozooplankton, commonly *Daphnia spp.*, receive 47-98% of their MeHg from diet (Tsui and Wang 2004). Kainz and Mazumder (2005) found that MeHg concentrations in coastal lake zooplankton are more correlated to bacterial (R^2=0.50) than algal (R^2=0.35) consumption. Heterotrophic bacteria use DOM as an energy source (Moran and Hodson 1990), receiving mercury bound to the DOM in either MeHg or Hg(II) form and recycling both organic matter and mercury from detritus. Bacterial diet sources stimulate the uptake of MeHg more than algal diets of zooplankton (de Wit et al. 2012) and perhaps it also matters what the bacteria use as a carbon source and where that carbon came from.

Algae presence and growth is driven by light, temperature and nutrient availability. Seasonal variation in these components lead to an unstable food source for zooplankton, forcing zooplankton to shift their diet to bacteria and terrestrial detritus (de Wit et al. 2012). Bacteria can contain higher MeHg concentrations (Kainz and Mazumder 2005) because they can recycle material within a system or from allochtonous DOM

inputs and are therefore critical to the cycling of nutrients, cycling of mercury, and interactions with other microbial components of the community. A microbial loop can exist whereby detrital carbon and nutrients get cycled through several microbial consumers before being transferred to higher trophic organisms such as macrozooplankton (Sherr and Sherr 1988). In oligotrophic waters, phytoplankton can be too small (< 5 μm) to be effectively grazed by macrozooplankton and thus enter the microbial loop whereby microzooplankton (> 5 μm) feed on detritivores before they themselves are consumed by larger zooplankton (Sherr and Sherr 1988). Plankton community structure is an explicit consideration for mercury transfer and propagation in the lower trophic levels of aquatic food chains.

Periphyton is composed of algae, bacteria, and detritus contained within a gelatinous polymer that can colonize the surfaces of macrophytes, rocks, or any other submerged structure (Vander Zanden et al. 1997). Due to structural inhibition the exact ratio and taxa composition present in periphyton can be difficult to delineate (de Wit et al. 2012). Unique microhabitats of periphyton can enable high mercury methylation rates more than twice that of the adjacent sediment (Hamelin et al. 2015). Periphyton can also be a direct food source for grazers and scrapers in the littoral zone where macrophytes are present (Hamelin et al. 2015). Comparatively, macrophytes themselves are generally low in MeHg; grazers relying on this food source will also have low MeHg concentrations (Mason et al. 2000; Tsui et al. 2009). The source and availability of MeHg as a dietary component dictates the concentrations of MeHg that can enter food chains and be transferred to consumers.

3.4.3 Bioaccumulation and biomagnification of mercury

The inclusion and retention of mercury in food webs depends on bioaccumulation and biomagnification properties. When concentrations in an organism are higher than those in the surrounding water this is referred to as bioconcentration. The greatest bioconcentration of MeHg occurs in the lowest trophic levels of the food web, with concentrations of MeHg in phytoplankton being 1,000,000 times greater than those in water (Watras et al. 1998; Engstrom 2007). Bioaccumulation includes both mercury uptake from water and transfer between trophic levels. When the ratio of mercury concentration in an organism is greater than the concentration of mercury in water, the bioaccumulation factor, is greater than one. Bioaccumulation factors (BAFs) can be greater in long-lived, large-bodied organisms than shorter-lived, smaller-bodied organisms (Watras et al. 1998). In a controlled mesocosm experiment that identified mercury concentrations in three zooplankton species, a large Cladoceran species (*Daphnia mendotae*) had MeHg levels 2 - 3 times higher than the two smaller copepod species (*Leptodiaptomus minutus* and *Mesocyclops edax*) (Pickhardt et al. 2005). While this size trend is generally accepted, concentrations of MeHg vary greatly between and within invertebrate species depending on habitat-specific mercury loadings (Chételat and Amyot 2009) and different prey for the raptorial cladocerans versus filter-feeding copepods. Biomagnification is an increase in contaminant concentration at each trophic step and biomagnification factors (BMFs) are the ratio of mercury concentration in predator versus prey, which are documented to range between 2 and 10 in aquatic food webs (Watras et al. 1998). Diet sources of MeHg accounted for 47 - 98% of the MeHg in *Daphnia spp.*, common macrozooplankton (Tsui and Wang 2004). Biomagnification

occurs in all aquatic ecosystems and is the process that causes top predators, such as fish, to have MeHg concentrations at levels that cause neurological effects (Watras et al. 1998). Remote pristine environments can have high mercury levels in consumers due to the presence of mercury in prey species (Depew et al. 2013b) and the process of MeHg biomagnification (Rasmussen et al. 1990).

A study of many mid-latitude lakes in Nova Scotia showed that pH was not a strong control on mercury in top predators, but rather mercury concentrations at lower trophic levels (zookplankton, amphipods, and dragonfly nymphs) best predicted mercury in fish (yellow perch), further supporting the hypothesis that variation in consumer species mercury levels is driven by mercury exposure in lower trophic levels (Wyn et al. 2009). That being said, the lakes studied by Wyn et al. (2009) had similar community composition, so any differences in biomagnification rates would be due to varying ecosystem properties and consequential influences on physiology. Physiological controls on biomagnification rates may be influenced by physical and chemical ecosystem properties that contribute to mercury contamination in organisms.

3.4.4 Trophic and habitat-specific transfer of energy and mercury

Food chains are delineated by organism size and function. Heterotrophic organisms gain energy (OM source) and nutrients through diet, but they can also acquire nonessential elements and compounds that are not required for metabolic function that may be detrimental to organism health. Some organisms have mechanisms for detoxifying MeHg but these rates are too slow to remove all mercury from an organism before predation (Trudel and Rasmussen 1997). Algae and macrozooplankton can

demethylate 68.9 ± 4.9% and 13.5 ± 1.3% of the MeHg, respectively, over 2-weeks in a mesocosm experiment (Pickhardt et al. 2005). These rates are relatively slow considering this was a closed system experiment. Since mercury has no biological benefit to any organism, there are limited methods for its removal from most consumer organisms once in MeHg form. The proportion of total mercury that is MeHg (%MeHg) increases from primary producers to primary consumers to consumers with multiple food sources (Mason et al. 2000). In this fashion mercury piggybacks through the food chain accumulating at each successive step, since more energy (in the form of organic matter) is required for higher organism function and these higher organisms also receive more mercury along with energy and nutrients.

Freshwater habitats vary in organic matter source, nutrient availability, and the types of biota that can be sustained in a specific area. Likewise, each habitat will also vary in MeHg bioavailability and food chain mercury burdens. Streams can facilitate mercury transfer between terrestrial and aquatic biota (Walters et al. 2008). Littoral habitats are similar to riverine habitats because they receive terrestrial detritus, which includes nutrients and mercury, but have still waters that allow for development of macrophytes and small metazoan community food webs. Wetlands positioned on lake margins provide high MeHg concentrations to littoral habitats (Kidd et al. 2011) and periphyton growing on macrophytes can also be a large source of MeHg (Hamelin et al. 2015). Along with MeHg source and concentration in primary producers and consumers, the nutrient status of the lake will control biodilution, the balance between mercury uptake and organism growth (Cabana et al. 1994; Sunda and Huntsman 1998). Benthic habitats can have high mercury methylation potential due to low redox conditions that

promote sulfate reducing bacteria (Gilmour et al. 1998), but amphipod and fish mercury concentrations are not always related to high sediment MeHg levels if the mercury is from historical anthropogenic contamination (Hodson et al. 2014) or legacy mercury.

Almost all of the mercury added to a lake surface can be quickly (<3 years) incorporated into food webs, which is evidence that new allochtonous inputs of mercury are likely more bioavailable than legacy mercury already present in the ecosystem (Harris et al. 2007). This result also highlights that atmospherically deposited mercury is likely more bioavailable. The bioavailability of mercury declines over time, possibly through photochemical processing of DOM which can lead to decreased methylation potential (Luo et al. 2016). Based on a study of 52 oligotrophic lakes in North America, pelagic food webs may have the most efficient uptake of MeHg of any specific habitat with non-point source contamination (Chételat et al. 2011). Zooplankton in pelagic habitats consume bacteria, algae, and microzooplankton forming a microbial loop (Sherr and Sherr 1988), which results as a MeHg enrichment mechanism for lower trophic level species which then propagates through food chains to higher trophic level consumers. This microbial loop may actually extend the food chain length in low trophic levels concentrating mercury levels before invertebrate consumption. Concurrently, pelagic food webs incorporate MeHg enriched plankton from low redox potential environments, such as the hypolimnion, during diurnal cycles and fall turnover mixing of the water column (Harris et al. 2007). At the landscape and large scale, global syntheses of metadata have highlighted uncertainties on universal controls for bioaccumulation factors among freshwater ecosystems likely driven by site specific water chemistry characteristics like

pH, nutrients, and mercury concentrations available for methylation and not spatial trends such as latitude (Lavoie et al. 2013).

3.5 Photodemethylation knowledge gaps and key uncertainties

A proposed framework for addressing mercury contamination in remote freshwater lakes should include methylation potential, bioavailability, and photodemethylation potential that focus on ubiquitous water chemistry parameters like pH, sulfur, and DOM (Figure 1.7) with the strength of each parameter depending on the specific ecosystem in question. Methylation of mercury is the primary factor that can promote or inhibit mercury contamination in organisms. Without methylation, environments that contain background levels of Hg(II) pose little risk to aquatic food web health. Methylation increases in acidic environments with low redox potential and high concentrations of sulfate however there is still some uncertainty regarding the influence of DOM on this predominantly bacteria mediated process. Once formed the bioavailability of MeHg is strongly controlled again by pH and sulfur or thiol groups but there is high uncertainty regarding the direct and indirect influences of DOM on this process.

Methylmercury can be removed from a lake physically by outflows and sediment burial although these processes do not eliminate risk of MeHg to another lake or if sediment disturbance occurs. Shifting the speciation of mercury away from MeHg to Hg(II) or Hg^0 is ideal for reducing MeHg exposure to food webs. In lake water columns the dominant pathway for demethylation is photodemethylation. However, the strength of this sink is highly variable and depends on pH, reduced sulfur groups, and DOM for

photochemical reactiveness. Dissolved organic matter must be present in order for this demethylation pathway to occur; however concentrations of DOM naturally present in the environment quickly complicate photodemethylation predictability by limiting the quantity of photoreactions that can involve MeHg. The source and structure of DOM greatly affects the ability of DOM to absorb radiation and therefore fundamental relationships such as optical parameters of DOM require further examination with regard to MeHg photoreactions.

Universal photodemethylation rate constants have even been proposed for specific wavebands because values found throughout the literature are comparable, within one order of magnitude of each other (Fernández-Gómez et al. 2013; Fleck et al. 2014; Poste et al. 2015). The caveat with the application of this idea is that the DOM between areas will differ in quantity and optical properties. The way in which DOM absorbs radiation and photoreacts can affect the efficiency of photodemethylation (Klapstein et al. 2016) and prediction of MeHg losses using only DOM concentration without knowing the photoreactivity can increase the error associated with these calculations and lead to underestimates of photodemethylation rate constants (Black et al. 2012). Because ice and snow cover water surfaces (and columns) for large portions of the year ecosystems with temperate and Arctic climate regimes will have dramatic shifts in photodemethylation potential between seasons (Poste et al. 2015). A comprehensive analysis of the relationship between DOM, MeHg, and solar radiation exposure is necessary to better predict the potential for photodemethylation to occur in natural remote freshwater ecosystems. The balance between MeHg formation and MeHg removal from a system (physical isolation or degradation) is essential for predicting when and where excess

MeHg will be available for biological uptake (Figure 1.7). We propose further investigation of the complex relationship between DOM and photodemethylation will help elucidate risk of mercury exposure to organisms.

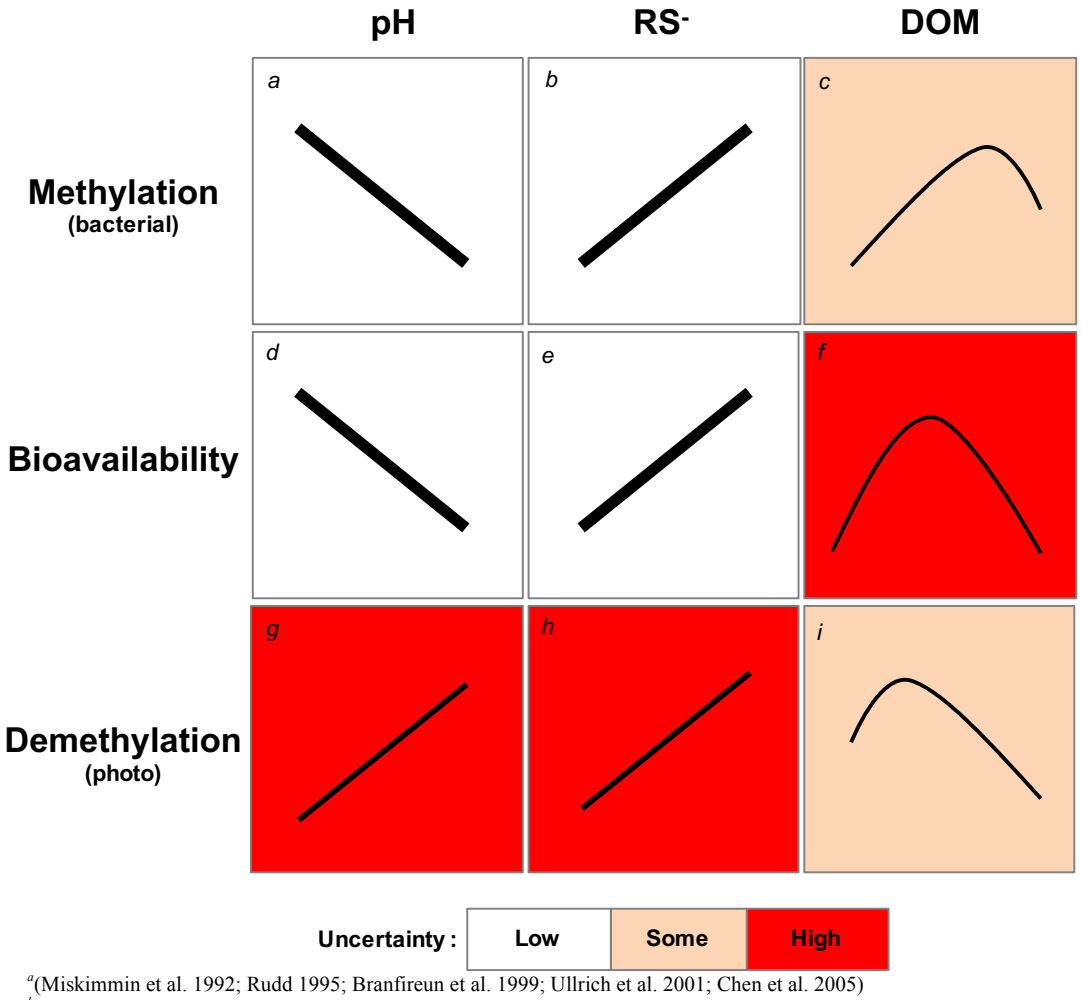

[a](Miskimmin et al. 1992; Rudd 1995; Branfireun et al. 1999; Ullrich et al. 2001; Chen et al. 2005)
[b](Compeau and Bartha 1985; Gilmour et al. 1992, 1998, Benoit et al. 1999, 2003; Branfireun et al. 1999)
[c](Miskimmin 1991; Mason and Lawrence 1999; Krabbenhoft et al. 2002; Meng et al. 2005; Mazrui et al. 2016)
[d](Watras et al. 1998; Ullrich et al. 2001)
[e](Benoit et al. 1999, 2001)
[f](Miskimmin et al. 1992; Driscoll et al. 1995; French et al. 2014; Isidorova et al. 2016)
[g](Zhang et al. 2016; Kim et al. 2017)
[h](Ni et al. 2006; Hammerschmidt and Fitzgerald 2010; Bridou et al. 2011; Qian et al. 2014; Jeremiason et al. 2015; Zhang et al. 2016)
[i](Krabbenhoft et al. 2002; Hammerschmidt and Fitzgerald 2006; Lehnherr and St Louis 2009; Zhang and Hsu-Kim 2010; Li et al. 2010; Black et al. 2012; Tai et al. 2014; Qian et al. 2014; Poste et al. 2015; Jeremiason et al. 2015; Fleck et al. 2016; Klapstein et al. 2016)

Figure 1.7 Summary of general uncertainty (low, some, high) associated with bacterial methylation of methylmercury (MeHg), bioavailability of MeHg to organisms, and MeHg photodemethylation given three key water chemistry parameters: pH, sulfur groups (RS^-), and dissolved organic matter (DOM). The water chemistry parameters themselves also covary but are not visually described here.

References

Baker, A., and R. G. M. Spencer. 2004. Characterization of dissolved organic matter from source to sea using fluorescence and absorbance spectroscopy. Sci. Total Environ. **333**: 217–232. doi:10.1016/j.scitotenv.2004.04.013

Barkay, T., and I. Wagner-Döbler. 2005. Microbial transformations of mercury: Potentials, challenges, and achievements in controlling mercury toxicity in the environment, p. 1–52. *In* B.-A. in A. Microbiology [ed.]. Academic Press.

Batchelar, K. L., K. A. Kidd, P. E. Drevnick, K. R. Munkittrick, N. M. Burgess, A. P. Roberts, and J. D. Smith. 2013. Evidence of impaired health in yellow perch (*Perca flavescens*) from a biological mercury hotspot in northeastern North America. Environ. Toxicol. Chem. **32**: 627–637. doi:10.1002/etc.2099

Benoit, J. M., C. C. Gilmour, A. Heyes, R. P. Mason, and C. L. Miller. 2003. Geochemical and biological controls over methylmercury production and degradation in aquatic ecosystems. *ACS symposium series*. Washington, DC; American Chemical Society; 1999. 262–297.

Benoit, J. M., C. C. Gilmour, and R. P. Mason. 2001. The influence of sulfide on solid-phase mercury bioavailability for methylation by pure cultures of *Desulfobulbus propionicus* (1pr3). Environ. Sci. Technol. **35**: 127–132. doi:10.1021/es001415n

Benoit, J. M., C. C. Gilmour, R. P. Mason, and A. Heyes. 1999. Sulfide controls on mercury speciation and bioavailability to methylating bacteria in sediment pore waters. Environ. Sci. Technol. **33**: 951–957. doi:10.1021/es9808200

Bertilsson, S., and L. J. Tranvik. 2000. Photochemical transformation of dissolved organic matter in lakes. Limnol. Oceanogr. **45**: 753–762.

Black, F. J., B. A. Poulin, and A. R. Flegal. 2012. Factors controlling the abiotic photo-degradation of monomethylmercury in surface waters. Geochim. Cosmochim. Acta **84**: 492–507. doi:10.1016/j.gca.2012.01.019

Blais, J. M., R. W. Macdonald, D. Mackay, E. Webster, C. Harvey, and J. P. Smol. 2007. Biologically mediated transport of contaminants to aquatic systems. Environ. Sci. Technol. **41**: 1075–1084. doi:10.1021/es061314a

Bloom, N. S. 1992. On the chemical form of mercury in edible fish and marine invertebrate tissue. Can. J. Fish. Aquat. Sci. **49**.

Branfireun, B. A., N. T. Roulet, C. A. Kelly, and J. W. M. Rudd. 1999. In situ sulphate stimulation of mercury methylation in a boreal peatland: Toward a link between

acid rain and methylmercury contamination in remote environments. Glob. Biogeochem. Cycles **13**: 743–750. doi:10.1029/1999GB900033

Bridou, R., M. Monperrus, P. R. Gonzalez, R. Guyoneaud, and D. Amouroux. 2011. Simultaneous determination of mercury methylation and demethylation capacities of various sulfate-reducing bacteria using species-specific isotopic tracers. Environ. Toxicol. Chem. **30**: 337–344. doi:10.1002/etc.395

Burgess, N. M., and M. W. Meyer. 2007. Methylmercury exposure associated with reduced productivity in common loons. Ecotoxicology **17**: 83–91. doi:10.1007/s10646-007-0167-8

Cabana, G., A. Tremblay, J. Kalff, and J. B. Rasmussen. 1994. Pelagic food chain structure in Ontario lakes: a determinant of mercury levels in lake trout (*Salvelinus namaycush*). Can. J. Fish. Aquat. Sci. **51**: 381–389.

Calder, R. S. D., A. T. Schartup, M. Li, A. P. Valberg, P. H. Balcom, and E. M. Sunderland. 2016. Future impacts of hydroelectric power development on methylmercury exposures of Canadian indigenous communities. Environ. Sci. Technol. **50**: 13115–13122. doi:10.1021/acs.est.6b04447

Campbell, P. G., M. R. Twiss, and K. J. Wilkinson. 1997. Accumulation of natural organic matter on the surfaces of living cells: implications for the interaction of toxic solutes with aquatic biota. Can. J. Fish. Aquat. Sci. **54**: 2543–2554. doi:10.1139/f97-161

Chasar, L. C., B. C. Scudder, A. R. Stewart, A. H. Bell, and G. R. Aiken. 2009. Mercury cycling in stream ecosystems. 3. Trophic dynamics and methylmercury bioaccumulation. Environ. Sci. Technol. **43**: 2733–2739. doi:10.1021/es8027567

Chen, C. Y., R. S. Stemberger, N. C. Kamman, B. M. Mayes, and C. L. Folt. 2005. Patterns of Hg bioaccumulation and transfer in aquatic food webs across multi-lake studies in the northeast US. Ecotoxicology **14**: 135–147. doi:10.1007/s10646-004-6265-y

Chételat, J., and M. Amyot. 2009. Elevated methylmercury in high Arctic *Daphnia* and the role of productivity in controlling their distribution. Glob. Change Biol. **15**: 706–718. doi:10.1111/j.1365-2486.2008.01729.x

Chételat, J., M. Amyot, and E. Garcia. 2011. Habitat-specific bioaccumulation of methylmercury in invertebrates of small mid-latitude lakes in North America. Environ. Pollut. **159**: 10–17. doi:10.1016/j.envpol.2010.09.034

Clayden, M. G., K. A. Kidd, B. Wyn, J. L. Kirk, D. C. G. Muir, and N. J. O'Driscoll. 2013. Mercury biomagnification through food webs is affected by physical and

chemical characteristics of lakes. Environ. Sci. Technol. **47**: 12047–12053. doi:10.1021/es4022975

Clements, W. H., C. W. Hickey, and K. A. Kidd. 2012. How do aquatic communities respond to contaminants? It depends on the ecological context. Environ. Toxicol. Chem. **31**: 1932–1940. doi:10.1002/etc.1937

Compeau, G. C., and R. Bartha. 1985. Sulfate-reducing bacteria: Principal methylators of mercury in anoxic estuarine sediment. Appl. Environ. Microbiol. **50**: 498–502.

Cory, R. M., E. W. Boyer, and D. M. McKnight. 2011. Spectral methods to advance understanding of dissolved organic carbon dynamics in forested catchments, p. 117–135. *In* D.F. Levia, D. Carlyle-Moses, and T. Tanaka [eds.], Forest Hydrology and Biogeochemistry. Springer Netherlands.

Depew, D. C., N. M. Burgess, and L. M. Campbell. 2013a. Modelling mercury concentrations in prey fish: Derivation of a national-scale common indicator of dietary mercury exposure for piscivorous fish and wildlife. Environ. Pollut. **176**: 234–243. doi:10.1016/j.envpol.2013.01.024

Depew, D. C., N. M. Burgess, and L. M. Campbell. 2013b. Spatial patterns of methylmercury risks to common loons and piscivorous fish in Canada. Environ. Sci. Technol. **47**: 13093–13103. doi:10.1021/es403534q

Driscoll, C. T., V. Blette, C. Yan, C. L. Schofield, R. Munson, and J. Holsapple. 1995. The role of dissolved organic carbon in the chemistry and bioavailability of nercury in remote Adirondack lakes, p. 499–508. *In* D.B. Porcella, J.W. Huckabee, and B. Wheatley [eds.], Mercury as a Global Pollutant. Springer Netherlands.

Dyrssen, D., and M. Wedborg. 1991. The sulphur-mercury(II) system in natural waters. Water. Air. Soil Pollut. **56**: 507–519. doi:10.1007/BF00342295

Eckley, C. S., and H. Hintelmann. 2006. Determination of mercury methylation potentials in the water column of lakes across Canada. Sci. Total Environ. **368**: 111–125.

Eckley, C. S., C. J. Watras, H. Hintelmann, K. Morrison, A. D. Kent, and O. Regnell. 2005. Mercury methylation in the hypolimnetic waters of lakes with and without connection to wetlands in northern Wisconsin. Can. J. Fish. Aquat. Sci. **62**: 400–411.

Engstrom, D. R. 2007. Fish respond when the mercury rises. Proc. Natl. Acad. Sci. **104**: 16394–16395. doi:10.1073/pnas.0708273104

Evers, D. C., Y.-J. Han, C. T. Driscoll, and others. 2007. Biological mercury hotspots in the Northeastern United States and Southeastern Canada. BioScience **57**: 29–43. doi:10.1641/B570107

Evers, D. C., J. D. Kaplan, M. W. Meyer, P. S. Reaman, W. E. Braselton, A. Major, N. Burgess, and A. M. Scheuhammer. 1998. Geographic trend in mercury measured in common loon feathers and blood. Environ. Toxicol. Chem. **17**: 173–183. doi:10.1002/etc.5620170206

Fernández-Gómez, C., A. Drott, E. Björn, S. Díez, J. M. Bayona, S. Tesfalidet, A. Lindfors, and U. Skyllberg. 2013. Towards universal wavelength-specific photodegradation rate constants for methyl mercury in humic waters, exemplified by a boreal lake-wetland gradient. Environ. Sci. Technol. 130529101435009. doi:10.1021/es400373s

Filip, D. S., and R. I. Lynn. 1972. Mercury accumulation by the fresh water alga *Selenastrum capricornutum*. Chemosphere **1**: 251–254. doi:10.1016/0045-6535(72)90028-8

Fitzgerald, W. F., D. R. Engstrom, R. P. Mason, and E. A. Nater. 1998. The case for atmospheric mercury contamination in remote Areas. Environ. Sci. Technol. **32**: 1–7. doi:10.1021/es970284w

Fleck, J. A., G. Gill, B. A. Bergamaschi, T. E. C. Kraus, B. D. Downing, and C. N. Alpers. 2014. Concurrent photolytic degradation of aqueous methylmercury and dissolved organic matter. Sci. Total Environ. **484**: 263–275. doi:10.1016/j.scitotenv.2013.03.107

Fleck, J. A., M. Marvin-DiPasquale, C. A. Eagles-Smith, and others. 2016. Mercury and methylmercury in aquatic sediment across western North America. Sci. Total Environ. doi:10.1016/j.scitotenv.2016.03.044

French, T. D., A. J. Houben, J.-P. W. Desforges, and others. 2014. Dissolved organic carbon thresholds affect mercury bioaccumulation in Arctic lakes. Environ. Sci. Technol. **48**: 3162–3168. doi:10.1021/es403849d

Gherini, S. A., R. J. M. Hudson, C. J. Watras, and D. B. Porcella. 1994. Modeling the biogeochemical cycle of mercury in lakes: the mercury cycling model (MCM) and its application to the MTL study lakes. 473–522.

Gilmour, C. C., E. A. Henry, and R. Mitchell. 1992. Sulfate stimulation of mercury methylation in freshwater sediments. Environ. Sci. Technol. **26**: 2281–2287.

Gilmour, C. C., G. S. Riedel, M. C. Ederington, J. T. Bell, G. A. Gill, and M. C. Stordal. 1998. Methylmercury concentrations and production rates across a trophic

gradient in the northern Everglades. Biogeochemistry **40**: 327–345. doi:10.1023/A:1005972708616

Hamelin, S., D. Planas, and M. Amyot. 2015. Mercury methylation and demethylation by periphyton biofilms and their host in a fluvial wetland of the St. Lawrence River (QC, Canada). Sci. Total Environ. **512**–**513**: 464–471. doi:10.1016/j.scitotenv.2015.01.040

Hammerschmidt, C. R., and W. F. Fitzgerald. 2006. Photodecomposition of methylmercury in an Arctic Alaskan lake. Environ. Sci. Technol. **40**: 1212–1216. doi:10.1021/es0513234

Hammerschmidt, C. R., and W. F. Fitzgerald. 2010. Iron-mediated photochemical decomposition of methylmercury in an Arctic Alaskan lake. Environ. Sci. Technol. **44**: 6138–6143. doi:10.1021/es1006934

Harris, R. C., J. W. Rudd, M. Amyot, and others. 2007. Whole-ecosystem study shows rapid fish-mercury response to changes in mercury deposition. Proc. Natl. Acad. Sci. **104**: 16586–16591.

Haverstock, S., T. Sizmur, J. Murimboh, and N. J. O'Driscoll. 2012. Modeling the photo-oxidation of dissolved organic matter by ultraviolet radiation in freshwater lakes: Implications for mercury bioavailability. Chemosphere **88**: 1220–1226. doi:10.1016/j.chemosphere.2012.03.073

Helms, J. R., A. Stubbins, J. D. Ritchie, E. C. Minor, D. J. Kieber, and K. Mopper. 2008. Absorption spectral slopes and slope ratios as indicators of molecular weight, source, and photobleaching of chromophoric dissolved organic matter. Limnol. Oceanogr. **53**: 955.

Hill, J. R., N. J. O'Driscoll, and D. R. S. Lean. 2009. Size distribution of methylmercury associated with particulate and dissolved organic matter in freshwaters. Sci. Total Environ. **408**: 408–414. doi:10.1016/j.scitotenv.2009.09.030

Hines, N. A., and P. L. Brezonik. 2004. Mercury dynamics in a small Northern Minnesota lake: water to air exchange and photoreactions of mercury. Mar. Chem. **90**: 137–149. doi:10.1016/j.marchem.2004.03.013

Hintelmann, H., P. M. Welbourn, and R. D. Evans. 1995. Binding of methylmercury compounds by humic and fulvic acids. Water. Air. Soil Pollut. **80**: 1031–1034. doi:10.1007/BF01189760

Hodson, P. V., K. Norris, M. Berquist, L. M. Campbell, and J. J. Ridal. 2014. Mercury concentrations in amphipods and fish of the Saint Lawrence River (Canada) are

unrelated to concentrations of legacy mercury in sediments. Sci. Total Environ. **494–495**: 218–228. doi:10.1016/j.scitotenv.2014.06.137

Isidorova, A., A. G. Bravo, G. Riise, S. Bouchet, E. Björn, and S. Sobek. 2016. The effect of lake browning and respiration mode on the burial and fate of carbon and mercury in the sediment of two boreal lakes: Carbon and mercury burial. J. Geophys. Res. Biogeosciences **121**: 233–245. doi:10.1002/2015JG003086

Jeremiason, J., J. C. Portner, G. Aiken, K. T. Tran, M. T. Dvorak, A. Hiranaka, and D. Latch. 2015. Photoreduction of Hg(II) and photodemethylation of methylmercury: The key role of thiol sites on dissolved organic matter. Environ. Sci. Process. Impacts. doi:10.1039/C5EM00305A

Kainz, M., M. Lucotte, and C. C. Parrish. 2003. Relationships between organic matter composition and methyl mercury content of offshore and carbon-rich littoral sediments in an oligotrophic lake. Can. J. Fish. Aquat. Sci. **60**: 888–896. doi:10.1139/f03-075

Kainz, M., and A. Mazumder. 2005. Effect of algal and bacterial diet on methyl mercury concentrations in zooplankton. Environ. Sci. Technol. **39**: 1666–1672. doi:10.1021/es049119o

Kerin, E. J., C. C. Gilmour, E. Roden, M. T. Suzuki, J. D. Coates, and R. P. Mason. 2006. Mercury methylation by dissimilatory iron-reducing bacteria. Appl. Environ. Microbiol. **72**: 7919–7921. doi:10.1128/AEM.01602-06

Kidd, K., M. Clayden, and T. Jardine. 2011. Bioaccumulation and biomagnification of mercury through food webs, p. 453–499. *In* G. Liu, Y. Cai, and N. O'Driscoll [eds.], Environmental Chemistry and Toxicology of Mercury. John Wiley & Sons, Inc.

Kim, M.-K., A.-Y. Won, and K.-D. Zoh. 2017. Effects of Molecular Size Fraction of DOM on Photodegradation of Aqueous Methylmercury. Chemosphere. doi:10.1016/j.chemosphere.2017.02.033

Kim, M.-K., and K.-D. Zoh. 2013. Effects of natural water constituents on the photo-decomposition of methylmercury and the role of hydroxyl radical. Sci. Total Environ. **449**: 95–101. doi:10.1016/j.scitotenv.2013.01.039

Klapstein, S. J., S. E. Ziegler, D. A. Risk, and N. J. O'Driscoll. 2016. Quantifying the effects of photoreactive dissolved organic matter on methylmercury photodemethylation rates in freshwaters. Environ. Toxicol. Chem. **9999**: 1–10. doi:10.1002/etc.3690

Krabbenhoft, D. P., M. L. Olson, J. F. Dewild, D. W. Clow, R. G. Striegl, M. M. Dornblaser, and P. VanMetre. 2002. Mercury loading and methylmercury production and cycling in high-altitude lakes from the Western United States. Water Air Soil Pollut. Focus **2**: 233–249. doi:10.1023/A:1020162811104

Lavoie, R. A., T. D. Jardine, M. M. Chumchal, K. A. Kidd, and L. M. Campbell. 2013. Biomagnification of mercury in aquatic food webs: A worldwide meta-analysis. Environ. Sci. Technol. **47**: 13385–13394. doi:10.1021/es403103t

Lehnherr, I. 2014. Methylmercury biogeochemistry: a review with special reference to Arctic aquatic ecosystems. Environ. Rev. 1–15. doi:10.1139/er-2013-0059

Lehnherr, I., and V. L. St Louis. 2009. Importance of ultraviolet radiation in the photodemethylation of methylmercury in freshwater ecosystems. Environ. Sci. Technol. **43**: 5692–5698.

Li, Y., Y. Mao, G. Liu, G. Tachiev, D. Roelant, X. Feng, and Y. Cai. 2010. Degradation of methylmercury and its effects on mercury distribution and cycling in the Florida Everglades. Environ. Sci. Technol. **44**: 6661–6666. doi:10.1021/es1010434

Li, Y., Y. Yin, G. Liu, G. Tachiev, D. Roelant, G. Jiang, and Y. Cai. 2012. Estimation of the major source and sink of methylmercury in the Florida Everglades. Environ. Sci. Technol. **46**: 5885–5893. doi:10.1021/es204410x

Lin, C.-C., N. Yee, and T. Barkay. 2011. Microbial transformations in the mercury cycle, p. 155–191. *In* G. Liu, Y. Cai, and N. O'Driscoll [eds.], Environmental Chemistry and Toxicology of Mercury. John Wiley & Sons, Inc.

Lindberg, S., R. Bullock, R. Ebinghaus, and others. 2007. A synthesis of progress and uncertainties in attributing the sources of mercury in deposition. AMBIO J. Hum. Environ. **36**: 19–33. doi:10.1579/0044-7447(2007)36[19:ASOPAU]2.0.CO;2

Lindqvist, O., K. Johansson, L. Bringmark, and others. 1991. Mercury in the Swedish environment — Recent research on causes, consequences and corrective methods. Water. Air. Soil Pollut. **55**: xi-261. doi:10.1007/BF00542429

Little, M. E., N. M. Burgess, H. G. Broders, and L. M. Campbell. 2015. Distribution of mercury in archived fur from little brown bats across Atlantic Canada. Environ. Pollut. **207**: 52–58. doi:10.1016/j.envpol.2015.07.049

Luo, H.-W., X. Yin, A. M. Jubb, and others. 2016. Photochemical reactions between mercury (Hg) and dissolved organic matter decrease Hg bioavailability and methylation. Environ. Pollut. doi:10.1016/j.envpol.2016.10.099

Marcarelli, A. M., C. V. Baxter, M. M. Mineau, and R. O. Hall. 2011. Quantity and quality: Unifying food web and ecosystem perspectives on the role of resource subsidies in freshwaters. Ecology **92**: 1215–1225. doi:10.1890/10-2240.1

Marvin-DiPasquale, M. C., and R. S. Oremland. 1998. Bacterial methylmercury degradation in Florida Everglades peat sediment. Environ. Sci. Technol. **32**: 2556–2563. doi:10.1021/es971099l

Mason, R. P., J.-M. Laporte, and S. Andres. 2000. Factors controlling the bioaccumulation of mercury, methylmercury, arsenic, selenium, and cadmium by freshwater invertebrates and fish. Arch. Environ. Contam. Toxicol. **38**: 283–297. doi:10.1007/s002449910038

Mason, R. P., and A. L. Lawrence. 1999. Concentration, distribution, and bioavailability of mercury and methylmercury in sediments of Baltimore Harbor and Chesapeake Bay, Maryland, USA. Environ. Toxicol. Chem. **18**: 2438–2447.

Mason, R. P., J. R. Reinfelder, and F. M. M. Morel. 1996. Uptake, toxicity, and trophic transfer of mercury in a coastal diatom. Environ. Sci. Technol. **30**: 1835–1845. doi:10.1021/es950373d

Mazrui, N. M., S. Jonsson, S. Thota, J. Zhao, and R. P. Mason. 2016. Enhanced availability of mercury bound to dissolved organic matter for methylation in marine sediments. Geochim. Cosmochim. Acta. doi:10.1016/j.gca.2016.08.019

McClain, M. E., E. W. Boyer, C. L. Dent, and others. 2003. Biogeochemical hot spots and hot moments at the interface of terrestrial and aquatic ecosystems. Ecosystems **6**: 301–312.

Meng, F.-R., P. Arp, A. Sangster, and others. 2005. Modeling dissolved organic carbon, total and methyl mercury in Kejimkujik freshwaters, p. 1–19. *In* Mercury cycling in a wetland-dominated ecosystem: a multidisciplinary study. Society of Environmental Toxicology and Chemistry (SETAC).

Mergler, D., H. A. Anderson, L. H. M. Chan, K. R. Mahaffey, M. Murray, M. Sakamoto, A. H. Stern, and Panel on Health Risks and Toxicological Effects of Methylmercury. 2007. Methylmercury exposure and health effects in humans: A worldwide concern. Ambio J. Hum. Environ. **36**: 3–11.

Miskimmin, B. M. 1991. Effect of natural levels of dissolved organic carbon (DOC) on methyl mercury formation and sediment-water partitioning. Bull. Environ. Contam. Toxicol. **47**: 743–750. doi:10.1007/BF01701144

Miskimmin, B. M., J. W. M. Rudd, and C. A. Kelly. 1992. Influence of dissolved organic carbon, pH, and microbial respiration rates on mercury methylation and

demethylation in lake water. Can. J. Fish. Aquat. Sci. **49**: 17–22. doi:10.1139/f92-002

Mitchell, C. P. J., B. A. Branfireun, and R. K. Kolka. 2008. Spatial characteristics of net methylmercury production hot spots in peatlands. Environ. Sci. Technol. **42**: 1010–1016. doi:10.1021/es0704986

Moran, M. A., and R. E. Hodson. 1990. Bacterial production on humic and nonhumic components of dissolved organic carbon. Limnol. Oceanogr. **35**: 1744–1756.

Morel, F. M. M., A. M. L. Kraepiel, and M. Amyot. 1998. The chemical cycle and bioaccumulation of mercury. Annu. Rev. Ecol. Syst. **29**: 543–566.

Morris, D. P., H. Zagarese, C. E. Williamson, E. G. Balseiro, B. R. Hargreaves, B. Modenutti, R. Moeller, and C. Queimalinos. 1995. The attenuation of solar UV radiation in lakes and the role of dissolved organic carbon. Limnol. Oceanogr. **40**: 1381–1391.

Munthe, J., R. A. (Drew) Bodaly, B. A. Branfireun, and others. 2007. Recovery of mercury-contaminated fisheries. AMBIO J. Hum. Environ. **36**: 33–44. doi:10.1579/0044-7447(2007)36[33:ROMF]2.0.CO;2

Ni, B., J. R. Kramer, R. A. Bell, and N. H. Werstiuk. 2006. Protonolysis of the Hg−C bond of chloromethylmercury and dimethylmercury. A DFT and QTAIM study. J. Phys. Chem. A **110**: 9451–9458. doi:10.1021/jp061852+

Nriagu, J. O. 1993. Legacy of mercury pollution. Nature **363**: 589–589. doi:10.1038/363589a0

O'Driscoll, N. J., and R. D. Evans. 2000. Analysis of methyl mercury binding to freshwater humic and fulvic acids by gel permeation chromatography/hydride generation ICP-MS. Environ. Sci. Technol. **34**: 4039–4043. doi:10.1021/es0009626

O'Driscoll, N. J., S. D. Siciliano, D. Peak, R. Carignan, and D. R. S. Lean. 2006. The influence of forestry activity on the structure of dissolved organic matter in lakes: Implications for mercury photoreactions. Sci. Total Environ. **366**: 880–893. doi:10.1016/j.scitotenv.2005.09.067

Oremland, R. S., C. W. Culbertson, and M. R. Winfrey. 1991. Methylmercury decomposition in sediments and bacterial cultures: Involvement of methanogens and sulfate reducers in oxidative demethylation. Appl. Environ. Microbiol. **57**: 130–137.

Osburn, C. L., L. Retamal, and W. F. Vincent. 2009. Photoreactivity of chromophoric dissolved organic matter transported by the Mackenzie River to the Beaufort Sea. Mar. Chem. **115**: 10–20. doi:10.1016/j.marchem.2009.05.003

Parks, J. M., A. Johs, M. Podar, and others. 2013. The genetic basis for bacterial mercury methylation. Science **339**: 1332–1335. doi:10.1126/science.1230667

Pickhardt, P. C., and N. S. Fisher. 2007. Accumulation of inorganic and methylmercury by freshwater phytoplankton in two contrasting water bodies. Environ. Sci. Technol. **41**: 125–131. doi:10.1021/es060966w

Pickhardt, P. C., C. L. Folt, C. Y. Chen, B. Klaue, and J. D. Blum. 2005. Impacts of zooplankton composition and algal enrichment on the accumulation of mercury in an experimental freshwater food web. Sci. Total Environ. **339**: 89–101. doi:10.1016/j.scitotenv.2004.07.025

Podar, M., C. C. Gilmour, C. C. Brandt, and others. 2015. Global prevalence and distribution of genes and microorganisms involved in mercury methylation. Sci. Adv. **1**: e1500675. doi:10.1126/sciadv.1500675

Poste, A. E., H. F. V. Braaten, H. A. de Wit, K. Sørensen, and T. Larssen. 2015. Effects of photodemethylation on the methylmercury budget of boreal Norwegian lakes. Environ. Toxicol. Chem. n/a-n/a. doi:10.1002/etc.2923

Poulin, B. A., J. N. Ryan, and G. R. Aiken. 2014. Effects of iron on optical properties of dissolved organic matter. Environ. Sci. Technol. **48**: 10098–10106. doi:10.1021/es502670r

Qian, Y., X. Yin, H. Lin, B. Rao, S. C. Brooks, L. Liang, and B. Gu. 2014. Why dissolved organic matter enhances photodegradation of methylmercury. Environ. Sci. Technol. Lett. **1**: 426–431. doi:10.1021/ez500254z

Rasmussen, J. B., D. J. Rowan, D. R. S. Lean, and J. H. Carey. 1990. Food chain structure in Ontario lakes determines PCB levels in lake trout (*Salvelinus namaycush*) and other pelagic fish. Can. J. Fish. Aquat. Sci. **47**: 2030–2038. doi:10.1139/f90-227

Reinfelder, J. R., and N. S. Fisher. 1991. The assimilation of elements ingested by marine copepods. Science **251**: 794–796.

Rudd, J. W. M. 1995. Sources of methyl mercury to freshwater ecosystems: A review. Water. Air. Soil Pollut. **80**: 697–713. doi:10.1007/BF01189722

Schaefer, J. K., and F. M. M. Morel. 2009. High methylation rates of mercury bound to cysteine by *Geobacter sulfurreducens*. Nat. Geosci. **2**: 123–126. doi:10.1038/ngeo412

Schaefer, J. K., A. Szczuka, and F. M. M. Morel. 2014. Effect of divalent metals on Hg(II) uptake and methylation by bacteria. Environ. Sci. Technol. **48**: 3007–3013. doi:10.1021/es405215v

Schartup, A. T., P. H. Balcom, A. L. Soerensen, K. J. Gosnell, R. S. D. Calder, R. P. Mason, and E. M. Sunderland. 2015. Freshwater discharges drive high levels of methylmercury in Arctic marine biota. Proc. Natl. Acad. Sci. **112**: 11789–11794. doi:10.1073/pnas.1505541112

Scully, N. M., and D. R. S. Lean. 1994. The attenuation of ultraviolet radiation in temperate lakes. Erg Limnol **43**: 135–144.

Sellers, P., C. A. Kelly, and J. W. M. Rudd. 2001. Fluxes of methylmercury to the water column of a drainage lake: The relative importance of internal and external sources. Limnol. Oceanogr. **46**: 623–631. doi:10.4319/lo.2001.46.3.0623

Sellers, P., C. A. Kelly, J. W. M. Rudd, and A. R. MacHutchon. 1996. Photodegradation of methylmercury in lakes. Nature **380**: 694–697. doi:10.1038/380694a0

Sherr, E., and B. Sherr. 1988. Role of microbes in pelagic food webs: A revised concept. Limnol. Oceanogr. **33**: 1225–1227. doi:10.4319/lo.1988.33.5.1225

Singer, M. B., L. R. Harrison, P. M. Donovan, J. D. Blum, and M. Marvin-DiPasquale. 2016. Hydrologic indicators of hot spots and hot moments of mercury methylation potential along river corridors. Sci. Total Environ. **568**: 697–711. doi:10.1016/j.scitotenv.2016.03.005

Stewart, A. R., M. K. Saiki, J. S. Kuwabara, C. N. Alpers, M. Marvin-DiPasquale, and D. P. Krabbenhoft. 2008. Influence of plankton mercury dynamics and trophic pathways on mercury concentrations of top predator fish of a mining-impacted reservoir. Can. J. Fish. Aquat. Sci. **65**: 2351–2366. doi:10.1139/F08-140

Strock, K. E., J. E. Saros, S. J. Nelson, S. D. Birkel, J. S. Kahl, and W. H. McDowell. 2016. Extreme weather years drive episodic changes in lake chemistry: implications for recovery from sulfate deposition and long-term trends in dissolved organic carbon. Biogeochemistry **127**: 353–365. doi:10.1007/s10533-016-0185-9

Sunda, W. G., and S. A. Huntsman. 1998. Processes regulating cellular metal accumulation and physiological effects: Phytoplankton as model systems. Sci. Total Environ. **219**: 165–181. doi:10.1016/S0048-9697(98)00226-5

Tai, C., Y. Li, Y. Yin, L. J. Scinto, G. Jiang, and Y. Cai. 2014. Methylmercury photodegradation in surface water of the Florida Everglades: Importance of

dissolved organic matter-methylmercury complexation. Environ. Sci. Technol. **48**: 7333–7340. doi:10.1021/es500316d

Tossell, J. A. 1998. Theoretical study of the photodecomposition of methyl Hg complexes. J. Phys. Chem. A **102**: 3587–3591. doi:10.1021/jp980244u

Trudel, M., and J. B. Rasmussen. 1997. Modeling the elimination of mercury by fish. Environ. Sci. Technol. **31**: 1716–1722. doi:10.1021/es960609t

Tsui, M. T. K., J. C. Finlay, and E. A. Nater. 2009. Mercury bioaccumulation in a stream network. Environ. Sci. Technol. **43**: 7016–7022. doi:10.1021/es901525w

Tsui, M. T. K., and W.-X. Wang. 2004. Uptake and elimination routes of inorganic mercury and methylmercury in *Daphnia magna*. Environ. Sci. Technol. **38**: 808–816. doi:10.1021/es034638x

Ullrich, S. M., T. W. Tanton, and S. A. Abdrashitova. 2001. Mercury in the aquatic environment: A review of factors affecting methylation. Crit. Rev. Environ. Sci. Technol. **31**: 241–293. doi:10.1080/20016491089226

Vander Zanden, M. J., G. Cabana, and J. B. Rasmussen. 1997. Comparing trophic position of freshwater fish calculated using stable nitrogen isotope ratios ($\delta^{15}N$) and literature dietary data. Can. J. Fish. Aquat. Sci. **54**: 1142–1158. doi:10.1139/f97-016

Walters, D. M., K. M. Fritz, and R. R. Otter. 2008. The dark side of subsidies: Adult stream insects export organic contaminants to riparian predators. Ecol. Appl. **18**: 1835–1841. doi:10.1890/08-0354.1

Walters, D. M., T. D. Jardine, B. S. Cade, K. A. Kidd, D. C. G. Muir, and P. Leipzig-Scott. 2016. Trophic magnification of organic chemicals: A global synthesis. Environ. Sci. Technol. doi:10.1021/acs.est.6b00201

Watras, C. J., R. C. Back, S. Halvorsen, R. J. M. Hudson, K. A. Morrison, and S. P. Wente. 1998. Bioaccumulation of mercury in pelagic freshwater food webs. Sci. Total Environ. **219**: 183–208. doi:10.1016/S0048-9697(98)00228-9

Watras, C. J., and N. S. Bloom. 1992. Mercury and methylmercury in individual zooplankton: Implications for bioaccumulation. Limnol. Oceanogr. **37**: 1313–1318.

Weishaar, J. L., G. R. Aiken, B. A. Bergamaschi, M. S. Fram, R. Fujii, and K. Mopper. 2003. Evaluation of specific ultraviolet absorbance as an indicator of the chemical composition and reactivity of dissolved organic carbon. Environ. Sci. Technol. **37**: 4702–4708. doi:10.1021/es030360x

Wetzel, R. G. 2001. 23 - Detritus: Organic carbon and ecosystem metabolism, p. 731–783. *In* R.G. Wetzel [ed.], Limnology (Third Edition). Academic Press.

de Wit, H. A., A. Granhus, M. Lindholm, M. J. Kainz, Y. Lin, H. F. V. Braaten, and J. Blaszczak. 2014. Forest harvest effects on mercury in streams and biota in Norwegian boreal catchments. For. Ecol. Manag. **324**: 52–63. doi:10.1016/j.foreco.2014.03.044

de Wit, H. A., M. J. Kainz, and M. Lindholm. 2012. Methylmercury bioaccumulation in invertebrates of boreal streams in Norway: Effects of aqueous methylmercury and diet retention. Environ. Pollut. **164**: 235–241. doi:10.1016/j.envpol.2012.01.041

de Wit, H. A., S. Valinia, G. A. Weyhenmeyer, and others. 2016. Current browning of surface waters will Be further promoted by wetter climate. Environ. Sci. Technol. Lett. doi:10.1021/acs.estlett.6b00396

Wyn, B., K. A. Kidd, N. M. Burgess, and R. A. Curry. 2009. Mercury biomagnification in the food webs of acidic lakes in Kejimkujik National Park and National Historic Site, Nova Scotia. Can. J. Fish. Aquat. Sci. **66**: 1532–1545. doi:10.1139/F09-097

Wyn, B., K. A. Kidd, N. M. Burgess, R. A. Curry, and K. R. Munkittrick. 2010. Increasing mercury in yellow perch at a hotspot in Atlantic Canada, Kejimkujik National Park. Environ. Sci. Technol. **44**: 9176–9181.

Xun, L., N. E. R. Campbell, and J. W. M. Rudd. 1987. Measurements of specific rates of net methyl mercury production in the water column and surface sediments of acidified and circumneutral lakes. Can. J. Fish. Aquat. Sci. **44**: 750–757. doi:10.1139/f87-091

Zepp, R. G., P. F. Schlotzhauer, and R. M. Sink. 1985. Photosensitized transformations involving electronic energy transfer in natural waters: role of humic substances. Environ. Sci. Technol. **19**: 74–81. doi:10.1021/es00131a008

Zhang, D., Y. Yin, Y. Li, Y. Cai, and J. Liu. 2016. Critical role of natural organic matter in photodegradation of methylmercury in water: Molecular weight and interactive effects with other environmental factors. Sci. Total Environ. doi:10.1016/j.scitotenv.2016.10.222

Zhang, T., and H. Hsu-Kim. 2010. Photolytic degradation of methylmercury enhanced by binding to natural organic ligands. Nat. Geosci. **3**: 473–476. doi:10.1038/ngeo892

CO-AUTHORSHIP STATEMENT

Initial ideas for the project were proposed by Dr. Nelson O'Driscoll in response to my interest in addressing a research question of importance to Atlantic Canada, specifically with a Nova Scotia focus and application. The practical aspects of the research were performed by myself, under the direct supervision of Dr. David Risk and then Dr. Nelson O'Driscoll, and the remote supervision of Dr. Susan Ziegler. I designed, carried out, and collected samples for each field campaign in 2013 (June, August, October, November), 2014 (May, June, August, September, December) and 2015 (February, April, May, June, August, October) in Kejimkujik National Park, NS, Canada. This location was chosen as a field site due to the mercury sensitive characteristics of the ecosystem and the resultant long studied history of elevated mercury concentrations in organisms. On each field visit an assistant accompanied me from Memorial University of Newfoundland, St. Francis Xavier University, Dalhousie University, Acadia University, or an individual with no professional research affiliation. These field assistants were essential to sample collection however they did not contribute conceptually to project design. I independently developed and carried out each set of laboratory experiments and field studies and performed the laboratory analyses to acquire the data presented in this thesis, with analytical equipment consultation from Dr. Erin Mann. Full supervisory committee meetings were held at minimum once per academic year to discuss experimental design, corresponding results, and steps for moving forward with data interpretation and writing.

Once each experimental dataset was collected, interpreted, and discussed via supervisory committee meetings and/or email correspondence with all co-authors I

prepared manuscript drafts that were then shared with Dr. O'Driscoll for initial feedback before being circulated to Dr. Ziegler and Dr. Risk. Feedback, concerns, and suggested revisions from all co-authors are incorporated into each data chapter of this thesis. Anonymous reviewer feedback is also incorporated into Chapter 3.

Chapter 2 : PHOTOREACTIVITY OF DISSOLVED ORGANIC MATTER IN THE LAKES OF KEJIMKUJIK NATIONAL PARK NOVA SCOTIA: IMPLICATIONS FOR METHYLMERCURY PHOTOCHEMISTRY

Sara J. Klapstein[a,b,c], Susan E. Ziegler[a], David A. Risk[b], Nelson J. O'Driscoll[c]

[a]Department of Environmental Science, Memorial University of Newfoundland, St. John's NL, Canada

[b]Department of Earth Sciences, St. Francis Xavier University, Antigonish NS, Canada

[c]Department of Earth and Environmental Science, Acadia University, Wolfville NS, Canada

Abstract

Methylmercury (MeHg) bioaccumulation is a growing concern in many ecosystems worldwide. The absorption of solar radiation by dissolved organic matter (DOM) and other photoreactive ligands can convert MeHg into a less toxic form of mercury through photodemethylation. In this study, measurement of spectral changes and photoreactivity of DOM were tracked in order to assess the potential for controlling photoreactions involving MeHg. Water samples collected from a series of lakes in southwestern Nova Scotia in June, August, and September were exposed to controlled ultraviolet-A (UV-A) radiation for up to 24 hours. Ultraviolet-A photoreactivity, defined here as the loss of absorbance at 350 nm following constant UV irradiation over a 24 h period, was highly dependent on the initial DOM concentration in lake water (r^2=0.94). This trend was consistent over time; both DOM concentration and UV-A photoreactivity increased from summer into fall across lakes. Lake *in situ* MeHg concentration was positively correlated with DOM concentration and likely catchment transport in summer (r=0.77) but was not later in the year for the other sampling seasons. A 3-year dataset (2013, 2014, and 2015) from the 6 study lakes showed that DOM concentrations were significantly positively correlated with Fe concentrations (r=0.91) and MeHg concentrations (r=0.51). Both DOM and Fe followed clear seasonal patterns across years but the inter-annual variation and correlation overrode any quantifiable seasonal relationship with MeHg. Lakes with higher DOM photoreactivity tended to have higher MeHg concentrations and the correlation between MeHg sources (DOM-Fe inputs) are likely to overwhelm losses of MeHg via photodemethylation in high DOM lakes. These results highlight the seasonal complexity of DOM-mercury interactions and the need for further experimentation examining DOM

photoreactivity and MeHg availability in natural waters in the future with climate perturbations.

1. INTRODUCTION

The amount of methylmercury (MeHg) available for uptake at the base of the food web is partially controlled by the balance between methylation and demethylation reactions (Xun et al. 1987). While a lot of research has focused on methylation processes, the demethylation processes are not well constrained in natural waters. MeHg can be demethylated both biotically and abiotically, however in water columns of freshwater lakes the primary pathway for demethylation has been identified as photodemethylation by solar radiation (Sellers et al. 1996). Photodegradation experiments have evaluated MeHg photodemethylation rate constants both at water body surfaces (Sellers et al. 1996; Lehnherr et al. 2012a) and within lake water columns (Krabbenhoft et al. 2002; Zhang and Hsu-Kim 2010; Lehnherr et al. 2012b) using bottle incubations at various depths. Rate constants of this photochemical process have been quantified for several specific ecosystems (ranging from 0.006 to 0.015 E^{-1} m^2 for photon flux from 330 – 700 nm) (Black et al. 2012). However, less attention has been given to the photochemically active components themselves, such as the chromophoric portions of dissolved organic matter (DOM) and dissolved ions present within these ecosystems (Fleck et al. 2014; Klapstein et al. 2016), and how these constituents may also interact with solar radiation and mercury.

When considering the fate of MeHg in freshwater lakes, it is important to address how MeHg may be influenced by indirect or direct reactions with dissolved entities. Radiation attenuation by chromophoric DOM and iron (Fe) will reduce the depth of solar radiation penetration as well as the spectral distribution of radiation (Scully and Lean 1994; Poulin et al. 2014) and therefore can restrict photoreactions, including those that

involve MeHg to shallow water layers (Li et al. 2010). Dissolved organic matter serves many functions in freshwater lake ecosystems. Along with being a significant carbon pool, DOM is a microbial energy and nutrient source (De Lange et al. 2003), contains binding sites for cations such as mercury and other metals (O'Driscoll and Evans 2000; Ravichandran 2004), and is photoreactive, meaning some portions of DOM (including Fe complexes) will absorb solar radiation, particularly ultraviolet (UV) radiation and visible wavebands, resulting in visibly brown or dark waters (Bertilsson and Tranvik 2000; Osburn et al. 2009; Granéli et al. 1996). A study from 65 sites across North America has shown that more than 85% of the between-lake variation in UV attenuation may be attributed to bulk DOM concentrations alone (Morris et al. 1995). The depth of penetration for UV radiation has been shown to vary substantially between low carbon temperate lakes (35-150% of the mixed layer depth throughout a year; DOM=1.09 mg C L^{-1}; 41-41°N) and higher carbon lakes (4-8% of the mixed layer depth; DOM=4.80-5.28 mg C L^{-1}) (Morris and Hargreaves 1997). Even though both UV-A (320-400 nm) and UV-B (280-320 nm) radiation have been shown to be important drivers of the photomineralization of DOM (Morris and Hargreaves 1997), in high DOM lakes (DOM=3.3 –12.3 mg C L^{-1}) the flux of UV-A and particularly UV-B radiation in water columns can be quickly quenched in surface waters (Haverstock et al. 2012). UV-A radiation may be the main driver of MeHg photochemistry in lakes (Lehnherr and St Louis 2009; Kim and Zoh 2013). In waters that have a large contribution of chromophoric DOM, the potential for photodemethylation of MeHg may be limited in space to the top layer of the lake where UV-A radiation is present and limited in time when UV-A is

diurnally and seasonally sufficient within the water column. The impact of photoreactive DOM on MeHg photoreactions across seasons is not clear.

Correlation between concentrations of total mercury, MeHg, and dissolved organic carbon (DOC - the portion of DOM commonly quantified) are repeatedly reported in the literature, however sometimes this relationship is positive and sometimes negative (Ravichandran 2004; Meng et al. 2005; Li et al. 2010; Kim and Zoh 2013). This inconsistency highlights the need for more research regarding the relationships between *in situ* lake water photochemical characteristics, such as DOM photoreactivity, in order to gain insight into factors governing MeHg concentrations. To begin to address this research gap, we quantified UV-A photoreactivity (absorption loss at 350 nm) and DOM loss (photomineralization to inorganic carbon) from water collected multiple times per year from 6 lakes in southwestern Nova Scotia and exposed to UV-A radiation (320-400 nm) in a controlled experimental environment. We hypothesized that if there was a reduction of UV radiation entering lakes from summer through to fall that lead to a decrease of associated losses of chromophoric structures from *in situ* DOM, then we predicted that UV-A photoreactivity of lake water would increase over the sampling season. We also predicted that higher concentrations of photoreactive DOM would facilitate an increased rate of photoreactions involving DOM, and that these reactions could interact with MeHg in the lakes. As such, we expected that UV-A photoreactivity would be negatively correlated with MeHg concentration.

2. MATERIALS AND METHODS

2.1 Water collection and monitoring

Located in southwestern Nova Scotia, Canada, Kejimkujik National Park (44.399°N, 65.218°W) is a temperate region characterized by mixed coniferous and deciduous vegetation, high wetland cover, and an abundance of freshwater lakes. The park's bedrock is split between the Meguma Group of the Cambro-Ordovician and South Mountain Batholith, both of which are known to contain mercury and are associated with low alkalinity bedrock and soils (Smith et al. 2005). Six lakes with DOM concentrations ranging from 3 to 26 mg C L^{-1} were sampled over a 3-day period in each of summer (late-June; Week 25), late-summer (mid-August; Week 33), and fall (September; Week 40) in 2013. Lakes sampled included: Big Dam East Lake (BDE), Puzzle Lake (PUZ), North Cranberry Lake (NC), Peskawa Lake (PES), Big Dam West Lake (BDW), and Pebbleloggitch Lake (PEB) (Figure 2.1). At the time of sampling diffuse integrated solar radiation attenuation coefficients with depth (K_d) were calculated for each lake using the slope of the natural log of irradiance intensity and depth (Scully and Lean 1994). We measured diffuse integrated irradiance intensity for UV-A at the center of each lake every 5 cm over a minimum water column depth of 30 cm using an Ocean Optics USB-4000 spectrometer with fiber optic cable (3900 μm diameter; 10 m length) and a cosine corrected watertight probe with diffuse integrator. The instrument was calibrated with a National Institute for Standards and Technology (NIST) compliant and traceable calibration light source (Ocean Optics Inc. DH-2000 UV-VIS NIR).

Water was collected in amber glass 1.0 L bottles with PTFE lined caps at 30 cm depth from the side of a canoe in the middle of each lake. Bottles were pre-cleaned with 20% HCl and triple-rinsed with Milli-Q water before being rinsed three times with lake water, filled with zero headspace, and stored in a dark cooler with ice during transportation back to the lab for analysis. All water was vacuum filtered with 0.45 μm hydrophilic polyethersulfone Supor Membrane Disc Filters (Pall), recommended through rigorous testing for DOC leaching by Karanfil et al. (2003), and refrigerated in the dark for less than 48 hours before experiment initiation. We also collected and filtered water samples for DOM, MeHg, and Fe concentrations in each sampling season of 2014 and 2015.

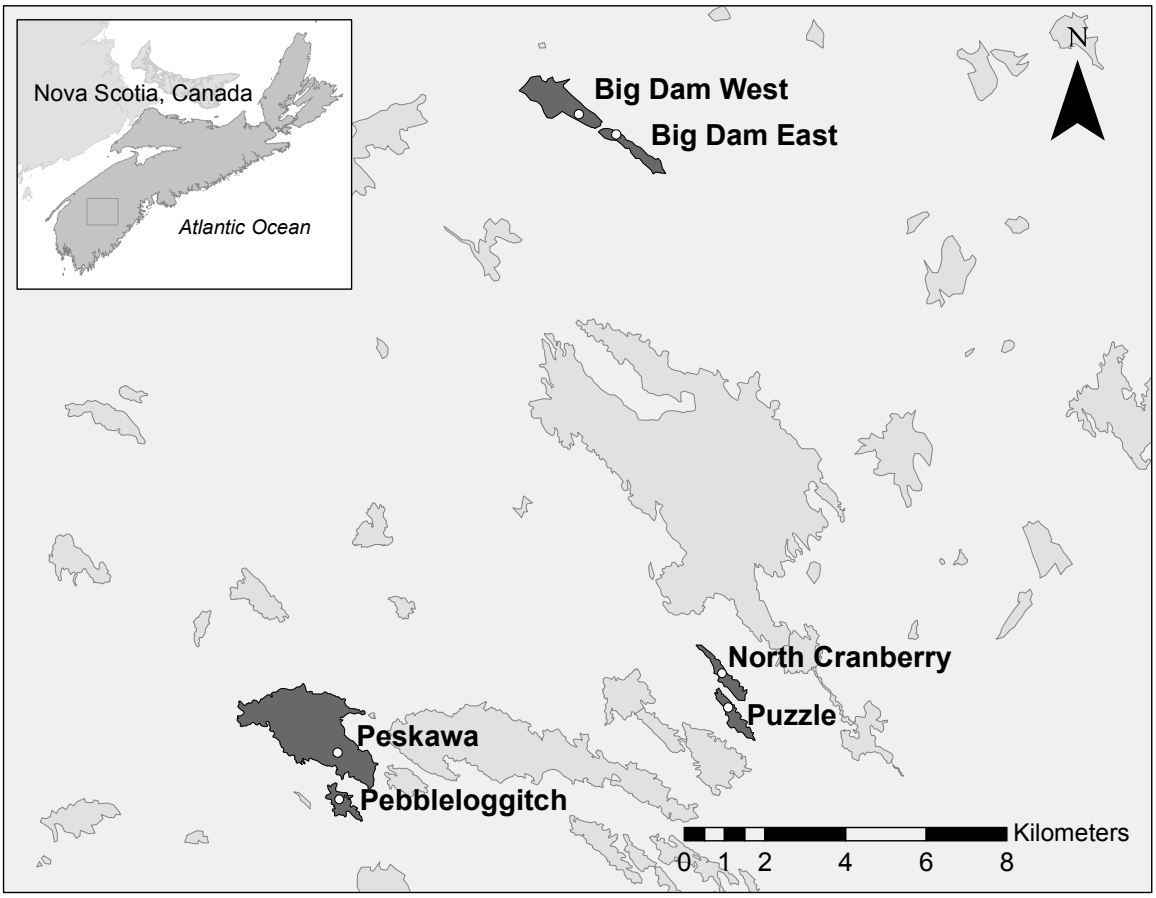

Figure 2.1 Map showing location of lakes sampled (dark grey) in Kejimkujik National Park, Nova Scotia with specific sampling locations as white circles.

2.2 Chemical analyses

All water samples from each lake and collection period were analyzed for concentrations of DOM, dissolved ions, and MeHg. Dissolved organic matter concentrations were measured as the difference between total dissolved carbon and dissolved inorganic carbon by acidic oxidation and thermal oxidation with non-dispersive infrared detection respectively using a Shimadzu TOC-V CPH/TOC-CPN Total Organic Carbon Analyzer with an ASI-V autosampler. Samples were blank corrected and 5 ppm inorganic and 5 ppm total carbon check standards were run to ensure the internal

instrument calibration within 5% of expected concentration range. Total Fe concentrations were measured on a PerkinElmer Inductively Coupled Plasma-Mass Spectrometer following acidification to 1% HNO_3. MeHg water samples were acidified to 1% HCl and analyzed on a Model III Brooks Rand Spectrophotometer following distillation using aqueous ethylation, purge and trap, and cold vapour atomic fluorescence spectrometry (EPA Method 1630). Six-point calibration curves were analyzed each day. All samples were blank corrected (Milli-Q) and samples were distillation recovery corrected if recoveries were outside of 100 ± 10%. Check standards (repeated 50 pg standards) were analyzed throughout each daily run to ensure accuracy and precision of the instrument and the limit of detection was calculated as 3x the standard deviation of repeated blanks (LOD=1.58 pg; n=9).

2.3 Experiments to characterize photoreactive DOM

Filtered water subsamples from each lake collection in 2013 were placed in sealed 9.5 mL quartz vials on a rotating Luzchem carousel in a Luzchem LZC-5 photoreactor for up to 24 hours and exposed to 47 W m^{-2} of constant UV-A radiation. These irradiations were comparable to total cumulative UV-A exposure of less than 1 week, including diurnal dark periods, at the field site, at 20°C temperature. The path length for each vial was 1.0 cm to avoid attenuation effects within each vial. Therefore, UV-A radiation was not limited in these incubations by internal sample self-shading. UV-A exposure was determined inside the quartz vials using the Ocean Optics USB 4000 and fiber optic probe described above. Triplicate vials were removed from the photoreactor at 0, 4, 8, 12, 16, 20, and 24 hours, equivalent to 0, 0.64, 1.29, 1.93, 2.57, 3.21, and 3.86 kJ cumulative

UV-A exposure in each vial. Triplicate dark sample controls for each lake were analyzed for absorbance and DOM concentration at the 24-hour mark to test for microbial degradation of DOM. Absorbance spectra from 200-800 nm were obtained for each subsample using an Ultrospec 3100pro UV/Vis spectrophotometer with a 1.0 cm quartz cuvette and with Milli-Q water as a reference blank. Absorption coefficients were calculated as the absorbance (A) at a specific wavelength (i.e. 350 nm) divided by the path length (0.01 m) multiplied by 2.303 ((A_{350} = 2.303 x (A/L)); see Kirk et al. (1994)). The contribution of Fe to the overall water absorptivity was calculated for each water sample using the method outlined in Poulin et al. (2014). Specific UV absorbance at 350 nm ($SUVA_{350}$) was calculated using the absorbance at 350 nm divided by the DOM concentration. Spectral slopes ($S_{275\text{-}295\ nm}$, $S_{350\text{-}400\ nm}$) were calculated using linear regressions of log transformed absorbance across 275-295 and 350-400 nm, respectively. The spectral ratio (S_R) was then calculated as the $S_{275\text{-}295\ nm}$:$S_{350\text{-}400\ nm}$ and the S_R was used as an index of the relative amount of high molecular weight to low molecular weight chromophoric DOM (Helms et al. 2008). In this study we define UV-A photoreactivity as the loss of absorbance at 350 nm in our controlled incubation experiments.

2.4 Data analyses

Linear regressions were used to determine whether there was a significant reduction in DOM concentration and absorbance between initial lake water and irradiated experiment lake water. Confidence intervals were calculated to determine if rates of DOM loss varied between lakes and across season. To test whether shifts in S_R were significantly different between lakes and collection month, a two-way ANOVA with

Tukey's Test was applied to the data. We used Pearson's correlations to determine if DOM concentration or DOM photoreactivity were correlated with MeHg concentration and linear regression to determine whether photoreactivity varied with changing DOM concentration. All tests of significance were performed in R version 3.0.1 (The R Foundation for Statistical Computing Platform) at 95% confidence (α=0.05) unless otherwise stated.

3. RESULTS AND DISCUSSION

3.1 DOM concentration is a good predictor of its UV-A photoreactivity

UV-A photoreactivity of DOM will inevitably affect bound MeHg through photoreactions and therefore the DOM must be critically studied from an optical perspective. We quantified lake water UV-A photoreactivity using 24-hour experiments by exposing filtered water samples to controlled UV-A irradiation to better hypothesize how DOM and MeHg react photolytically in combination. Every 4 hours triplicate samples were removed and analyzed for absorbance and DOM concentration. Reduction of absorbance over time in these types of experiments can be due to two linked and sometimes inseparable processes, photomineralization (conversion of organic carbon to inorganic carbon) and photobleaching (loss of chromophoric absorbing bonds). Loss of DOM after 24 hours of UV-A radiation was significant across lakes and months (all p<0.05; Figure A1.1A) except in two circumstances, PUZ lake in June, and BDE lake in September (these lakes consistently had lower carbon concentrations; see Figure 2.2A). On average lakes lost 16 ± 7.3% of the initial DOM concentration and rates of photomineralization normalized by initial DOM concentrations were greater in August

than June for PES and BDW lakes (Figure A1.1A). Lower carbon lakes will have attenuated less radiation *in situ* and therefore more radiation gets transmitted through these water columns compared to higher carbon lakes. Therefore, the lack of detectable DOM concentration loss in these lakes (June PUZ and September BDE) are a result of lowered UV-A photoreactivity possibly because of photochemical processing of DOM in lower carbon lakes, prior to sampling. Our sampling depth of 30 cm in the water column still had UV-A present for the two lowest carbon lakes (BDE and PUZ; Figure A1.2). This prior exposure and the possibility that the 24-hour period and UV-A intensity used in the experiment were too short or low may have reduced DOM photomineralization in these lake waters.

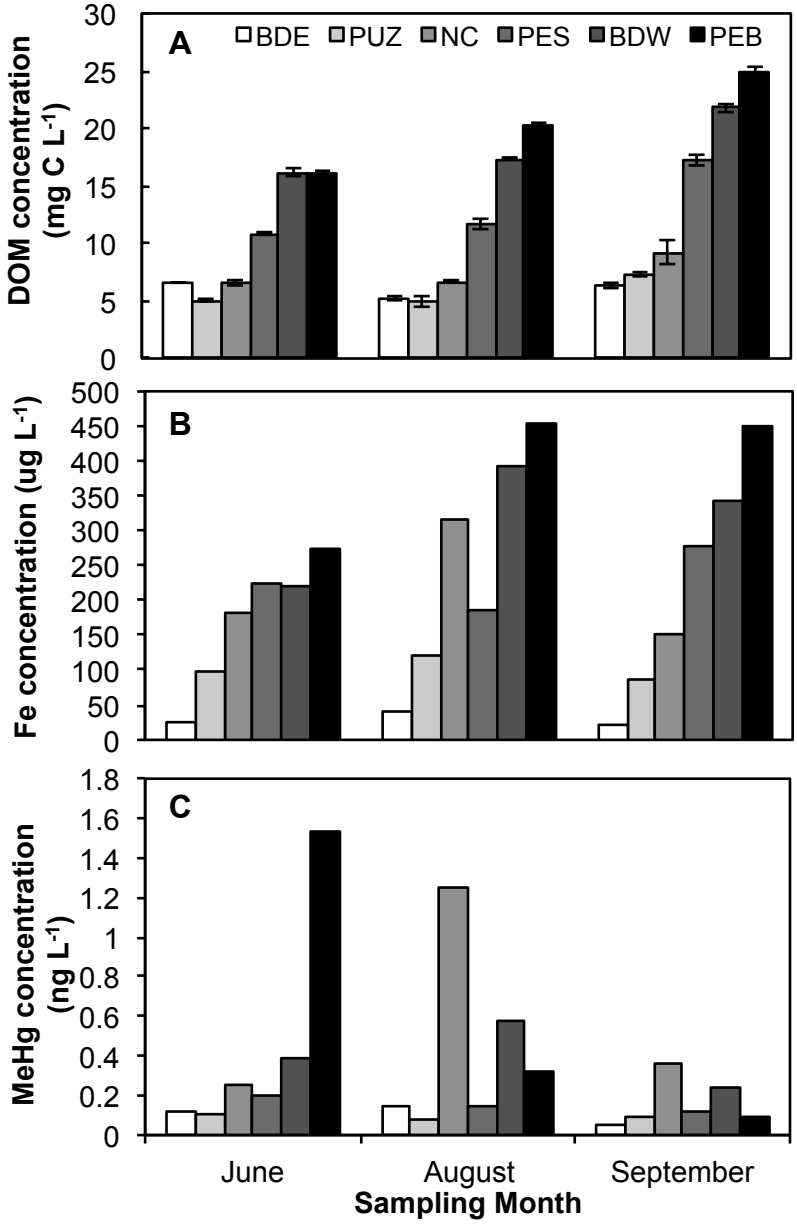

Figure 2.2 (A) Dissolved organic matter (DOM) concentration, (B) iron (Fe) concentrations, and (C) methylmercury (MeHg) concentration from June, August, and September in Kejimkujik National Park. Lakes arranged by increasing average DOM concentration. DOM values are expressed as means ± 1 standard deviation (n=3).

Photomineralization losses of DOM for natural waters reported in the literature range from negligible in California surface waters (Fleck et al. 2014) to less than 10% of

initial DOM concentrations in lab incubations of boreal stream waters (Franke et al. 2012). The California study used bottles containing water from different wetland types floated in a pond to include natural diurnal radiation exposure intensities and noted possible shading effects due to sample path lengths (Fleck et al. 2014). In contrast, our study applied a constant UV-A radiation source and a short path length of 1 cm to reduce possible within-sample attenuation and shading. Our irradiation experiments more closely resembled methods used for the boreal stream water lab incubation, although Franke et al. (2012) focused on a combination of visible and UV radiation (300-800 nm). All studies were equivalent to several days of natural radiation exposure but used different wavelength and intensity exposures and this distinction may explain the small yet significant variation in DOM loss across similar study types.

Dissolved organic matter can be defined on the basis of molecular weight and origin. In irradiation experiments it is important to consider the fractions of DOM and the chemical structures that are photodegraded. High molecular weight (HMW) DOM can attenuate more UV due to the presence of more aromatic carbon structures and may therefore be preferentially photo-oxidized, compared to lower molecular weight (LMW) DOM (Helms et al. 2008). Much of the DOM in Kejimkujik is thought to be allochtonous due to terrestrial inputs and low productivity within these dystrophic lakes. The difference in UV-A attenuation between lakes in Kejimkujik noted by Haverstock et al. (2012) could be due to differences in chemical structure or quantity of DOM between lakes. Interestingly, when Haverstock et al. (2012) used a depth-integrated model to predict annual DIC production through photomineralization across lakes of various DOM concentration (4 of the lakes used in this study), similar total amounts of DIC were

predicted to be produced by UV-A. This finding suggests that the structure of the DOM between samples lakes may not vary greatly and was not a significant factor in the total photomineralization of DOM. Lakes that contained higher concentrations of DOM attenuated more radiation and therefore the predicted DIC produced across lakes was similar. Radiation availability plays a major role in regulating potential photochemical reactions in these lakes, and DOM concentration itself will regulate radiation availability.

Variability in UV-A photoreactivity between our study lakes appears to be largely related to DOM concentration. We use the measure of UV-A photoreactivity as a way to quantitatively compare DOM as a competitive sink for photons used in UV-A mediated photoreactions within lake waters. Absorbance coefficients for high carbon lakes were up to one order of magnitude greater than absorbance coefficients for low carbon lakes throughout the entire incubation (Figure A1.3). Regardless of between lake variations in absorbance values, UV-A photoreactivity across all samples for our 6 study lakes in all 3 sampling periods had a highly significant positive linear relationship with DOM concentration (r^2=0.94; Figure 2.3A). Higher carbon lakes also exhibited larger variation in UV-A photoreactivity than lower carbon lakes (shown in Figure 2.3A). The $SUVA_{350}$ values were different among lakes (Figure 2.4B) and suggested that the higher DOM lakes were more photoreactive and had greater photobleaching and photomineralization than the lower DOM lakes. Initial absorption values at 350 nm and UV-A photoreactivity values that were normalized by DOM concentration still showed variation among lakes (Figure A1.1B & A1.1A). Lakes with higher DOM had greater UV-A photoreactivity and the DOM concentration loss increased with DOM concentration (Figure 2.3B).

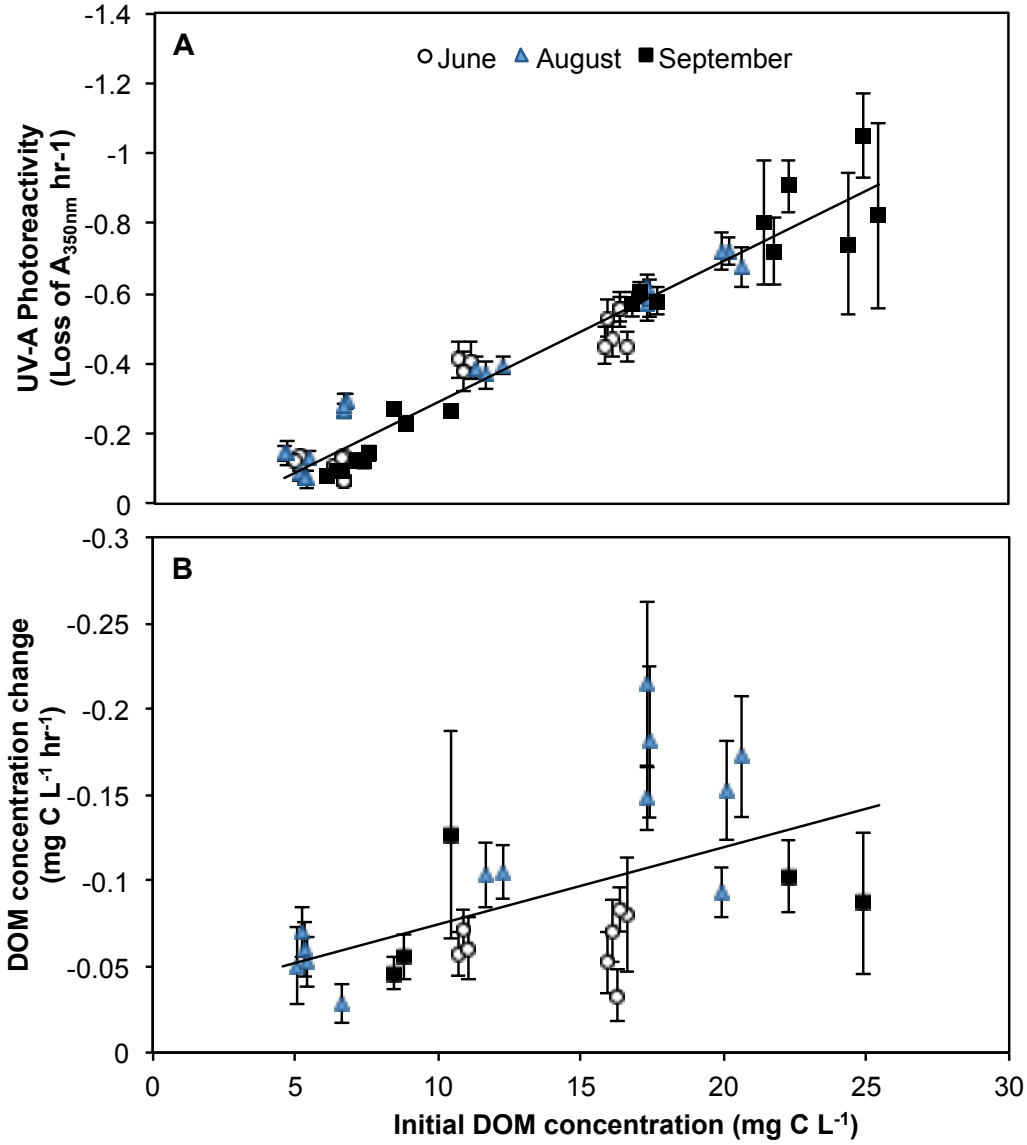

Figure 2.3 (A) UV-A photoreactivity of lake water (quantified as the loss of absorptivity at 350 nm) and (B) significant (p<0.1) detectable dissolved organic matter (DOM) losses versus the initial DOM concentration for all six lakes in triplicate over all months (UV-A photoreactivity = -0.04[DOM] + 0.14, r^2=0.94, *p*<0.001; DOM loss = -0.005[DOM] -0.008, r^2=0.31, *p*=0.003). Open circles represent June) blue triangles August, and black squares September. Note the inverted y-axis showing negative slope values for photoreactivity; more negative y-values indicate higher photoreactivity. Error bars are the standard error on photoreactivity slopes for each experimental triplicate over the 3 sampling periods and 6 lakes.

Changes in spectral slopes and subsequently spectral slope ratios (S_R) reflect changes in the composition of DOM following UV-A exposure. Spectral slopes ($S_{275\text{-}295nm}$ and $S_{350\text{-}400nm}$) for Kejimkujik lakes ranged from 0.011 to 0.017 nm^{-1} for $\lambda_{275\text{-}295}$ and 0.015 to 0.020 nm^{-1} for $\lambda_{350\text{-}400}$ similar to sites reported in temperate streams and freshwater bodies (Helms et al. 2008) but higher than those reported in boreal streams (Franke et al. 2012). Spectral slope ratios ranged from 0.63 to 0.85, similar to the boreal streams and bogs sampled by Franke et al. (2012). All spectral slopes and slope ratios increased significantly ($p<0.05$) during irradiation experiments suggesting a decrease in the relative abundance of HMW DOM to LMW chromophoric DOM with UV-A exposure (Helms et al. 2008) (Figure A1.4). This trend is widely supported in the literature across many freshwater ecotypes (Helms et al. 2008; Franke et al. 2012; Fleck et al. 2014). Our data suggest that lakes and collection times that had higher DOM concentrations will have greater potential to participate in DOM photoreactions during irradiation experiments and there was no significant difference in spectral slope shifts between lake samples (all $p>0.185$). This finding establishes that the chromophoric DOM composition was similar across lakes and months. Furthermore, lake water of varying UV-A photoreactivity behaved similar in terms of the DOM components vulnerable to UV-A photoreactions. Our research shows DOM concentration is a useful predictor of UV-A photoreactivity of DOM in the 6 lakes studied.

3.2 Seasonal patterns and observations of DOM, Fe, MeHg in Kejimkujik lakes

Seasonal variation in DOM and Fe along with solar radiation can be used to uncover possible mechanisms controlling MeHg levels in natural waters. Many

photochemistry studies and experiments in natural lakes focus on one time point or a short sampling period with few studies using repeated sampling strategies, particularly sampling campaigns over multiple seasons. Our study lakes were chosen based on previous research to cover a wide gradient of DOM, Fe, and MeHg concentrations representative of the National Park (O'Driscoll et al. 2005) and southwestern Nova Scotia in general. Dissolved organic matter concentrations typically increased in the lakes over the 2014 sampling season (Figure 2.2A). All 6 lakes were significantly different in DOM concentration ($p<0.05$) except for the two lakes with the lowest DOM concentrations: BDE and PUZ lakes ($p=0.99$). Lake DOM concentrations were not significantly different in June and August ($p=0.95$). Mean DOM concentrations across all lakes in June and August were significantly lower than in September ($p<0.05$) supporting an overall increase in DOM throughout the region in fall compared to the summer months. Increased wetland and landscape export of DOM through leaf litter and plant senescence without dilution from heavy precipitation or concentration through evaporative water flux could be factors in the increased DOM concentrations observed. Historical long-term stream and river data from Kejimkujik National Park shows that May-November are low-flow periods (Kerekes and Freedman 1989) and that DOM concentrations are positively linked to lake flushing rates (times per year the entire lake volume will be replaced) (Hirtle and Rencz 2003). The spatial and temporal hydrology of lake systems will control both the water entering the lake (dilution factor) and pulses of DOM and mercury species (concentration factor). Apart from PEB lake, DOM concentrations in our study lakes were positively correlated with catchment area ($r=0.80$, $p=0.10$) and flushing rate per year ($r=0.87$, $p=0.05$) further supporting the link between DOM in these lakes with the

physical hydrology of the region (Table A1.1). In-lake attenuation coefficients (K_d) varied across lakes and months from 0.05 to 2.17 cm^{-1} (Figure 2.4A) and are comparable to previous attenuation measurements in these lakes (Haverstock et al. 2012). In all lakes, except BDE and PUZ, which were lakes with the lowest DOM concentrations in our study set, K_d varied with season and positively corresponded with an increase in DOM concentration within the lakes supporting the importance of DOM to seasonal attenuation of radiation in the water columns of these lakes.

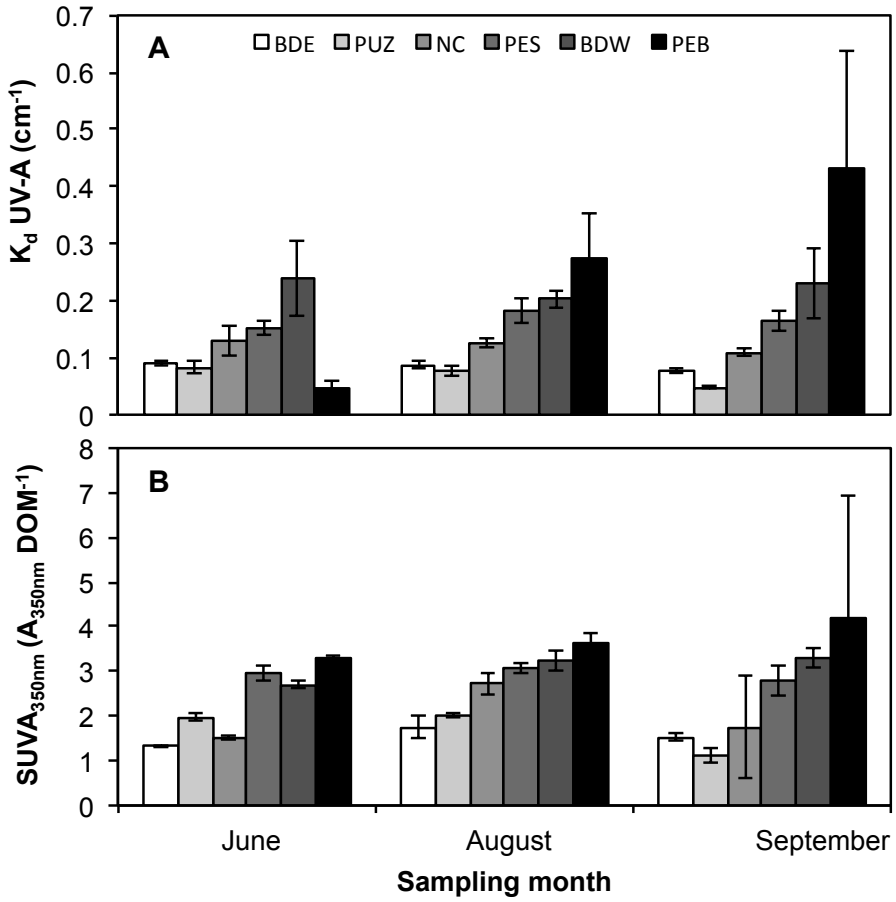

Figure 2.4 (A) UV-A attenuation coefficients (K_d) and (B) specific ultraviolet absorbance at 350 nm ($SUVA_{350}$) in June, August, and September in Kejimkujik National Park. Lakes are arranged by increasing average dissolved organic matter (DOM) concentration. Values are expressed as means ± standard deviation (n=3).

Increased DOM concentrations across the 2013 season also corresponded with increased Fe concentrations ranging from 20 to 453 μg L^{-1} (Figure 2.2B). Dissolved Fe in the Fe(III) form, is known to absorb UV appreciably (Zepp et al. 1992) and total Fe was positively correlated with DOM concentration (r=0.81, p<0.01) in the lakes and accounted for 0.6 – 13.5% of the absorbance at 350 nm using the Fe extinction coefficient (method outlined in Poulin et al. (2014); Figure A1.5). All lakes except for PUZ and NC lakes exhibited little (<2%) effect of Fe on A_{350nm} based on this Fe extinction coefficient. These two lakes both had relatively low DOM concentrations and were paired in sampling location (Figure 2.2A & Figure 2.1) suggesting a small spatial effect of Fe or DOM. Iron could play a greater role in water photoreactions at PUZ and NC than the other lakes, although the effect is still quite minor (<15% of A_{350} could be attributed to Fe) and overall is likely not a strong predictor of absorbance or photoreactions in the study lakes. Additionally, natural organic matter can inhibit the effect of Fe on photoreactions involving MeHg (Zhang et al. 2016), an effect that is amplified in high DOM waters.

MeHg concentrations ranged from lowest in BDE lake (lowest carbon) in September (0.05 ng L^{-1}) to highest in PEB lake (highest carbon) in June (1.54 ng L^{-1}; Figure 2.2C). There was no consistent temporal pattern in our MeHg concentrations across sampling periods, however, a previous study that included brooks, creeks, and lakes in Kejimkujik showed that total mercury and MeHg concentrations were positively correlated with DOM concentration in pooled data from August (summer) and April (spring) (Meng et al. 2005). We also looked at three years of monitoring of DOM, Fe, and MeHg in summer (late-June), late-summer (mid-August), and fall (late-September/early-

October) from all 6 lakes. Overall there was an excellent pooled correlation between DOM and Fe (r=0.90, $p<0.01$; Figure 2.5A). DOM concentrations were also well correlated with MeHg concentrations (r=0.51, $p<0.01$; Figure 2.5B) with greater scatter occurring in the higher DOM lakes (BDW and PEB lakes in particular).

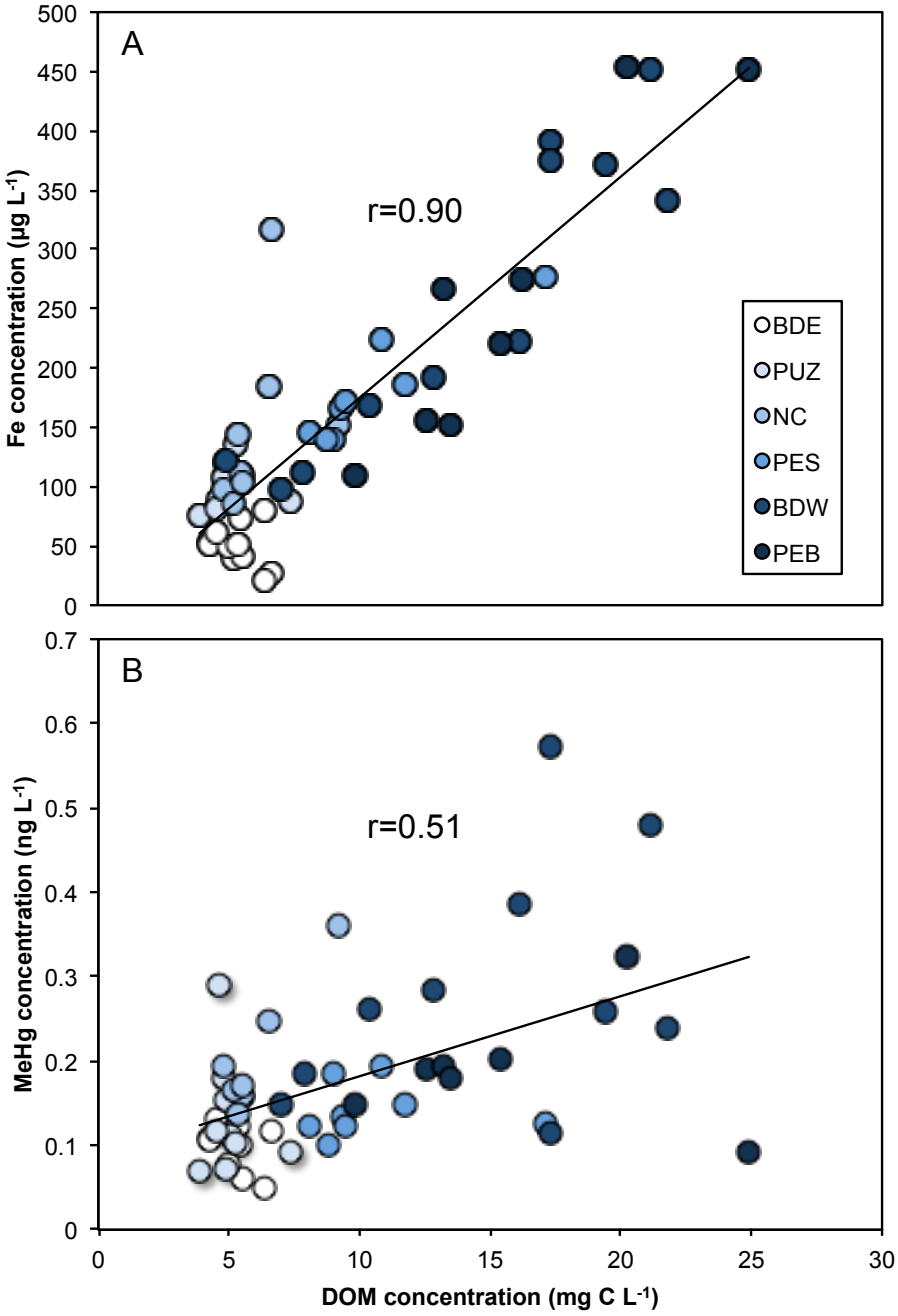

Figure 2.5 Correlation between dissolved organic matter (DOM) and (A) iron (Fe) concentrations (r=0.91, p<0.01), and (B) methylmercury (MeHg) concentrations (r=0.51, p<0.01) in summer, late-summer, and fall from 2013, 2014, and 2015.

This inconsistency supports the idea that the timing of water sampling is critical when drawing conclusions about the relationship between DOM and MeHg concentrations in lakes. The correlation between DOM and MeHg concentration was high in summer (r=0.77, n=18, p=0.12) and was not observed in late-summer (r=0.09, n=18, p=0.78), and fall (r=-0.09, n=18, p=0.94). The lack of correlation between DOM concentration and MeHg later in the year suggests that DOM may have the greatest effect on MeHg concentration in early summer through transport processes. However, as the season transitions into late-summer and fall, DOM has less direct influence on MeHg concentrations likely due to reduced transport and greater importance of biological and photo-induced processes within the lakes. In addition, increased DOM and Fe concentrations later in the summer season may shield more of the water column limiting *in situ* photochemical processing. Methylmercury concentrations may have also been influenced seasonally by some other factor not studied in this study (such as biological uptake, mixing through upwelling, or in lake photochemical processing). These data highlight the importance of seasonal monitoring as well as mechanistic studies for capturing ecosystem variations in MeHg and DOM photochemistry.

3.3 Relating DOM photoreactivity to MeHg availability

Concentrations of DOM and MeHg both varied substantially with season and across lakes (MeHg range: 0.05 – 1.54 ng L^{-1}; DOM range: 3.9 – 24.9 mg C L^{-1}) but some trends were visible in the data: DOM tended to increase and MeHg tended to decrease within individual lakes from summer to fall (Figure 2.2A; Figure 2.2C). Concentrations of DOM and MeHg were correlated in June but MeHg concentrations were not

significantly correlated with UV-A photoreactivity as determined in irradiation experiments in any of the sampling months (June: r=-0.36, p=0.46, August: r=-0.25, p=0.64, September: r=0.04, p=0.94). This observation suggests that bioaccumulation studies examining the lower trophic levels must account for these seasonal shifts and the timing of MeHg entry to the base of food webs. Compelling evidence from an 11-lake study in Kejimkujik suggested that DOM may be linked to biomagnification of MeHg, with lower carbon lakes exhibiting higher ranges of biomagnification (Clayden et al. 2013). Another study from 26 Arctic lakes showed that low DOM concentrations (<8.5 mg C L^{-1}) promoted mercury bioaccumulation in aquatic invertebrates and that high DOM concentrations inhibited mercury bioaccumulation (French et al. 2014). These results must be considered within the context of the significant seasonal shifts in DOM and dissolved MeHg concentrations observed in this study. Seasonal variations in DOM photoreactivity and effects on MeHg photodemethylation are difficult to assess *in situ* because of the dynamic nature of the aquatic environment.

The effect of DOM photoreactivity on *in situ* MeHg concentrations and availability in freshwaters is still not well characterized. The uncertainty in this research area is due to the difficulty in separating DOM photoreactions that are *intra*-molecular (MeHg bound directly to DOM subjected to photoreactions) versus *inter*-molecular (MeHg not bound directly to DOM subjected to photoreactions). High carbon freshwaters, like those lakes used in our study, can efficiently attenuate UV radiation and may theoretically inhibit or facilitate MeHg photodemethylation by acting as a photoreactive species within the water column (Sellers et al. 1996; Li et al. 2010). The influence of DOM concentrations on MeHg photodemethylation rate constants has been

documented as negligible or inhibitory. In Californian wetlands MeHg photodemethylation rate constants were only significantly related to cumulative solar radiation exposure and not to naturally different DOM concentrations at different sampling sites, which varied from 8 – 34 mg C L^{-1} (Fleck et al. 2014). Cumulative solar radiation will decrease rapidly across a given path length at higher DOM concentrations and this attenuation of UV-A can be used to predict rates of MeHg photodemethylation. However, a predicted decrease of 34% due to an increase in DOM concentration by 1.5 to 11.2 mg C L^{-1} only resulted in a 6% decrease in MeHg photodemethylation rate constants (Black et al. 2012). This suggested that the influence of DOM on MeHg photodemethylation is not solely inhibitory and dependent on just radiation availability. In our experimental treatments by removing the limitation of radiation extinction via attenuation by using quartz vials with a short path length (1.0 cm) we were able to show that DOM concentrations directly controlled the DOM photoreactivity (Figure 2.3A; r^2=0.94). This finding is key if MeHg photodemethylation is intramolecular and requires energy transfer from bound organic ligands (Tai et al. 2014; Qian et al. 2014); DOM must be present in order for this process to occur but photoreactive DOM may also attenuate the majority of photoreactive energy and thereby inhibit photodemethylation (Figure 2.6).

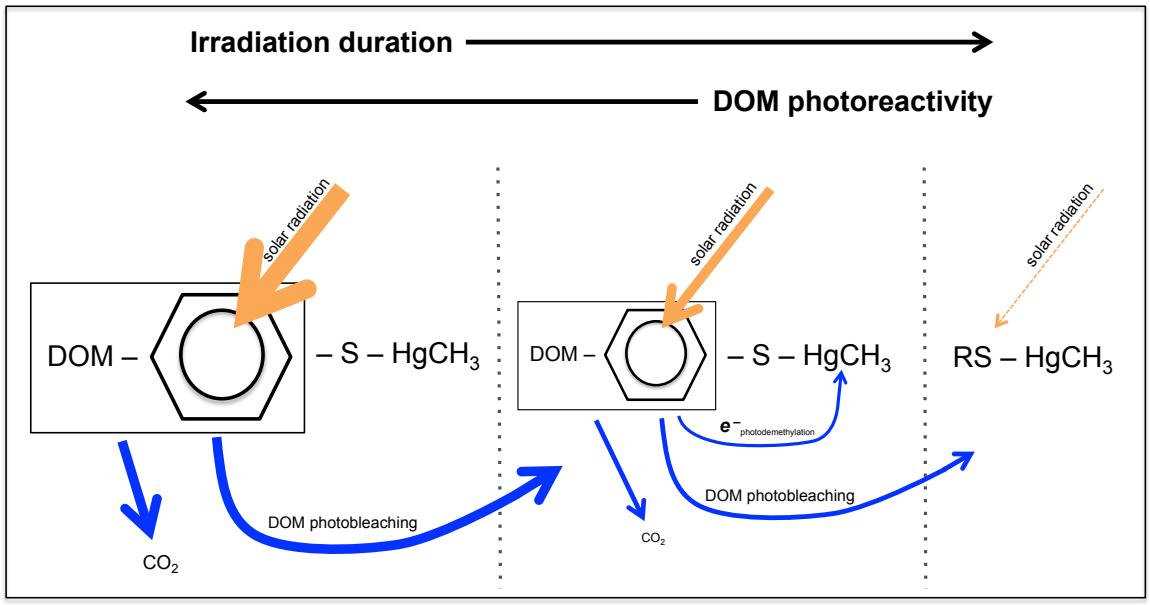

Figure 2.6 Increased irradiation duration will decrease dissolved organic matter (DOM) photoreactivity through DOM photomineralization and the production of carbon dioxide (CO_2) as well as DOM photobleaching, leading to less photoreactive DOM. Highly photoreactive DOM will absorb a lot of solar radiation and DOM phototransformations will dominate the photoreactions. Less photoreactive DOM will absorb less radiation and therefore methylmercury ($HgCH_3$) associated with sulfur groups may photodemethylate through internal charge transfer (e^-). When DOM is no longer present, photodemethylation will not occur. The sizes of the arrows indicate the relative strength of each action with absorbed radiation in orange arrows and resultant photoreactions in blue.

4. CONCLUSIONS

Our study found that across seasonal samplings, UV-A photoreactivity (calculated based on the absorptivity loss at 350 nm over each incubation time) was significantly and positively related to DOM concentration in freshwater oligotrophic lake waters in southwestern Nova Scotia. This UV-A photoreactivity-DOM relationship was independent of season even though DOM concentration itself was affected by seasonality. Other chromophoric dissolved constituents, such as Fe, may also contribute to the absorptivity of the lake water studied but these effects were small and spatially specific in

our study area. Irradiation exposure caused significant loss of absorbance at 350 nm and losses of DOM concentration through photomineralization in the majority of the experiment treatments resulting in significant declines in DOM concentration across sampling seasons. Given the strong correlation between DOM concentration and UV-A photoreactivity, high carbon systems may be characterized by increased photoreactions with DOM and not MeHg whereas less photoreactive DOM in lower carbon lakes will likely facilitate MeHg photodemethylation (Figure 2.6). Periods of time with high photoreactivity (such as fall) may also experience this paradigm of increased DOM photoreactions but limited MeHg photoreactions. We saw some correlation between DOM concentration and *in situ* MeHg concentration in the June sampling period however, this study found no consistent relationship between UV-A photoreactivity of DOM and MeHg concentration over the 2013 sampling season and therefore this hypothesis requires further controlled experimentation. The inclusion of 3 years of sampling in summer, late-summer, and fall showed a positive relationship between DOM and MeHg, suggesting that higher MeHg concentrations tend to be present in lakes with greater DOM photoreactivity. Our results also highlight a wide variation in DOM and MeHg concentrations within individual lakes across season, which may significantly affect the timing of mercury entry at the base of the food web. Further work, including controlled lab and field studies, should identify if and how photoreactive DOM in lake water directly influences the photodemethylation rate constant of MeHg and its importance in temporal dynamics.

Acknowledgments

Funding for this research was provided from the National Science and Engineering Council (NSERC) of Canada in the form of a discovery grant to N.J.O and an NSERC CREATE scholarship to S.J.K. In addition, Canada Research Chair, and Canadian Foundation for Innovation funding was provided to N.J.O., Canada Research Chair to S.E.Z., and NSERC Discovery Grant to D.A.R.. Logistical field and laboratory support provided by Parks Canada (Chris McCarthy), E. Mann, H. MacDonell, L. Klapstein, S. Edmonds, the Mersey Tobeatic Research Institute, and Acadia University.

References

Bertilsson, S., and L. J. Tranvik. 2000. Photochemical transformation of dissolved organic matter in lakes. Limnol. Oceanogr. **45**: 753–762.

Black, F. J., B. A. Poulin, and A. R. Flegal. 2012. Factors controlling the abiotic photo-degradation of monomethylmercury in surface waters. Geochim. Cosmochim. Acta **84**: 492–507. doi:10.1016/j.gca.2012.01.019

Clayden, M. G., K. A. Kidd, B. Wyn, J. L. Kirk, D. C. G. Muir, and N. J. O'Driscoll. 2013. Mercury biomagnification through food webs is affected by physical and chemical characteristics of lakes. Environ. Sci. Technol. **47**: 12047–12053. doi:10.1021/es4022975

De Lange, H. J., D. P. Morris, and C. E. Williamson. 2003. Solar ultraviolet photodegradation of DOC may stimulate freshwater food webs. J. Plankton Res. **25**: 111–117.

Fleck, J. A., G. Gill, B. A. Bergamaschi, T. E. C. Kraus, B. D. Downing, and C. N. Alpers. 2014. Concurrent photolytic degradation of aqueous methylmercury and dissolved organic matter. Sci. Total Environ. **484**: 263–275. doi:10.1016/j.scitotenv.2013.03.107

Franke, D., M. W. Hamilton, and S. E. Ziegler. 2012. Variation in the photochemical lability of dissolved organic matter in a large boreal watershed. Aquat. Sci. **74**: 751–768. doi:10.1007/s00027-012-0258-3

French, T. D., A. J. Houben, J.-P. W. Desforges, and others. 2014. Dissolved organic carbon thresholds affect mercury bioaccumulation in Arctic lakes. Environ. Sci. Technol. **48**: 3162–3168. doi:10.1021/es403849d

Granéli, W., M. Lindell, and L. Tranvik. 1996. Photo-oxidative production of dissolved inorganic carbon in lakes of different humic content. Limnol. Oceanogr. **41**: 698–706. doi:10.4319/lo.1996.41.4.0698

Haverstock, S., T. Sizmur, J. Murimboh, and N. J. O'Driscoll. 2012. Modeling the photo-oxidation of dissolved organic matter by ultraviolet radiation in freshwater lakes: Implications for mercury bioavailability. Chemosphere **88**: 1220–1226. doi:10.1016/j.chemosphere.2012.03.073

Helms, J. R., A. Stubbins, J. D. Ritchie, E. C. Minor, D. J. Kieber, and K. Mopper. 2008. Absorption spectral slopes and slope ratios as indicators of molecular weight, source, and photobleaching of chromophoric dissolved organic matter. Limnol. Oceanogr. **53**: 955.

Hirtle, H., and A. Rencz. 2003. The relation between spectral reflectance and dissolved organic carbon in lake water: Kejimkujik National Park, Nova Scotia, Canada. Int. J. Remote Sens. **24**: 953–967. doi:10.1080/01431160210154957

Karanfil, T., I. Erdogan, and M. A. Schlautman. 2003. Selecting filter membranes for measuring DOC and UV_{254}. J. Am. Water Works Assoc. **95**: 86–100.

Kerekes, J., and B. Freedman. 1989. Seasonal variations of water chemistry in oligotrophic streams and rivers in Kejimkujik National Park, Nova Scotia. Water. Air. Soil Pollut. **46**: 131–144.

Kim, M.-K., and K.-D. Zoh. 2013. Effects of natural water constituents on the photo-decomposition of methylmercury and the role of hydroxyl radical. Sci. Total Environ. **449**: 95–101. doi:10.1016/j.scitotenv.2013.01.039

Kirk, J. T. O. 1994. Light and photosynthesis in aquatic ecosystems, Cambridge University Press.

Klapstein, S. J., S. E. Ziegler, D. A. Risk, and N. J. O'Driscoll. 2016. Quantifying the effects of photoreactive dissolved organic matter on methylmercury photodemethylation rates in freshwaters. Environ. Toxicol. Chem. **9999**: 1–10. doi:10.1002/etc.3690

Krabbenhoft, D. P., M. L. Olson, J. F. Dewild, D. W. Clow, R. G. Striegl, M. M. Dornblaser, and P. VanMetre. 2002. Mercury loading and methylmercury production and cycling in high-altitude lakes from the Western United States. Water Air Soil Pollut. Focus **2**: 233–249. doi:10.1023/A:1020162811104

Lehnherr, I., and V. L. St Louis. 2009. Importance of ultraviolet radiation in the photodemethylation of methylmercury in freshwater ecosystems. Environ. Sci. Technol. **43**: 5692–5698.

Lehnherr, I., V. L. St. Louis, C. A. Emmerton, J. D. Barker, and J. L. Kirk. 2012a. Methylmercury cycling in high Arctic wetland ponds: Sources and sinks. Environ. Sci. Technol. **46**: 10514–10522. doi:10.1021/es300576p

Lehnherr, I., V. L. St. Louis, and J. L. Kirk. 2012b. Methylmercury cycling in high Arctic wetland ponds: Controls on sedimentary production. Environ. Sci. Technol. **46**: 10523–10531. doi:10.1021/es300577e

Li, Y., Y. Mao, G. Liu, G. Tachiev, D. Roelant, X. Feng, and Y. Cai. 2010. Degradation of methylmercury and its effects on mercury distribution and cycling in the Florida Everglades. Environ. Sci. Technol. **44**: 6661–6666. doi:10.1021/es1010434

Meng, F.-R., P. Arp, A. Sangster, and others. 2005. Modeling dissolved organic carbon, total and methyl mercury in Kejimkujik freshwaters, p. 1–19. *In* Mercury cycling in a wetland-dominated ecosystem: a multidisciplinary study. Society of Environmental Toxicology and Chemistry (SETAC).

Morris, D. P., and B. R. Hargreaves. 1997. The role of photochemical degradation of dissolved organic carbon in regulating the UV transparency of three lakes on the Pocono Plateau. Limnol. Oceanogr. **42**: 239–249.

Morris, D. P., H. Zagarese, C. E. Williamson, E. G. Balseiro, B. R. Hargreaves, B. Modenutti, R. Moeller, and C. Queimalinos. 1995. The attenuation of solar UV radiation in lakes and the role of dissolved organic carbon. Limnol. Oceanogr. **40**: 1381–1391.

O'Driscoll, N. J., and R. D. Evans. 2000. Analysis of methyl mercury binding to freshwater humic and fulvic acids by gel permeation chromatography/hydride generation ICP-MS. Environ. Sci. Technol. **34**: 4039–4043. doi:10.1021/es0009626

O'Driscoll, N. J., A. N. Rencz, and D. R. S. Lean. 2005. Review of factors affecting mercury fate in Kejimkujik Park, Nova Scotia, p. 7–20. *In* Mercury cycling in a wetland-dominated ecosystem: a multidisciplinary study. SETAC.

Osburn, C. L., L. Retamal, and W. F. Vincent. 2009. Photoreactivity of chromophoric dissolved organic matter transported by the Mackenzie River to the Beaufort Sea. Mar. Chem. **115**: 10–20. doi:10.1016/j.marchem.2009.05.003

Poulin, B. A., J. N. Ryan, and G. R. Aiken. 2014. Effects of iron on optical properties of dissolved organic matter. Environ. Sci. Technol. **48**: 10098–10106. doi:10.1021/es502670r

Qian, Y., X. Yin, H. Lin, B. Rao, S. C. Brooks, L. Liang, and B. Gu. 2014. Why dissolved organic matter enhances photodegradation of methylmercury. Environ. Sci. Technol. Lett. **1**: 426–431. doi:10.1021/ez500254z

Ravichandran, M. 2004. Interactions between mercury and dissolved organic matter—a review. Chemosphere **55**: 319–331. doi:10.1016/j.chemosphere.2003.11.011

Scully, N. M., and D. R. S. Lean. 1994. The attenuation of ultraviolet radiation in temperate lakes. Erg Limnol **43**: 135–144.

Sellers, P., C. A. Kelly, J. W. M. Rudd, and A. R. MacHutchon. 1996. Photodegradation of methylmercury in lakes. Nature **380**: 694–697. doi:10.1038/380694a0

Smith, P. K., A. Sangster, and A.-M. O'Beirne-Ryan. 2005. Bedrock mercury at Kejimkujik National park, Nova Scotia, p. 131–195. *In* Mercury cycling in a wetland-dominated ecosystem: a multidisciplinary study. Society of Envrionmental Toxicology and Chemistry (SETAC).

Tai, C., Y. Li, Y. Yin, L. J. Scinto, G. Jiang, and Y. Cai. 2014. Methylmercury photodegradation in surface water of the Florida Everglades: Importance of dissolved organic matter-methylmercury complexation. Environ. Sci. Technol. **48**: 7333–7340. doi:10.1021/es500316d

Xun, L., N. E. R. Campbell, and J. W. M. Rudd. 1987. Measurements of specific rates of net methyl mercury production in the water column and surface sediments of acidified and circumneutral lakes. Can. J. Fish. Aquat. Sci. **44**: 750–757. doi:10.1139/f87-091

Zepp, R. G., B. C. Faust, and J. Hoigne. 1992. Hydroxyl radical formation in aqueous reactions (pH 3-8) of iron(II) with hydrogen peroxide: the photo-Fenton reaction. Environ. Sci. Technol. **26**: 313–319. doi:10.1021/es00026a011

Zhang, D., Y. Yin, Y. Li, Y. Cai, and J. Liu. 2016. Critical role of natural organic matter in photodegradation of methylmercury in water: Molecular weight and interactive effects with other environmental factors. Sci. Total Environ. doi:10.1016/j.scitotenv.2016.10.222

Zhang, T., and H. Hsu-Kim. 2010. Photolytic degradation of methylmercury enhanced by binding to natural organic ligands. Nat. Geosci. **3**: 473–476. doi:10.1038/ngeo892

Chapter 3 : QUANTIFYING THE EFFECTS OF PHOTOREACTIVE DISSOLVED ORGANIC MATTER ON METHYLMERCURY PHOTODEMETHYLATION RATES IN FRESHWATERS

Sara J. Klapstein[a,c], Susan E. Ziegler[a], David A. Risk[b], Nelson J. O'Driscoll[c]

[a]Department of Environmental Science, Memorial University of Newfoundland, St. John's NL, Canada

[b]Department of Earth Sciences, St. Francis Xavier University, Antigonish NS, Canada

[c]Department of Earth and Environmental Science, Acadia University, Wolfville NS, Canada

Reproduced with permission from: Klapstein, S.J., Ziegler, S.E., Risk, D.A., and O'Driscoll, N.J. 2016. Quantifying the effects of photoreactive dissolved organic matter on methylmercury photodemethylation rates in freshwaters. *Environmental Toxicology and Chemistry.* **9999**: 1-10. doi: 10.1002/etc.3690.

Abstract

The present study examined potential effects of seasonal variations in photoreactive dissolved organic matter (DOM) on methylmercury (MeHg) photodemethylation rate constants in freshwaters. A series of controlled experiments were carried out using natural and photochemically preconditioned DOM in water collected from one lake (Big Dam West) in June, August, and October. Natural DOM concentrations doubled between June and August (10.2 – 21.2 mg C L^{-1}) and then remained stable into October (19.4 mg C L^{-1}). Correspondingly, MeHg concentrations peaked in August (0.42 ng L^{-1}) along with absorbances at 350 nm (A_{350}) and 254 nm ($SUVA_{254}$). Up to 70% of the MeHg was photodemethylated in the short 48-hour irradiation experiments with June having significantly higher rates than the other sampling months ($p<0.001$). Photodemethylation rate constants were not affected by photoreactive DOM nor were they affected by initial MeHg concentrations ($p>0.10$). However, MeHg photodemethylation efficiencies (quantified in mole MeHg lost/mole photon absorbed) were higher in treatments with less photoreactive DOM. Congruently, MeHg photodemethylation efficiencies also decreased over summer by up to 10× across treatments in association with increased photoreactive DOM, and were negatively correlated with DOM concentration. These results suggest that an important driver of MeHg photodemethylation is the interplay between MeHg and DOM with greater potential for photodemethylation in freshwaters with more photobleached DOM and lower DOM content.

1. INTRODUCTION

Methylmercury (MeHg) is the form of mercury that poses the greatest risk to organism health through its neurotoxic effects (Mergler et al. 2007) and its ability to bioaccumulate and biomagnify through food webs (Morel et al. 1998; Walters et al. 2016). As a result, higher trophic level organisms accumulate and retain primarily the MeHg form of mercury (Bloom 1992). Variation in available MeHg in the water column is an important factor controlling food web bioaccumulation. Dissolved MeHg concentrations in freshwater lakes are governed by a number of production and loss processes, including both abiotic and biotic methylation, uptake to the food web, complexation and flocculation with organic matter particles, and photodemethylation. Photodemethylation varies in importance to MeHg budgets but can account for up to 80% of the MeHg loss in oligotrophic water columns (Sellers et al. 2001; Hammerschmidt and Fitzgerald 2006, 2010; Lehnherr and St Louis 2009). Rates of photodemethylation are consistently dependent on availability of incoming solar radiation and absorbance in water columns (Sellers et al. 1996, 2001; Lehnherr and St Louis 2009; Li et al. 2010; Black et al. 2012), and therefore environmental variables that affect solar radiation availability can also influence the mechanisms underlying this photoreaction and still require further research. In particular, the role of dissolved organic matter (DOM), a major factor regulating water column radiation availability (Scully and Lean 1994; Haverstock et al. 2012), in MeHg photodemethylation reactions is important to consider (Black et al. 2012; Fleck et al. 2014; Tai et al. 2014; Poste et al. 2015; Jeremiason et al. 2015).

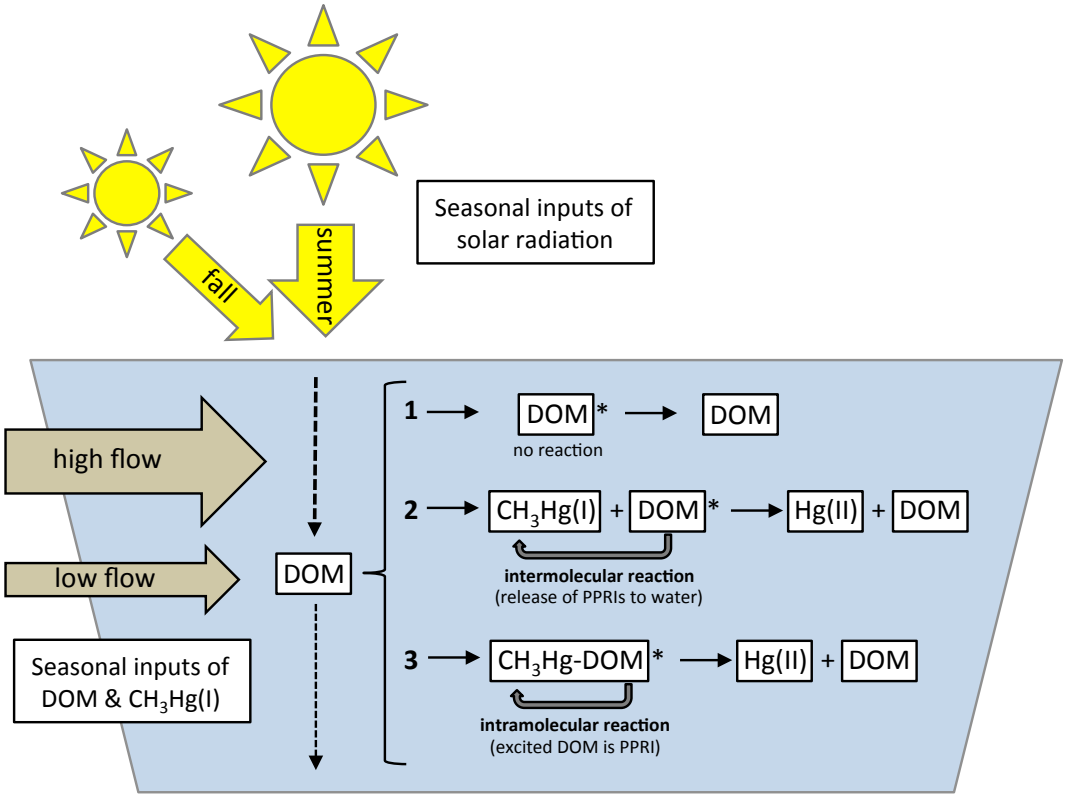

Figure 3.1 Conceptual diagram showing three possible outcomes between photoreactive dissolved organic matter (DOM) absorbing solar radiation and methylmercury ($CH_3Hg(I)$) in freshwater lakes: 1) no reaction: DOM undergoes photoreactions (i.e. photobleaching) but not with MeHg, 2) intermolecular reaction: photodemethylation occurs when DOM releases photochemically produced reactive intermediates (PPRIs) which photodemethylate $CH_3Hg(I)$, or 3) intramolecular reaction: photodemethylation occurs via an internal charge transfer within a DOM complex containing $CH_3Hg(I)$ (CH_3Hg-DOM). Reactions 2 and 3 produce divalent mercury (Hg(II)).

Two hypotheses to explain the role of DOM in MeHg photodemethylation reactions have been proposed in the current literature: (1) DOM can act as a photosensitizer through the attenuation of solar radiation and subsequent production of radicals such as singlet oxygen ($^1O_2$), triplet excited state DOM ($^3DOM^*$), hydrated electrons (e^-_{aq}), and hydroxyl radicals (•OH) (Zepp et al. 1985; Chen et al. 2003; Fernández-Gómez et al. 2013) that are involved in secondary oxidation and reduction

reactions with dissolved MeHg through intermolecular photoreactions (Zhang and Hsu-Kim 2010; Hammerschmidt and Fitzgerald 2010); and (2) DOM can bind cations such as mercury species and directly transfer electrons through intramolecular photoreactions (Tai et al. 2014; Jeremiason et al. 2015) (Figure 3.1 Pathways 2 & 3, respectively). While the relative role of these mechanisms is unclear, recent work using complexation agents and scavenger addition experiments suggest that the dominant photochemical mechanism is intramolecular charge transfer within MeHg-DOM complexes (Tai et al. 2014). Thiol and aromatic groups within the DOM may have synergistic effects on the overall mechanism for photodemethylation of MeHg (Qian et al. 2014). Thiol groups within DOM are important binding sites for MeHg (Qian et al. 2002), but the MeHg-S bond does not tend to absorb radiation (Jeremiason et al. 2015). Charge or energy transfer from chromophoric, or photoreactive, structures within the DOM such as aromatic organic ligands (Qian et al. 2014) are more likely responsible for instigating MeHg photodemethylation (Jeremiason et al. 2015). However, experiments that used combinations of DOM isolates found that DOM isolates with greater aromaticity ($SUVA_{254}$) are less effective than DOM isolates with a lower $SUVA_{254}$ at promoting the photodegradation of MeHg (Qian et al. 2014). This fact, however, could be an artifact of the experiment given that the reactant solutions were prepared using specific DOM isolates and are not representative of naturally occurring DOM. Nevertheless, specific optical characteristics of DOM are important to consider with regard to photodemethylation mechanisms and rate determination because MeHg may more favourly bind, or be found, with thiol containing portions of DOM but the aromatic portions of DOM are what will facilitate photon absorption and therefore

photodemethylation. The role of DOM in facilitating photodemethylation is likely to be dependent on the photoreactivity of the DOM.

The addition of DOM isolates to simulated freshwaters has been shown to facilitate photodemethylation by increasing the rate at which MeHg is photochemically destroyed through radicals or photochemically produced reactive intermediates (PPRIs) (Jeremiason et al. 2015). Dissolved organic matter concentration is a fairly reliable predictor of MeHg concentration in high carbon lake systems because both are linked to catchment characteristics (Meng et al. 2005; Fleck et al. 2014; Jeremiason et al. 2016) and although a link between photochemically active DOM and the photodegradation of MeHg intuitively should exist, one dominant pathway has not yet been validated (Black et al. 2012; Fleck et al. 2014; Tai et al. 2014). Optical tools such as UV-vis absorbance spectroscopy have been used for characterizing DOM optical properties to elucidate which portions of the DOM are vulnerable to photolytic degradation and subsequently which portions of the DOM change concurrently with changes in MeHg concentration via photodegradation (Black et al. 2012; Fleck et al. 2014). Absorbance techniques are beneficial because they are non-destructive, quick, and require minimal manipulation of the sample. Overall, a loss in DOM absorbance has been shown to occur following prolonged solar radiation exposure and spectral analysis shows the losses are particularly linked to photochemically labile chromophoric DOM portions (e.g. 330-450 nm) of the DOM (Fleck et al. 2014). As such, DOM concentration (often measured as dissolved organic carbon) alone is unlikely to be the best predictor of mercury photochemical activity due to the complex nature of DOM structure and variables affecting DOM sources to freshwaters.

DOM source will influence the types of photoreactions that take place in freshwater ecosystems. Terrestrially sourced DOM tends to be more aromatic than aquatic-sourced DOM and absorbs radiation more strongly at shorter wavelengths (Twardowski et al. 2004). When the DOM within freshwaters is pre-dominantly from the terrestrial environment these DOM compounds will readily absorb UV radiation resulting in potential for primary and secondary photoreactions (Scully et al. 1995; Morris and Hargreaves 1997). DOM can be photochemically active through absorption of solar radiation, specifically ultraviolet (UV) wavebands, which can result in photobleaching, direct photolysis of carbon bonds, or radical formation. Direct photolysis by UV-B (280-320 nm) can cause photomineralization of DOM (Haverstock et al. 2012) and theoretically photodemethylation of MeHg (Tossell 1998), however, UV-B wavebands, that have not been filtered by atmospheric absorption and reach Earth's surface, are quickly absorbed in the first few centimeters of many freshwater lakes (Haverstock et al. 2012). Absorption of UV-A (320-400 nm) by DOM generates chemically reactive species that can indirectly affect MeHg through secondary reactions. Laboratory studies have shown that DOM acts as a mediator for photochemical degradation of MeHg (Tai et al. 2014; Qian et al. 2014; Jeremiason et al. 2015), however, the mechanism and explicit role of DOM to photodemethylation is still unclear. While previous studies have found that DOM presence influences mercury photoreaction rates in laboratory studies, there is little research examining naturally occurring photoreactive DOM and its role in photodemethylation pathways.

The principal objective of the present study was to determine if variability in photoreactive DOM (A_{350}) from the same source could affect photodemethylation

reaction rates. We hypothesized that the rate of MeHg photodemethylation would be positively related to photoreactive DOM due to an intramolecular photodemethylation reaction involving charge transfer within DOM to DOM-bound MeHg. We tested this hypothesis using water from one lake sampled over a summer-to-fall seasonal transition and used pre-irradiation exposure of the water and MeHg additions to attain 3 water quality treatments (combinations of photoreactive DOM and MeHg concentrations) within each set of experiments in June, August, and October. This experimental design allowed us to test both the influence of the photoreactive DOM on MeHg photodemethylation efficiency, as well as seasonal variations in photoreactive DOM and MeHg.

2. METHODS

2.1 Sampling site description

Kejimkujik National Park is located in southwestern Nova Scotia, Canada (44.399°N, 65.218°W); a region characterized by low alkalinity and low pH soils. There is a high percentage of wetlands in lake catchments (up to 15%) and as such lakes in this region can range in DOM concentration from very low (1-2 mg C L^{-1}) in groundwater fed systems to very high (>30 mg C L^{-1}) in surface water fed systems (O'Driscoll et al. 2005). Kejimkujik has long been identified as a biological hot spot for mercury contamination and mercury concentrations in fish are still increasing (Evers et al. 2007; Wyn et al. 2010). Big Dam West lake, studied in Chapter 2, was chosen due to previously published information on both DOM and MeHg concentrations as well as recorded seasonal variability in these concentrations (Meng et al. 2005; O'Driscoll et al. 2005).

2.2 Water sampling and filtration

Bulk surface water samples were collected at 30 cm depth in the center of the lake from a plastic canoe using pre-cleaned (triple-rinsed with both deionized water and then lake water) 26 L HDPE containers and transported in the dark to the CARE lab at Acadia University (http://care.acadiau.ca/) for experiments and analyses. Lake water was vacuum filtered into a glass flask using 0.45 μm hydrophilic polyethersulfone Supor Membrane Disc Filters (Pall) within 24 hours of sampling and refrigerated in the dark at 4^{o}C. Each set of experiments was initiated immediately following filtering in June, August, and October.

2.3 Irradiation experimental design

For each experimental treatment 200 mL of water was poured into twelve triple-rinsed acid-washed (20% HCl) 200 mL quartz beakers (5 cm diameter) and acclimated to room temperature for one hour. There were triplicates for each time point (0, 1, and 2 days) as well as the dark control. Three experimental treatments were performed in each sampling month with varied proportions of photoreactive DOM, DOM concentration, and MeHg concentration. In the present study we refer to photoreactive DOM as the portion of the lake water DOM that absorbs radiation, and specifically UV-A radiation, using absorbance at 350 nm (A_{350}) as a proxy. The chemical conditions for each of the 3 treatments were as follows: Treatment 1. 100% photoreactive DOM: the original amount of photoreactive DOM of the lake water sampled plus a 1 ng L^{-1} addition of MeHg (as MeHg(II)OH Strem Chemicals, Inc.), Treatment 2. <30% photoreactive DOM: <30% remaining of the original amount of photoreactive DOM plus a 1 ng L^{-1} MeHg addition,

and Treatment 3. 100% photoreactive DOM no MeHg spike: the original amount of photoreactive DOM of the lake water sampled but with no MeHg addition (Table 3.1). We chose to spike 2 out of 3 treatments to ensure MeHg concentrations would be detectable in the pre-irradiated treatment (2) and to compare whether the spike would have an effect on photodemethylation rates (Treatment 1 vs Treatment 3). All spiked samples were left in the dark covered by parafilm at room temperature for 1 hour before spiking and 24 hours following MeHg additions to allow for equilibrium between the MeHg and DOM complexes (Hintelmann et al. 1995). Treatment 3 was also kept in the dark at room temperature for 24 hours prior to irradiation.

In the lowered photoreactive DOM experiment (Treatment 2), lake water samples were photochemically preconditioned using irradiation exposure in 200 mL quartz beakers in a LuzChem ORG photoreactor for up to 2 weeks at 47 W m^{-2} UV-A (see Figure A2.1A for solar spectrum graph) until the absorbance at 350 nm was <30% of initial photoreactive DOM absorbance. During each experiment of 12 beakers, 3 beakers were analyzed immediately following the 24 hour post-spike acclimation period, 6 beakers were placed in the photoreactor at 47 W m^{-2} with 3 beakers removed at 24 hours (the equivalent of up to 1 week of *in-situ* summer field solar radiation exposure), 3 beakers removed at 48 hours (the equivalent of up to 2 weeks of *in-situ* summer field solar radiation exposure), and 3 beakers were kept in the dark at room temperature for the duration of the 48 hour experiment as dark controls. Constant radiation was received by each beaker over the exposure time period and due to the short pathlength of each beaker (5 cm) these experiments mimicked surface processes within lakes where solar radiation is not limited. The sum of cumulative UV-A radiation received by each sample at each

beaker location was measured using an Ocean Optics USB 4000 Spectroradiometer with fiber optic probe (see Figure A2.1B for experimental setup in the photoreactor). Cumulative UV-A amounts were corrected for the 11.8% attenuation of UV-A by the quartz beaker walls. Post-irradiation aliquots from each beaker were analyzed for UV-vis absorbance, then preserved using 1% HCl for MeHg analysis and 0.5% BrCl for total mercury analysis, and remaining unpreserved samples refrigerated for a maximum of 48 hours for DOC analysis.

Table 3.1 Initial experimental water characteristics for each treatment (combinations of photoreactive dissolved organic matter (DOM) and methylmercury (MeHg) speikes) (t=0) including DOM concentration, absorbance at 350 nm (A_{350}), specific ultraviolet absorbance ($SUVA_{254}$), ultraviolet spectral slope ratio (UV S_R: $S_{275-290}/S_{350-400}$), MeHg concentration, and corresponding photodemethylation rate constants (k_{PD} for kJ^{-1} and k_{PD}* for UV-A E^{-1}). Concentrations are expressed as means ± 1 standard deviation and rate constants are expressed with standard error associated with the rate.

Month	Treatment	DOM (mg C L^{-1})	A_{350} (AU cm^{-1})	$SUVA_{254}$ (m^{-1} mgC L^{-1})	UV S_R	MeHg (ng L^{-1})	k_{PD} (kJ^{-1})	k_{PD}^* (x 10^{-6} E^{-1})
June	(1) 100% DOM_p + 1ng L^{-1} MeHg spike	10.3 ± 0.0	0.113	3.89	0.93	1.57 ± 0.08	0.125 ± 0.009	6.07 ± 0.45
	(2) <30% DOM_p + 1ng L^{-1} MeHg spike	3.8 ± 0.2	0.017	1.38	1.25	0.87 ± 0.07	0.098 ± 0.015	4.76 ± 0.72
	(3) 100% DOM_p	10.2 ± 0.1	0.117	3.87	0.91	0.29 ± 0.02	0.103 ± 0.016	5.02 ± 0.76
August	(1) 100% DOM_p + 1ng L^{-1} MeHg spike	21.0 ± 0.1	0.251	4.05	0.94	1.54 ± 0.05	0.070 ± 0.005	3.42 ± 0.27
	(2) <30% DOM_p + 1ng L^{-1} MeHg spike	7.2 ± 1.3	0.067	2.05	1.06	0.89 ± 0.03	0.064 ± 0.039	5.42 ± 1.88
	(3) 100% DOM_p	21.2 ± 0.0	0.253	4.08	0.94	0.42 ± 0.02	0.061 ± 0.005	2.97 ± 0.22
October	(1) 100% DOM_p + 1ng L^{-1} MeHg spike	19.1 ± 0.2	0.225	4.03	0.95	1.45 ± 0.07	0.076 ± 0.011	3.68 ± 0.52
	(2) <30% DOM_p + 1ng L^{-1} MeHg spike	6.2 ± 0.7	0.027	1.49	1.47	0.68 ± 0.17	0.089 ± 0.022	4.32 ± 1.07
	(3) 100% DOM_p	19.4 ± 0.0	0.153	2.87	0.98	0.33 ± 0.01	0.057 ± 0.008	2.79 ± 0.40

2.4 Methylmercury analyses

All MeHg aliquots were analyzed using derivatization, purge and trap, and cold vapour atomic fluorescence spectrometry (US EPA Method 1630 was modified for direct ethylation using optimization techniques described by Mansfield and Black (Mansfield and Black 2015) and in Brooks Rand Analytical Notes). Methylmercury was extracted from June samples by distillation while August and October samples were analyzed following direct aqueous ethylation analysis with a Brooks-Rand automated MERX system. All samples were analyzed using the same Model III Brooks-Rand detector. Distillation spike recoveries were on average 62 ± 9% SD (n=11) and direct ethylation spike recoveries were on average 106 ± 8% SD (n=9). Recovery rates were tested in triplicate in all analytical runs (n=1:2 ratio between recovery spikes and analytical samples) and all samples were recovery corrected. Direct aqueous ethylation methods required pH adjustment in the 4.5-5.0 range by 25% KOH addition to ensure efficiency of the 2 M acetate buffer and ethylating agent (1.33 M tetraethylborate in 2% potassium hydroxide) (Brooks-Rand Analytical Notes and tested by (Mansfield and Black 2015)). Samples were also Milli-Q blank corrected (distillation: 0.024 ± 0.016 pg; n=12, and direct ethylation: 0.236 ± 0.326 pg; n=32) with the limit of detection calculated as 3 times standard deviation of blanks (<1 pg; 0.04 ng L^{-1}). Concentrations were calculated based on external calibration curves with a minimum of 5-points ($r^2 > 0.999$). Certified reference material (DORM-3, National Research Council Canada) and ongoing precision and recovery check standards were used to ensure accuracy of the instrument and

calibration with an average recovery of 97% (MeHg concentration = 0.344 ± 0.032 mg kg^{-1}).

2.5 DOC, Fe, and UV-vis absorbance analysis

A Shimadzu TOC-V CPH/TOC-CPN Total Organic Carbon Analyzer with an ASI-V autosampler and internal calibration was used to measure dissolved organic carbon concentration, the quantified measure for DOM concentration (following methods outlined in Haverstock et al. (2012)). Samples were blank corrected with blanks being consistently low (0.1 ± 0.1 mg C L^{-1}; n=49) and 5 ppm inorganic carbon and 5 ppm total carbon check standards had good recoveries (>95%). Limit of detection was calculated as 3 times the standard deviation of the blanks (0.2 mg C L^{-1}). Total iron (Fe) concentrations were measured for each bulk water sample using a PerkinElmer ICP-MS following acidification to 1% HNO_3. The absorbance of each sample was measured using 200-800 nm wavescans on an Ultrospec 3100pro UV/Vis spectrophotometer in a 1.0 cm quartz cuvette with Milli-Q water as a paired reference blank for each scan.

Absorbance coefficients (α) were calculated for all wavelengths (200-800 nm) using the following equation

$$\alpha = A \times 2.303/L \quad \text{(Equation 3.1)}$$

where A is the absorbance intensity at a given wavelength and L is the pathlength (0.01 m). Specific ultraviolet absorbance at 254 nm ($SUVA_{254}$) was then calculated as the absorbance coefficient divided by the DOM concentration (L $(mg\ C)^{-1}$ m^{-1}) using method discussed by Weishaar et al. (2003).

$$SUVA_{254} = (A/L)/[DOM] \quad \text{(Equation 3.2)}$$

Spectral slopes were calculated as linear regressions between wavelength ranges outlined by Helms et al. (2008) and corresponding absorbance coefficients to determine a UV spectral slope ratio (UV $S_R = S_{275\text{-}295}:S_{290\text{-}350}$) as an indicator/index of relative molecular weight/size of photoreactive DOM (Helms et al. 2008). Changes in α, $SUVA_{254}$, and spectral slope ratios were calculated over each experiment and then we correlated those rates with photodemethylation rate constants.

2.6 Data analyses

T-tests were used to determine if the MeHg concentrations significantly ($p<0.05$) changed in dark controls for each treatment to determine if any net dark microbial demethylation or methylation had occurred. If significant loss occurred, treatment samples were corrected for loss of MeHg based on the assumption that microbial activity was a function of time (this occurred in one treatment and is noted in results). While MeHg concentration losses over the experiment had good linear fit ($r's>0.70$; $p's<0.03$), 1st order rate constants were a better fit for photodemethylation and allowed comparison of results with other studies (Lehnherr and St Louis 2009; Fleck et al. 2014; Qian et al. 2014; Jeremiason et al. 2015). Photodemethylation rate constants (k_{PD}; kJ^{-1}) were calculated relative to cumulative UV-A (kJ) energy received as the slope of the 1st order kinetic plot (see Figure A2.2).

$$\ln(MeHg)_{UV\text{-}A} = \ln(MeHg)_0 - (k_{PD} \times \text{cumulative UV-A}) \qquad \text{(Equation 3.3)}$$

The cumulative UV-A received by each beaker was calculated as the UV-A intensity (kJ m^{-2} s^{-1}) multiplied by the cross-sectional area of the beaker (m^2) and the time of exposure (s). Once calculated, these rate constants were then used in ANCOVA models to

determine whether the rates were significantly different across sampling months and within photoreactivity experiments. Pearson's product-moment correlation coefficients (r) were used to test for trends between DOM concentration, initial MeHg concentrations, spectral slope ratios (S_R), and photodemethylation rate constants. Photodemethylation rate constants were also calculated for the cumulative UV-A in units of moles of photons (E^{-1}; Table 3.1).

To assess the impact of photoreactive DOM on photodemethylation of MeHg independent of the changes in photons absorbed between treatments we calculated photodemethylation efficiencies, which are unitless parameters based on the total photodemethylation (decrease of MeHg in moles) per photons absorbed (in moles) by each sample. Thus photodemethylation efficiency (PDE) was calculated as moles of MeHg loss between initial and final samples ($t_0 - t_{48hrs}$) divided by the incoming photons (moles) to the center each beaker (intensity in moles m^{-2} s^{-1} multiplied by the cross-sectional area of the beaker (m^2) and the time of exposure (s)) multiplied by the absorbance at 350 nm (A_{350nm} at 2.5 cm) at t_{24} as a proxy for absorbed UV-A radiation by each experimental treatment (n=3).

$$PDE = (MeHg_0 - MeHg_{48}) / (\text{cumulative UV-A photons @ } t_{48} * A_{350} @ t_{24}) \quad \text{(Equation 3.4)}$$

Absorbance loss over the 48 hour experiment was assumed to be linear given that the radiation intensity was constant and that linear dissolved organic carbon losses were reported in a similar irradiation study from this lake (Haverstock et al. 2012) and t_{24} is the most representative measurement for the entire incubation period. All data manipulation

and statistical analyses were performed in Microsoft Excel 2011 and RStudio version 0.98.501, respectively.

3. RESULTS

3.1 Temporal trends

DOM concentrations increased over 2-fold between the first 2 sampling events. June had the lowest concentrations (10.2 ± 0.1 mg C L^{-1}), whereas August had the highest (21.2 ± 0.0 mg C L^{-1}) followed by October (19.4 ± 0.0 mg C L^{-1}; Table 3.2). This wide range in DOM concentration was reflected in the absorbance at 350 nm (photoreactive DOM), ranging from 0.117 – 0.253 absorbance units (AU) cm^{-1}, however $SUVA_{254}$, an index for aromaticity of DOM source (Helms et al. 2008), was highest in the summer months (8.91 – 9.39 L (mg C)$^{-1}$ m^{-1}) compared to October (6.62 L (mg C)$^{-1}$ m^{-1}). UV S_R increased from summer into fall (June = 0.91, August = 0.94, October = 0.98). MeHg concentrations varied by a factor of almost 2 over the sampling period (0.29 – 0.42 ng L^{-1}) with the highest concentrations in August, followed by October, and then June consistent with DOM concentration trends (Table 3.2). Fe concentrations more than doubled from June to August (184 – 503 μg L^{-1}) and then decreased slightly in October (409 μg L^{-1}) similar to the seasonal pattern of MeHg and DOM concentrations observed.

Table 3.2 Dissolved organic carbon concentration (DOC), absorbance at 350 nm (A_{350}), specific ultraviolet absorbance ($SUVA_{254}$), ultraviolet spectral slope ratio (UV S_R), ultraviolet-visible spectral slope ratio (UV-vis S_R), methylmercury (MeHg) concentration, and total iron (Fe) concentration for Big Dam West lake water at each collection period. Concentration data except iron (n=1) are expressed as means ± 1 standard deviation (n=3).

Month	DOC (mg C L^{-1})	A_{350} (AU cm^{-1})	$SUVA_{254}$ (m^{-1} mgC L^{-1})	UV S_R	MeHg (ng L^{-1})	Fe (µg L^{-1})
June	10.2 ± 0.1	0.117	3.87	0.91	0.29 ± 0.02	184
August	21.2 ± 0.0	0.253	4.08	0.94	0.42 ± 0.02	503
October	19.4 ± 0.0	0.153	2.87	0.98	0.33 ± 0.01	409

3.2 Photodemethylation experiments

All experimental treatments displayed significant MeHg loss due to photodemethylation (Table 3.1; Figure A3.2). There were no significant net losses of MeHg in the dark controls compared to initial (t=0) samples (p's>0.1) with the exception of the June Treatment 3 (t=3.90, p=0.017), which exhibited losses in MeHg (up to 20%) measured in the dark controls. The June Treatment 1 (the same photoreactive DOM water as Treatment 3 but with a MeHg addition), however, did not display a significant net decline in the dark control MeHg (t=1.03, p=0.405). Therefore, only the June Treatment 3 was corrected for the additional dark loss in MeHg. In the irradiation experiments MeHg concentrations decreased by up to 85% in June, and 60% in August and October (Figure 3.2). All 100% photoreactive DOM treatments (Treatment 1 & 3) showed significant increases in UV S_R following irradiation in all sampling months (Table 3.3). Treatment 2 (<30% of original photoreactive DOM) showed no significant changes in UV S_R in any

sampling month (Table 3.3). DOM concentrations in Treatment 2 were also reduced by 63-67% from the *in-situ* lake DOM concentrations used in Treatment 1 and 3 (Table 3.1).

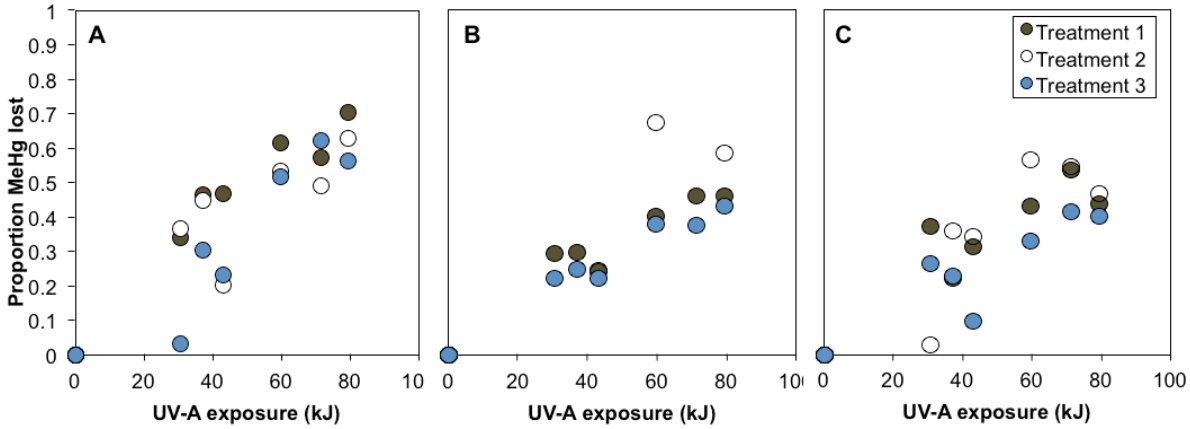

Figure 3.2 The proportion of methylmercury (MeHg) degraded via photodemethylation in each of the three water quality treatments in each of the months (A): June, (B): August, and (C): October. Treatment 1: 100% photoreactive dissolved organic matter (DOM) plus a MeHg spike, Treatment 2: <30% photoreactive DOM plus a MeHg spike, Treatment 3: 100% photoreactive DOM with no MeHg spike.

A MeHg spike of approximately 1 ng L^{-1} MeHg to lake water (Treatment 1; 100% photoreactive DOM) increased the MeHg concentrations by approximately 5 times (Table 3.1) and June photodemethylation rate constants were higher than both August (p<0.001) and October (p=0.044). August and October photodemethylation rate constants were not different (p=0.122). In reduced photoreactive DOM conditions with an addition of approximately 1 ng L^{-1} MeHg to lake water (<30% photoreactive DOM; Treatment 2), there was no significant effect of sampling month on photodemethylation (p=0.819). Within Treatment 3 (*in-situ* photoreactive DOM and MeHg concentrations) photodemethylation rate constants differed by sampling time (June vs. August: p<0.001, June vs. October: p<0.001, August vs. October: p<0.001; Figure 3.3A). Within each

sampling month there were no significant differences among photodemethylation rate constants due to the 3 water quality treatments tested (June: p=0.346, August: p=0.133, October: p=0.309).

Table 3.3 Change in ultraviolet spectral slope ratios (UV S_R; $S_{275-295}$:$S_{350-400}$) within each UV-A exposure experiment for the 3 water quality treatments (combinations of photoreactive dissolved organic matter (DOM_p) and methylmercury (MeHg) spikes) within the 3 collection months. Significant changes in UV S_R are noted by asterisks (*; α=0.05).

Month	Treatment	change in UV S_R	standard error	R^2	p
June	(1) 100% DOM_p + 1ngL^{-1} MeHg spike	0.0020*	0.00026	0.90	0.0006
	(2) <30% DOM_p + 1ngL^{-1} MeHg spike	-0.0075	0.00350	0.37	0.0862
	(3) 100% DOM_p	0.0015*	0.00042	0.66	0.0159
August	(1) 100% DOM_p + 1ngL^{-1} MeHg spike	0.0012*	0.00030	0.71	0.0110
	(2) <30% DOM_p + 1ngL^{-1} MeHg spike	0.0001	0.00471	-0.20	0.9833
	(3) 100% DOM_p	0.0015*	0.00013	0.96	0.0001
October	(1) 100% DOM_p + 1ngL^{-1} MeHg spike	0.0013*	0.00019	0.87	0.0013
	(2) <30% DOM_p + 1ngL^{-1} MeHg spike	-0.0019	0.00332	-0.13	0.5967
	(3) 100% DOM_p	0.0010*	0.00020	0.80	0.0044

Photodemethylation rate constants were not significantly correlated with initial MeHg concentrations over the concentration range tested (0.29 – 1.57 ng L^{-1}) in the irradiation experiments (r=0.290, p=0.450; Figure A2.3). Initial DOM concentration exhibited a weak trend with photodemethylation rate constants (r=-0.584, p=0.098; Figure

A2.4), however, UV S_R was positively correlated with photodemethylation rate constants (R=0.841, p=0.036; Figure A2.5).

Both photoreactive DOM (p<0.0001) and sampling month (p<0.003) affected MeHg photodemethylation efficiency calculated on a per mole of photons absorbed basis (Figure 3.3B). June exhibited greater photodemethylation efficiency than the other sampling months for Treatment 1 and Treatment 3 and both June and August had differences in photodemethylation efficiency between those with 100% of the photoreactive DOM (Treatments 1 & 3) and Treatment 2 where photoreactive DOM was decreased (all p's <0.05). Overall Treatment 2 had the greatest photodemethylation efficiency in June. MeHg photodemethylation efficiency was negatively and significantly correlated with initial DOM concentration (r=-0.786; p=0.012; Figure A2.6).

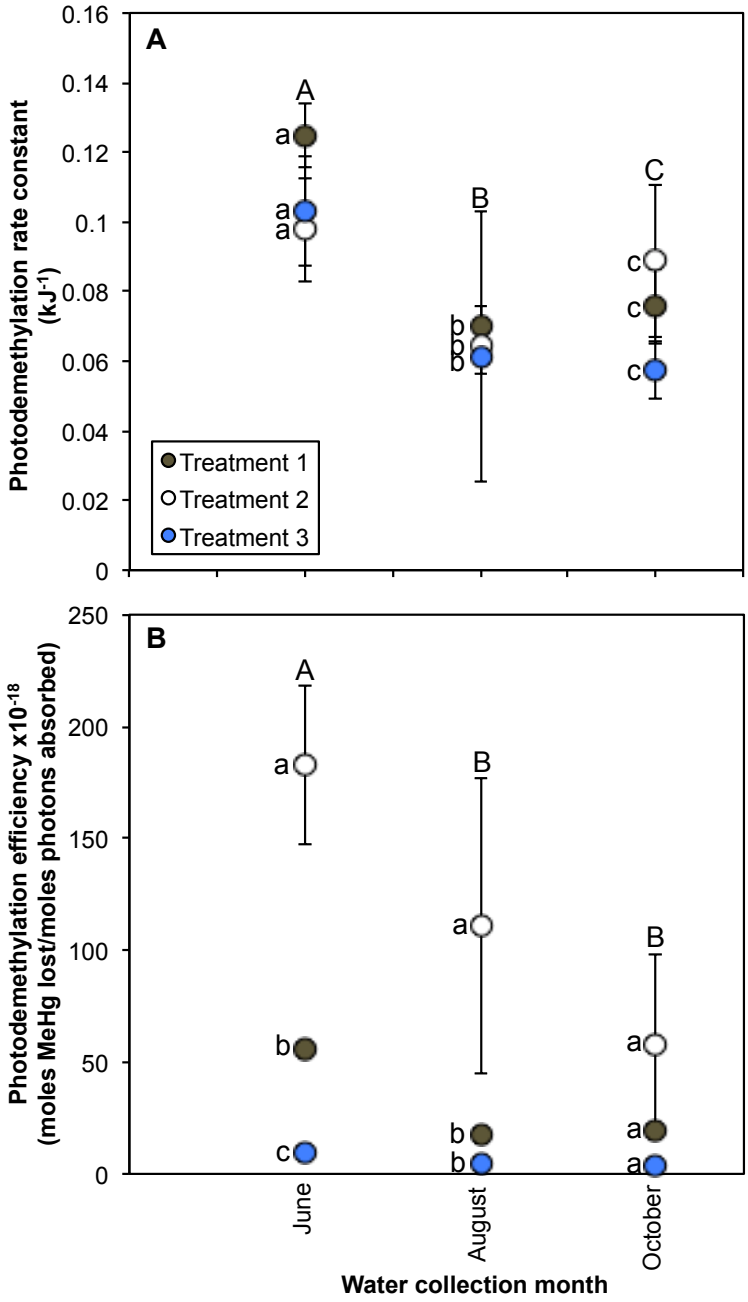

Figure 3.3 (A) Photodemethylation rate constants and (B) photodemethylation efficiency for each collection month's experiments and water quality treatments for each collection month (refer to Figure A2.2 for k_{PD} curves). Treatment 1: 100% photoreactive dissolved organic matter (DOM) plus a 1 ng L^{-1} spike of MeHg, Treatment 2: <30% photoreactive DOM plus a 1 ng L^{-1} addition of MeHg, and Treatment 3: 100% photoreactive DOM. Error bars are standard error on the photodemethylation rate constant calculated using Equation 4.3. Lettering indicates significance (α=0.05): capital letters compare months and small letters compare treatments within months.

4. DISCUSSION

4.1 Photoreactive DOM affects photodemethylation efficiency but not rate

An objective of the present study was to test if there was a relationship between photoreactive DOM and MeHg photodemethylation rate constants. This was carried out by direct photochemical alteration of photoreactive DOM in water samples from one lake. Contrary to our hypothesis that MeHg photodemethylation rate constants would be positively related to the concentration of photoreactive DOM, there were no significant differences between photodemethylation rate constants (using total UV-A energy exposure in kJ) observed across photoreactive DOM treatments (Figure 3.3A). Photoreactive DOM did not affect photodemethylation rate constants but did inversely affect photodemethylation efficiency. This outcome suggested that the loss of photoreactive DOM was balanced by increased photodemethylation efficiency of the DOM.

The influence of DOM is not as straightforward as just attenuating radiation (Li et al. 2010), especially in freshwaters with high concentrations of DOM (Black et al. 2012). Results from multiple scavenger experiments indicate that MeHg photodemethylation can occur through multiple pathways which will change depending on water chemistry and radiation quality (Li et al. 2010). Zhang and Hsu-Kim (2010) quantified photodemethylation occurrence in neutral waters (pH=7-7.4) whereas acidic waters are key for photo-Fenton reactions involving the oxidation of Fe(II) to Fe(III), a byproduct of which is hydroxyl radicals (Southworth and Voelker 2003). Recent work by Fleck et al. (2014) in water from rice fields and a wetland, showed strong relationships between absorbance loss in the 280-400 nm range and MeHg loss (r=0.88-0.88), highlighting that

MeHg may need to be bound directly to DOM in order to undergo photodemethylation. More specifically, lab experiments using targeted scavengers determined that solutions with molecules composed of both thiol and aromatic groups yielded faster rates of photodemethylation than solutions that had molecules containing only thiol or aromatics (Qian et al. 2014). Fluorescence excitation emission matrices (EEMs) confirmed that *in-situ* MeHg concentrations are related to DOM lability or source, whereas loss of MeHg through photodemethylation was correlated with the loss of fulvic or humic portions of DOM, further reiterating the idea of an intramolecular pathway (Fleck et al. 2014).

Lack of significant differences in photodemethylation rate constants reported in the present study between photoreactive DOM treatments (Treatment 1 & Treatment 2) over all sampling months suggest that photons, photoreactants, and PPRIs were not limited in these experiments over the range of photoreactive DOM tested using constant irradiation and beaker path lengths. The reduction of photoreactive DOM from 100% photoreactive DOM to less than 30% photoreactive DOM did not push the ratio between these PPRIs and MeHg below a threshold at which photodemethylation rate constant was enhanced (i.e. Figure 3.1 Pathway 1 is still dominant over Pathways 2 & 3). Additionally, we do not think that residual radicals from the pre-conditioning method, potentially present at the time of Treatment 2 MeHg spike additions, can explain the lack of statistical difference between photoreactive DOM treatments. Samples were stored in the dark for 1 hour prior to MeHg spike additions and the samples were then left at room temperature in the dark to equilibrate (Hintelmann et al. 1995) for 24 hours before experiments commenced. Therefore, any demethylation of MeHg by residual radicals would have happened in all of the pre-irradiated samples before the experiments started

and therefore could not explain the lack of difference in photodemethylation rate constants between the 3 treatments. Photodemethylation rate constants were calculated using Equation 4.3 that uses t_0 (samples that did not go in the photoreactor again), versus samples that were exposed to known amounts of UV-A (samples that were in the photoreactor for 24 to 48 hours).

Fernandez-Gomez et al. (2013) also found that photodemethylation rate constants at specific wavelengths were consistent between natural water samples of varying DOM concentration and absorbance, Fe concentrations, and pH when only the available photons were considered (i.e. when the attenuation effects of dissolved components were removed). Hammerschmidt and Fitzgerald (2010) identified that Fe is not a limiting reactant in Arctic lake photodemethylation reactions even though photo-Fenton reactions can produce reactive oxygen species which can facilitate photodemethylation. Similarly, Fe concentrations increased from June to October in the lake water sampled but there was no corresponding increase in photodemethylation, confirming that Fe was not a limiting reactant in our systems. More recent research by Black et al. (2012) has found that photodemethylation can occur in a variety of wetland surface water types without hydroxyl radical production.

MeHg photodemethylation efficiency is a useful measure to compare the total number of potential photoreactions (moles photons absorbed by DOM + DOM-MeHg complexes) with the number of measured photoreactions (moles MeHg lost; refer to Equation 4.4). Assessing molecular level photoreactions may be more helpful for understanding the relative proportions of photoreactions that are DOM phototransformations (Figure 3.1 Pathway 1) versus intramolecular MeHg

photodemethylation (Figure 3.1 Pathway 2). We hypothesized that treatments with greater photoreactive DOM would yield more photodemethylation (Figure 3.1 Pathways 2 & 3), however the results showed the opposite; the treatments with greater photoreactive DOM had a lower allocation of energy into photodemethylation pathways and therefore more DOM phototransformations that did not involve MeHg (Figure 3.1 Pathway 1). Similarly, there were significantly greater photodemethylation efficiencies in samples with less photoreactive DOM (Treatment 2 > Treatment 1 & Treatment 3; Figure 3.3B). These data further support the idea that freshwaters with lower DOM concentration and photobleached DOM will have greater photodemethylation potential than waters with more photoreactive and overall DOM concentration (Li et al. 2010; Black et al. 2012; Fleck et al. 2014; Poste et al. 2015). These data also support studies that have found lower rates of photodemethylation with depth in water columns, as less energy will be available for photoreactions that involve MeHg (Sellers et al. 1996; Krabbenhoft et al. 2002; Lehnherr and St Louis 2009; Li et al. 2010). More insight can be gained by examining photodemethylation efficiency when more energy is going into photoreactions with DOM and not DOM-MeHg complexes (Figure 3.1 Pathway 1 > Pathway 2 at higher concentrations of photoreactive DOM). The pre-irradiated and pre-photobleached DOM (Treatment 2) resulted in the highest MeHg photodemethylation efficiency and the least amount of DOM photobleaching during our experiments. Photodemethylation efficiencies were highest when there was less photoreactive DOM because a greater proportion of the energy was going into MeHg photoreactions. This conceptual framework for discussing MeHg photodemethylation is new and should not be simply labeled as shading because it provides a more mechanistic understanding of photoreactions in higher carbon systems.

There is still much debate in the literature concerning which PPRIs are driving photodemethylation. All proposed reaction pathways include a photosensitizer or PPRI, and other studies have confirmed that photoreactive DOM is an important variable driving photodemethylation. These previous studies that focused on photodemethylation used a number of physical techniques to alter water chemistry in general and did not specifically target the photoreactive portion of DOM. Specifically, these sample preparation techniques included: altering the DOM content of the water through dilution (Hammerschmidt and Fitzgerald 2010; Black et al. 2012), altering concentration of DOM using reverse osmosis (Black et al. 2012) and cross-flow ultrafiltration (Tai et al. 2014), and using DOM isolate additions to reagent-grade water (Zhang and Hsu-Kim 2010; Qian et al. 2014; Jeremiason et al. 2015). Our results presented here agree that some photoreactive DOM is necessary for this reaction to occur (Qian et al. 2014; Jeremiason et al. 2015) and that photodemethylation is actually more efficient in natural freshwaters with lower amounts of photoreactive DOM and we propose a conceptual mechanistic hypothesis based on competition for radiation energy between DOM and DOM-MeHg complexes. This hypothesis accounts for photoreactive DOM and not simply carbon concentration which could lead to poor prediction of photodemethylation rate constants when only DOM concentration is considered (Black et al. 2012). This finding was identified by quantifying changes in DOM optical properties and would not necessarily be apparent in studies focused on DOM structural analysis and those that used DOM isolates. To our knowledge this is the first study to use prior irradiation to photochemically alter naturally occurring DOM in order to test the effect of photoreactive DOM on photodemethylation of MeHg.

4.2 Seasonal variation in photodemethylation supports DOM competition hypothesis

Another objective of the present study was to examine the effects of seasonal variation in water chemistry on photodemethylation. This objective was carried out through the sampling of water from one freshwater lake 3 times during one year, spanning across the summer-to-fall seasonal transition to capture natural differences in concentrations of photoreactive DOM. Photodemethylation rate constants and efficiencies were greatest in our first sampling month's experimental treatments (June), with the other 2 sampling month's experimental treatments (August and October) being lower and similar.

This seasonal decrease in photodemethylation mirrored an increase in photoreactive DOM from June to the other sampling months and supports a DOM competition hypothesis (Figure 3.1, Pathway 1 vs. Pathway 3). June treatments had the highest rates of photodemethylation and the highest photodemethylation efficiencies, which corresponded to waters with the lowest DOM concentrations, A_{350}, and Fe concentrations, but not the lowest $SUVA_{254}$ (see Table 3.1). In contrast, August had the lowest photodemethylation rate constants, which corresponded with the highest DOM concentration, A_{350}, Fe concentrations and comparable $SUVA_{254}$. These results further suggest that photodemethylation is more likely to occur in waters with lower photoreactive DOM and indicate that photodemethylation was likely in competition for photons, more so in August relative to June or October experiments.

Lake water in June would have resided in the lake for less time since spring runoff (Meng et al. 2005) leading up to sampling compared to the other sampling events and, therefore, likely be the least photobleached relative to the other sampling months. The

lack of statistical differences between photoreactive DOM treatments (Treatments 1 versus 2) on photodemethylation rate constants in June suggests that *in-situ* photobleaching is likely not the reason behind June having the highest photodemethylation rate constants. However, the unaltered DOM in June (Treatments 1 & 3) exhibited the largest change in UV S_R during the irradiation experiments, which indicates that DOM in June was more susceptible to photobleaching than the other months and could explain the significantly higher photodemethylation rate constants overall in June than the other sampling months. June is closer to spring melt and wetland flushing; waters entering lakes in spring would have resided all winter in wetlands or porewaters and be subjected to microbial degradation prior to radiation exposure. The source of DOM was likely not different geographically for this sampling time point but may have been chemically different given other ongoing external processes (hydrology and biological processing).

In natural systems, particularly in shallow, well-mixed lakes, such as Big Dam West lake and many of the other lakes in Kejimkujik National Park, Nova Scotia, surface waters subjected to photobleaching are replenished through daily upwelling and mixing processes. This mixing of water also brings MeHg and DOM to the water surface and PPRIs would be limited to the very surface or few tens of centimeters of the entire lake water column (<10%). Mercury budgets in shallow Arctic ponds (<1 m depth) have highlighted that MeHg photodemethylation is limited to the top 30 cm of the water column, analogous to UV-A attenuation (Lehnherr and St Louis 2009). Our beaker size was chosen to have a maximum path length of 5 cm to avoid any inner shading of photons and mimic surface reactions at our well-mixed study lakes. In contrast, deeper

oligotrophic lakes (>5 m) in the Precambrian shield of the Experimental Lakes Area can have well developed thermal stratification that can facilitate MeHg photodemethylation in the epilimnion, while significant mercury methylation can occur in the hypolimnion (Sellers et al. 2001) with whole lake turnover and mixing only occurring in spring and fall (Morris and Hargreaves 1997). In drier years in-lake production of MeHg can dominate the MeHg budget whereas in wetter years terrestrial and wetlands sources are more important (Sellers et al. 2001) and less vertical mixing is more likely to occur in deeper lakes. In shallow well-mixed lakes, even during periods of low flow: minimal precipitation, outflow from wetlands, and overflow or runoff, these lakes will not develop any thermal stratification apart from the very shallow photic zone and will also not have a well-developed stratified zone of photochemically processed compounds.

Higher photodemethylation rate constants in June than the other sampling months could support the hypothesis that the photoreactive DOM and MeHg entering the lake at different times of years could behave differently in terms of PPRI production and therefore MeHg photodemethylation processes. Furthermore, the higher DOM concentrations in August and October would have reduced the lake's photic and PPRI production zone thus limiting the potential for *in-situ* photoreactions to the near surface of the water column (Scully and Lean 1994; Morris and Hargreaves 1997; Haverstock et al. 2012) prior to sampling and experiments. Seasonal variation of *in-situ* lake water properties caused higher rates of photodemethylation in June compared to later in the year in August and October. Poste et al. (2015) predict that MeHg losses through photodemethylation will be highest in the summer months (May-July) in Norwegian lakes due to incoming photon flux. However, that model (Poste et al. 2015) does not account

for seasonal differences in photoreactive DOM and photodemethylation rate constants were generated using water from one sampling time period, similar to most other MeHg photodemethylation studies (Sellers et al. 1996; Lehnherr and St Louis 2009; Black et al. 2012; Fleck et al. 2014). The observed seasonal variation in photodemethylation supports our experimental evidence that photoreactive DOM is inversely related to photodemethylation potential, due to a competition for photons. This trend could result in reduction of MeHg exposure to the base of food webs in early to mid-summer.

5. CONCLUSIONS

The present study highlights the important relationship between the phototransformation of DOM and MeHg photodemethylation pathways in quantifying the potential role of photodemethylation in high carbon lakes. These results indicate that photoreactions in high carbon systems are dominated by DOM photobleaching and photomineralization (Figure 3.1 Pathway 1) competing successfully with and reducing MeHg photodemethylation reactions. Whereas in lower carbon waters more photons are available for reactions involving DOM-MeHg complexes (Figure 3.1 Pathways 2 & 3) and MeHg photodemethylation efficiency will be greater. This observation of greater photodemethylation efficiency in lower carbon waters could be due to a number of seasonal ecosystem properties including hydrologic regimes that control carbon inputs to lakes, as well as lake water levels and therefore dilution or concentration of solutes within lake basins. The combination of DOM characteristics that result in the greatest reduction of MeHg availability (through photodemethylation pathways) to food webs may, however, correlate with times of the year when in situ MeHg concentrations are already

lowest. An important aspect for future research that examines seasonal bioaccumulation models in lakes. The present study focused on water from one lake but future studies should investigate the effect of DOM on MeHg photodemethylation in different lakes that encompass greater variation in DOM source and MeHg inputs. Future studies should also further address the use of photon absorption along with irradiance in modeling efforts for understanding the potential role of photodemethylation in freshwaters sensitive to mercury contamination.

Acknowledgments

Funding for the present research was provided from the National Science and Engineering Council (NSERC) of Canada in the form of Discovery and Canada Research Chair Grants to N.J.O and an NSERC CREATE scholarship to S.J.K. In addition, funding for N.J.O. through the Canada Foundation for Innovation and for D.A.R. through an NSERC Discovery Grant is acknowledged. Logistical field and laboratory support provided by Parks Canada (Chris McCarthy), E. Mann, L. Klapstein, L. Graham, J. Egan, the Mersey Tobeatic Research Institute, and Acadia University.

References

Black, F. J., B. A. Poulin, and A. R. Flegal. 2012. Factors controlling the abiotic photo-degradation of monomethylmercury in surface waters. Geochim. Cosmochim. Acta **84**: 492–507. doi:10.1016/j.gca.2012.01.019

Bloom, N. S. 1992. On the chemical form of mercury in edible fish and marine invertebrate tissue. Can. J. Fish. Aquat. Sci. **49**.

Chen, J., S. O. Pehkonen, and C.-J. Lin. 2003. Degradation of monomethylmercury chloride by hydroxyl radicals in simulated natural waters. Water Res. **37**: 2496–2504. doi:10.1016/S0043-1354(03)00039-3

Evers, D. C., Y.-J. Han, C. T. Driscoll, and others. 2007. Biological mercury hotspots in the Northeastern United States and Southeastern Canada. BioScience **57**: 29–43. doi:10.1641/B570107

Fernández-Gómez, C., A. Drott, E. Björn, S. Díez, J. M. Bayona, S. Tesfalidet, A. Lindfors, and U. Skyllberg. 2013. Towards universal wavelength-specific photodegradation rate constants for methyl mercury in humic waters, exemplified by a boreal lake-wetland gradient. Environ. Sci. Technol. 130529101435009. doi:10.1021/es400373s

Fleck, J. A., G. Gill, B. A. Bergamaschi, T. E. C. Kraus, B. D. Downing, and C. N. Alpers. 2014. Concurrent photolytic degradation of aqueous methylmercury and dissolved organic matter. Sci. Total Environ. **484**: 263–275. doi:10.1016/j.scitotenv.2013.03.107

Hammerschmidt, C. R., and W. F. Fitzgerald. 2006. Photodecomposition of methylmercury in an Arctic Alaskan lake. Environ. Sci. Technol. **40**: 1212–1216. doi:10.1021/es0513234

Hammerschmidt, C. R., and W. F. Fitzgerald. 2010. Iron-mediated photochemical decomposition of methylmercury in an Arctic Alaskan lake. Environ. Sci. Technol. **44**: 6138–6143. doi:10.1021/es1006934

Haverstock, S., T. Sizmur, J. Murimboh, and N. J. O'Driscoll. 2012. Modeling the photo-oxidation of dissolved organic matter by ultraviolet radiation in freshwater lakes: Implications for mercury bioavailability. Chemosphere **88**: 1220–1226. doi:10.1016/j.chemosphere.2012.03.073

Helms, J. R., A. Stubbins, J. D. Ritchie, E. C. Minor, D. J. Kieber, and K. Mopper. 2008. Absorption spectral slopes and slope ratios as indicators of molecular weight, source, and photobleaching of chromophoric dissolved organic matter. Limnol. Oceanogr. **53**: 955.

Hintelmann, H., P. M. Welbourn, and R. D. Evans. 1995. Binding of methylmercury compounds by humic and fulvic acids. Water. Air. Soil Pollut. **80**: 1031–1034. doi:10.1007/BF01189760

Jeremiason, J. D., T. K. Reiser, R. A. Weitz, M. E. Berndt, and G. R. Aiken. 2016. Aeshnid dragonfly larvae as bioindicators of methylmercury contamination in

aquatic systems impacted by elevated sulfate loading. Ecotoxicology. doi:10.1007/s10646-015-1603-9

Jeremiason, J., J. C. Portner, G. Aiken, K. T. Tran, M. T. Dvorak, A. Hiranaka, and D. Latch. 2015. Photoreduction of Hg(II) and photodemethylation of methylmercury: The key role of thiol sites on dissolved organic matter. Environ. Sci. Process. Impacts. doi:10.1039/C5EM00305A

Krabbenhoft, D. P., M. L. Olson, J. F. Dewild, D. W. Clow, R. G. Striegl, M. M. Dornblaser, and P. VanMetre. 2002. Mercury loading and methylmercury production and cycling in high-altitude lakes from the Western United States. Water Air Soil Pollut. Focus **2**: 233–249. doi:10.1023/A:1020162811104

Lehnherr, I., and V. L. St Louis. 2009. Importance of ultraviolet radiation in the photodemethylation of methylmercury in freshwater ecosystems. Environ. Sci. Technol. **43**: 5692–5698.

Li, Y., Y. Mao, G. Liu, G. Tachiev, D. Roelant, X. Feng, and Y. Cai. 2010. Degradation of methylmercury and its effects on mercury distribution and cycling in the Florida Everglades. Environ. Sci. Technol. **44**: 6661–6666. doi:10.1021/es1010434

Mansfield, C. R., and F. J. Black. 2015. Quantification of monomethylmercury in natural waters by direct ethylation: Interference characterization and method optimization. Limnol Ocean. Methods **13**: 81–91.

Meng, F.-R., P. Arp, A. Sangster, and others. 2005. Modeling dissolved organic carbon, total and methyl mercury in Kejimkujik freshwaters, p. 1–19. *In* Mercury cycling in a wetland-dominated ecosystem: a multidisciplinary study. Society of Environmental Toxicology and Chemistry (SETAC).

Mergler, D., H. A. Anderson, L. H. M. Chan, K. R. Mahaffey, M. Murray, M. Sakamoto, A. H. Stern, and Panel on Health Risks and Toxicological Effects of Methylmercury. 2007. Methylmercury exposure and health effects in humans: A worldwide concern. Ambio J. Hum. Environ. **36**: 3–11.

Morel, F. M. M., A. M. L. Kraepiel, and M. Amyot. 1998. The chemical cycle and bioaccumulation of mercury. Annu. Rev. Ecol. Syst. **29**: 543–566.

Morris, D. P., and B. R. Hargreaves. 1997. The role of photochemical degradation of dissolved organic carbon in regulating the UV transparency of three lakes on the Pocono Plateau. Limnol. Oceanogr. **42**: 239–249.

O'Driscoll, N. J., A. N. Rencz, and D. R. S. Lean. 2005. Review of factors affecting mercury fate in Kejimkujik Park, Nova Scotia, p. 7–20. *In* Mercury cycling in a wetland-dominated ecosystem: a multidisciplinary study. SETAC.

Poste, A. E., H. F. V. Braaten, H. A. de Wit, K. Sørensen, and T. Larssen. 2015. Effects of photodemethylation on the methylmercury budget of boreal Norwegian lakes. Environ. Toxicol. Chem. n/a-n/a. doi:10.1002/etc.2923

Qian, J., U. Skyllberg, W. Frech, W. F. Bleam, P. R. Bloom, and P. E. Petit. 2002. Bonding of methyl mercury to reduced sulfur groups in soil and stream organic matter as determined by x-ray absorption spectroscopy and binding affinity studies. Geochim. Cosmochim. Acta **66**: 3873–3885. doi:10.1016/S0016-7037(02)00974-2

Qian, Y., X. Yin, H. Lin, B. Rao, S. C. Brooks, L. Liang, and B. Gu. 2014. Why dissolved organic matter enhances photodegradation of methylmercury. Environ. Sci. Technol. Lett. **1**: 426–431. doi:10.1021/ez500254z

Scully, N. M., and D. R. S. Lean. 1994. The attenuation of ultraviolet radiation in temperate lakes. Erg Limnol **43**: 135–144.

Scully, N. M., D. J. McQueen, D. R. S. Lean, and W. J. Cooper. 1995. Photochemical formation of hydrogen peroxide in lakes: effects of dissolved organic carbon and ultraviolet radiation. Can. J. Fish. Aquat. Sci. **52**: 2675–2681.

Sellers, P., C. A. Kelly, and J. W. M. Rudd. 2001. Fluxes of methylmercury to the water column of a drainage lake: The relative importance of internal and external sources. Limnol. Oceanogr. **46**: 623–631. doi:10.4319/lo.2001.46.3.0623

Sellers, P., C. A. Kelly, J. W. M. Rudd, and A. R. MacHutchon. 1996. Photodegradation of methylmercury in lakes. Nature **380**: 694–697. doi:10.1038/380694a0

Southworth, B. A., and B. M. Voelker. 2003. Hydroxyl radical production via the photo-Fenton reaction in the presence of fulvic acid. Environ. Sci. Technol. **37**: 1130–1136. doi:10.1021/es020757l

Tai, C., Y. Li, Y. Yin, L. J. Scinto, G. Jiang, and Y. Cai. 2014. Methylmercury photodegradation in surface water of the Florida Everglades: Importance of dissolved organic matter-methylmercury complexation. Environ. Sci. Technol. **48**: 7333–7340. doi:10.1021/es500316d

Tossell, J. A. 1998. Theoretical study of the photodecomposition of methyl Hg complexes. J. Phys. Chem. A **102**: 3587–3591. doi:10.1021/jp980244u

Twardowski, M. S., E. Boss, J. M. Sullivan, and P. L. Donaghay. 2004. Modeling the spectral shape of absorption by chromophoric dissolved organic matter. Mar. Chem. **89**: 69–88. doi:10.1016/j.marchem.2004.02.008

Walters, D. M., T. D. Jardine, B. S. Cade, K. A. Kidd, D. C. G. Muir, and P. Leipzig-Scott. 2016. Trophic magnification of organic chemicals: A global synthesis. Environ. Sci. Technol. doi:10.1021/acs.est.6b00201

Weishaar, J. L., G. R. Aiken, B. A. Bergamaschi, M. S. Fram, R. Fujii, and K. Mopper. 2003. Evaluation of specific ultraviolet absorbance as an indicator of the chemical composition and reactivity of dissolved organic carbon. Environ. Sci. Technol. **37**: 4702–4708. doi:10.1021/es030360x

Wyn, B., K. A. Kidd, N. M. Burgess, R. A. Curry, and K. R. Munkittrick. 2010. Increasing mercury in yellow perch at a hotspot in Atlantic Canada, Kejimkujik National Park. Environ. Sci. Technol. **44**: 9176–9181.

Zepp, R. G., P. F. Schlotzhauer, and R. M. Sink. 1985. Photosensitized transformations involving electronic energy transfer in natural waters: role of humic substances. Environ. Sci. Technol. **19**: 74–81. doi:10.1021/es00131a008

Zhang, T., and H. Hsu-Kim. 2010. Photolytic degradation of methylmercury enhanced by binding to natural organic ligands. Nat. Geosci. **3**: 473–476. doi:10.1038/ngeo892

Chapter 4 : DISSOLVED ORGANIC MATTER INHIBITS FRESHWATER METHYLMERCURY PHOTODEMETHYLATION

Sara J. Klapstein[a,b], Susan E. Ziegler[a], Nelson J. O'Driscoll[b]

[a]Department of Environmental Science, Memorial University of Newfoundland, St. John's NL, Canada

[b]Department of Earth & Environmental Science, Acadia University, Wolfville NS, Canada

Abstract

Photodemethylation can be one of the primary processes for loss of neurotoxic methylmercury (MeHg) in freshwater lakes. Few studies have quantified seasonal variations in photodemethylation rate constants as a function of dissolved organic matter (DOM) concentration. We conducted 1-week irradiation experiments in two seasons to test for spatial and temporal differences in photodemethylation potential in temperate lake waters. Six study lakes in Kejimkujik National Park, Nova Scotia were sampled in summer and fall to include a range of naturally occurring DOM concentrations (4.4 – 13.4 and 3.9 – 16.4 mg C L^{-1}, respectively). A significant negative linear relationship (R^2=0.76, *p*=0.01) was found between DOM concentration and photodemethylation rate constant across seasons, indicating that DOM is a strong predictor of MeHg photodemethylation independent of seasonal effects. The two highest carbon lakes (BDW and PEB) had significantly higher energy-normalized photodemethylation rate constants in summer compared to fall corresponding with lower DOM concentrations in summer relative to fall. Additionally, there were negative linear relationships between MeHg photodemethylation and DOM photomineralization (R^2s=0.58-0.72) and DOM photobleaching (R^2s=0.83-0.90). This key finding suggests that competition for photons by DOM may reduce the potential for MeHg photodemethylation in high carbon waters and that this relationship persists across seasons.

1. INTRODUCTION

Methylmercury (MeHg) contamination through bioaccumulation and biomagnification in aquatic food webs is an issue in many remote ecosystems far from direct pollution sources (Evers et al. 2007; Wyn et al. 2010; Kidd et al. 2011; Lehnherr 2014). Understanding why some ecosystems are more sensitive to contamination following atmospheric mercury deposition and quantifying this effect is key to mercury fate modeling and mitigating mercury contamination in food webs. It is clear that dissolved organic matter (DOM) is a key variable in freshwaters. Once MeHg is in the water column it may be degraded through photodemethylation processes (Sellers et al. 1996) and the balance between the formation and degradation of MeHg will be an important factor controlling the availability of MeHg to the base of the food web (primary producers) in the water column.

Photodemethylation is an abiotic process that can be responsible for the majority (58-80%) of the MeHg loss in low nutrient freshwater Arctic ponds (Hammerschmidt and Fitzgerald 2006; Lehnherr et al. 2012) and temperate lakes (Sellers et al. 1996). The process of photodemethylation is also important in high carbon and nutrient-rich systems such as temperate California wetlands (Black et al. 2012; Fleck et al. 2014) and temperate-tropical Florida Everglades (Li et al. 2010). Solar radiation varies vertically as well as horizontally within a lake, and consequently, photodemethylation rate constants decrease dramatically with depth through freshwater lake columns (Sellers et al. 1996; Krabbenhoft et al. 2002) and this consistent pattern is due to the decrease in transmitted solar radiation (Scully and Lean 1994; Morris et al. 1995), particularly the ultraviolet (UV) wavebands (Lehnherr and St Louis 2009). The attenuation of UV wavelengths by

DOM occurs rapidly in temperate lakes (Scully and Lean 1994) with extinction of UV-A in high carbon lakes of Kejimkujik National Park, Nova Scotia occurring in the top 20-30 cm of the water column (Haverstock et al. 2012).

The purpose of this study was to determine how photodemethylation rate constants vary across a series of lakes in response to DOM (concentration and photoreactivity) and sampling season. Methylmercury is associated with DOM (DOM-MeHg) in complexes, however in high DOM waters the proportion of DOM that is associated with MeHg (DOM-MeHg) will decrease and this MeHg-free DOM may be critical in regulating photodemethylation reactions. We hypothesized that photodemethylation rate constants would decrease with increasing DOM concentration due to an increase in the ratio between DOM and DOM-MeHg complexes. An increase in that ratio would result in increased competition for photons in the photochemical reactions involving solely DOM versus DOM-MeHg complexes. At low DOM concentrations, DOM facilitates photodemethylation of a larger proportion of photoreactive DOM-MeHg complexes and DOM that is not associated with MeHg will not dominate the photoreactions in these waters (4.1a). Conversely, at higher DOM concentrations DOM inhibits photodemethylation by dominating the photoreactions through photon absorbance in these waters (Figure 4.1b). Photodemethylation will still occur in high DOM waters but at a limited rate because a smaller proportion of the photoreactions will involve DOM-MeHg complexes. To test these hypotheses, we used water collected from 6 lakes in both the summer and fall and exposed the water samples to the full natural solar radiation spectrum during each collection season. These findings present a simplified framework for predicting energy-normalized photodemethylation rate

constants among similar freshwaters using basic DOM characteristics (i.e. concentration and optical properties).

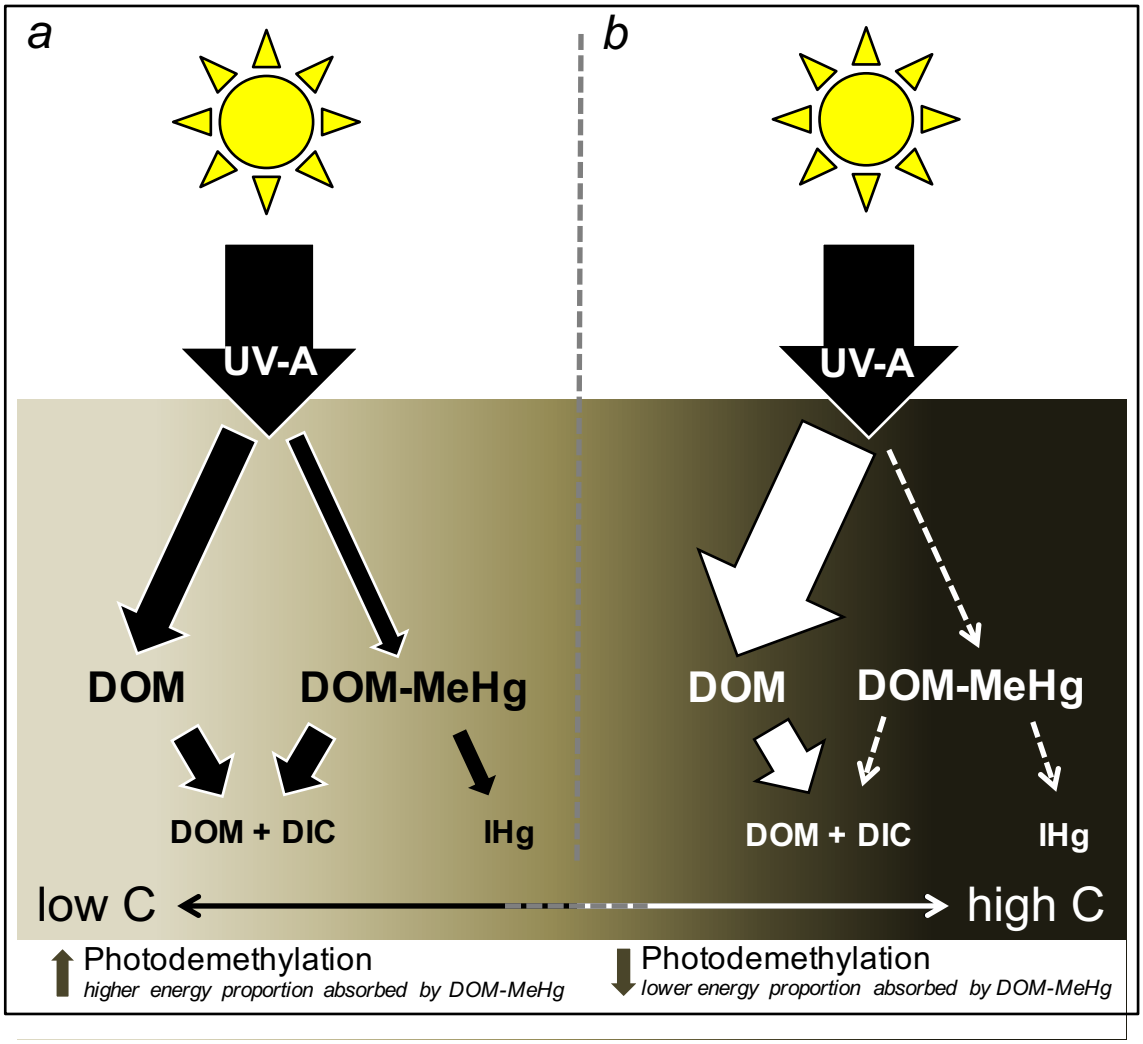

Figure 4.1 Conceptual figure displaying interactions between dissolved organic matter (DOM) and methylmercury (MeHg) with regard to the relative use of photons for photodemethylation as compared to photobleaching and photomineralization of DOM. At low carbon (C) concentrations (a), DOM facilitates photodemethylation through the creation of a larger proportion of photoreactive DOM-MeHg complexes and DOM that is not associated with MeHg will not dominate the photoreactions in these waters. At high C concentrations (b), DOM inhibits photodemethylation by dominating the photoreactions through photon absorbance. A smaller proportion of the photoreactions will involve DOM-MeHg complexes in higher than lower C freshwaters.

2. MATERIALS & METHODS

2.1 Sampling sites for freshwater of varying DOM

Six lakes in Kejimkujik National Park (Nova Scotia), a biological mercury hot spot (Evers et al. 2007; Wyn et al. 2010; Little et al. 2015), were sampled to include a range of DOM concentrations (3.9 – 16.4 mg C L^{-1}) (O'Driscoll et al. 2005). Sample sites included: Big Dam East (BDE), Puzzle (PUZ), North Cranberry (NCR), Peskawa (PES), Big Dam West (BDW), and Pebbleloggitch (PEB) lakes. Water was collected from BDW in spring (mid-May), all 6 lakes in summer (last week of June), and all 6 lakes in fall (last week of September). Bulk water samples were collected from the side of a plastic canoe in the middle of each lake at 30 cm depth using triple-rinsed (with Milli-Q and lake water) HDPE containers (>10 L).

2.2 Experimental setup

All irradiation experiments took place in the K.C. Irving Center experimental gardens at Acadia University. Sample bottles were placed in natural solar radiation conditions and HOBO® temperature data loggers (model #UA-001-64) programmed to record temperature (± 0.05°C) every 5 minutes were placed inside bottles (n=6 per experiment) to record temperature during each experiment. Solar radiation was measured and recorded every 5 minutes by an Ocean Optics USB 4000 spectroradiometer in spring and fall and an Ocean Optics Jaz spectroradiometer with a 10 m fiber optic cable and diffuse attenuation probe in summer. Cumulative solar radiation exposure (kJ m^{-2}) was calculated by measuring the incoming solar radiation intensity (W m^{-2}) at 5-minute intervals and summing for the corresponding exposure time periods. Meteorological

parameters such as wind speed and direction, humidity, total solar radiation energy, and rainfall were also recorded using a Davis Vantage Pro 2 meteorological station.

2.3 Sample preparation and analyses

In spring, experimental treatments included 0.45 μm filtered (polyethersulfone membrane) and unfiltered water from one lake (BDW lake) to test the effect of particulates on photodemethylation rate constants. In summer and fall 0.45 μm filtered water was collected from six lakes (BDE, PUZ, NCR, PES, BDW, and PES lakes) to quantify temporal and spatial differences in DOM on photodemethylation rate constants.

Polytetrafluoroethylene (PTFE) bottles were used for all irradiations in the experimental design to minimize losses in ultraviolet (UV) radiation due to absorption by the container walls (measured attenuation was 16 - 30% in the 320-400 nm region depending on bottle wall thickness) and the incoming UV-A was corrected for wall attenuation to determine the energy reaching each sample. Each 500 mL of lake water was spiked to have a concentration increase of 3 ng L^{-1} MeHgOH (Strem Chemicals, Inc.), swirled in the PTFE bottle to mix, and left capped in the dark at room temperature to equilibrate for 12 hours before being placed outside after sunset. This was done to allow for ambient temperature equilibrium prior to the solar radiation exposure. These spiked MeHg concentrations were within 10x of the naturally occurring MeHg concentrations in lakes within Kejimkujik National Park (O'Driscoll et al. 2005). Dark controls for each treatment were covered with 3 layers of aluminum foil to block radiation. Sample bottles for each lake were collected after sunset to minimize variations in radiation exposure between replicates after exposure times of 0, 1, 2, 3, 5, and 7 days.

Aliquots from each bottle were preserved for MeHg analysis to 0.5% HCl, total mercury (THg) to 0.5% BrCl, dissolved organic carbon with <1 week refrigeration, and optical measurements were measured immediately. The pH range across all treatments and lakes was 4.32 – 5.24 in summer and 3.67 – 5.22 in fall (Table A3.1). MeHg was measured using direct aqueous ethylation, purge and trap, and cold vapour atomic fluorescence spectrometry on a Brooks-Rand MERX system with a Modell III detector (US EPA Method 1630). Samples were pH adjusted to 4.5-5.0 using 25% KOH and 2M acetate buffer to optimize recovery efficiency of the method (Mansfield and Black 2015). Results were blank corrected and MeHg concentrations were calculated using appropriate calibration curves (MeHg stock: MeHg(II)OH Strem Chemicals, Inc.). Certified reference material DORM-4 (NRC; 102.5 ± 11.7% recovery, n=6), and check standards of 50 pg MeHg (99.8 ± 8.6% recovery, n=54) were run throughout each run to ensure accuracy and precision of the standards and the instrument. Matrix spikes were used to ensure ethylation efficiency within water samples and most measured as within 10% of expected concentrations (103.6 ± 9.5% recovery, n=42) and all sample MeHg concentrations were spike recovery corrected. The 1.39 pg limit of detection was calculated as three times the standard deviation of the blanks (0.28 ± 0.46 pg, n=42). THg was measured using reduction, purge and gold amalgamation trap, atomic fluorescence spectrometry (US EPA Method 1631) on a Tekran 2600. Results were blank corrected (0.13 ± 0.16 ng L^{-1}, n=29) and check standards were run every 10-12 runs (recoveries: 99.5 ± 6.2%, n=22). DOM was measured as DOC on a Shimadzu TOC-V_{CPH} total organic carbon analyzer with an ASI-V autosampler. Quality assurance included organic carbon and inorganic carbon calibration and blank correction (0.07 ± 0.12 mg C L^{-1}, n=38). Iron (Fe) concentration

was measured on a Perkin-Elmer ICP-MS. Absorbance for 200-800 nm was measured on each sample using a scanning spectrophotometer (Ultrospec 3100pro UV/Vis) with a 1.0 cm quartz cuvette with a paired reference blank of Milli-Q water. $SUVA_{254}$ was calculated as the absorbance at 254nm (A_{254}) divided by DOM concentration.

2.4 Data analyses

All data manipulation and statistical tests were carried out in Microsoft Excel for Mac 2011 and RStudio 0.98.501. Energy-normalized MeHg photodemethylation rate constants (k_{PD}; $m^2\ kJ^{-1}$) were calculated as the slope of the first-order kinetic plot of MeHg loss ($ng\ L^{-1}$) relative to cumulative UV-A (320-400 nm) energy received ($kJ\ m^{-2}$):

$$\ln(MeHg)_f = \ln(MeHg)_i - (k_{PD} * \text{cumulative UV-A}) \quad \text{(Equation 4.1)}$$

Similarly phototransformations of DOM were calculated/measured as the linear slope of DOM loss ($mg\ C\ L^{-1}$) relative to cumulative UV-A energy received ($kJ\ m^{-2}$) for DOM photomineralization (k_{PM}):

$$DOM_f = DOM_i + (k_{PM} * \text{cumulative UV-A}) \quad \text{(Equation 4.2)}$$

and the linear slope of the loss of absorbance at 350 nm (A_{350}) relative to cumulative UV-A energy received ($kJ\ m^{-2}$) for DOM photobleaching (k_{PB}):

$$A_{350f} = A_{350i} + (k_{PB} * \text{cumulative UV-A}) \quad \text{(Equation 4.3)}$$

For inter-study comparison of currently published photodemethylation rate constants, photodemethylation rate constants were also calculated as the slope of the first-order kinetic plot of MeHg loss ($ng\ L^{-1}$) relative to cumulative photosynthetically active radiation (PAR; 400-800 nm) photons received ($E\ m^{-2}$):

$$\ln(MeHg)_f = \ln(MeHg)_i - (k_{PD} * \text{cumulative PAR photons}) \quad \text{(Equation 4.4)}$$

Energy-normalized photodemethylation rate constants were compared using ANCOVA models to test for significant differences between experimental treatments. T-tests were used to test for differences in DOM concentrations between seasons for each individual lake. 95% confidence intervals for photodemethylation rate constants were calculated as 1.96 * standard error. Linear regression was used to quantify the dependence of photodemethylation rate constants on DOM concentration. Pearson's product-moment correlation coefficients (r) were used to test for relationships between DOM photoreactions (photomineralization and photobleaching) and photodemethylation. Linear regressions were used to define these relationships and ANCOVAs were used to test for the effects of season on photodemethylation versus photoreactions involving DOM (photomineralization and photobleaching).

3. RESULTS

3.1 Effects of season on MeHg photodemethylation

Seasonal trends in photodemethylation rate constants were measured in controlled experiments using water collected in summer and fall from 6 lakes. Quantified photodemethylation rate constants were significantly higher in 2 out of 6 lakes in summer as compared to fall (Figure 4.2a); the two lakes with the highest DOM concentration (BDW and PEB) where 95% confidence intervals did not overlap (Figure 4.2b). Over the 1-week summer experiment there was 5515 kJ m^{-2} of UV-A radiation received compared to a 1-week period in fall when there was 2596 kJ m^{-2} of UV-A radiation received, a two-fold difference (Table A3.1). Similarly, the proportion of MeHg lost over the 1-week irradiation period in each of these experiment sets was 78-94% in summer and 36-75% in

fall (Figure 4.3b & 4.3c). Within the lakes there were some significant temporal shifts in DOM and Fe concentrations, for example BDW increased over two-fold in DOM concentration from 7.0 ± 0.0, 12.8 ± 0.0, and 16.4 ± 0.4 mg C L^{-1} in spring, summer, and fall, respectively (Table 4.1). Dissolved organic matter concentrations significantly decreased from summer to fall in all lakes except BDW and PEB, which exhibited a significant increase in DOM concentration (all *p*'s <0.05; Figure 4.2b). Initial Fe concentrations also changed dramatically with season (Table 4.1) and were positively correlated with DOM concentration (r=0.92, $p<0.01$). BDE, BDW, and PEB increased in Fe from summer to fall, while PUZ decreased, and NCR and PES showed no significant change with season. Lakes with lower DOM concentration (BDE, PUZ, and NCR) consistently had less than 100 μg L^{-1} dissolved Fe compared to higher DOM lakes (PES, BDW, and PEB) which aside from BDW in spring (Fe = 86.5 μg L^{-1}), were always over 100 μg L^{-1}. Water temperatures were on average 21.41 ± 5.05°C in summer compared to 13.59 ± 3.57˚C in fall but were constant across the treatments (days) within each experiment in each season because the water temperatures reflect air temperature fluctuations, similar to very surface layers of lakes (Figure A3.4).

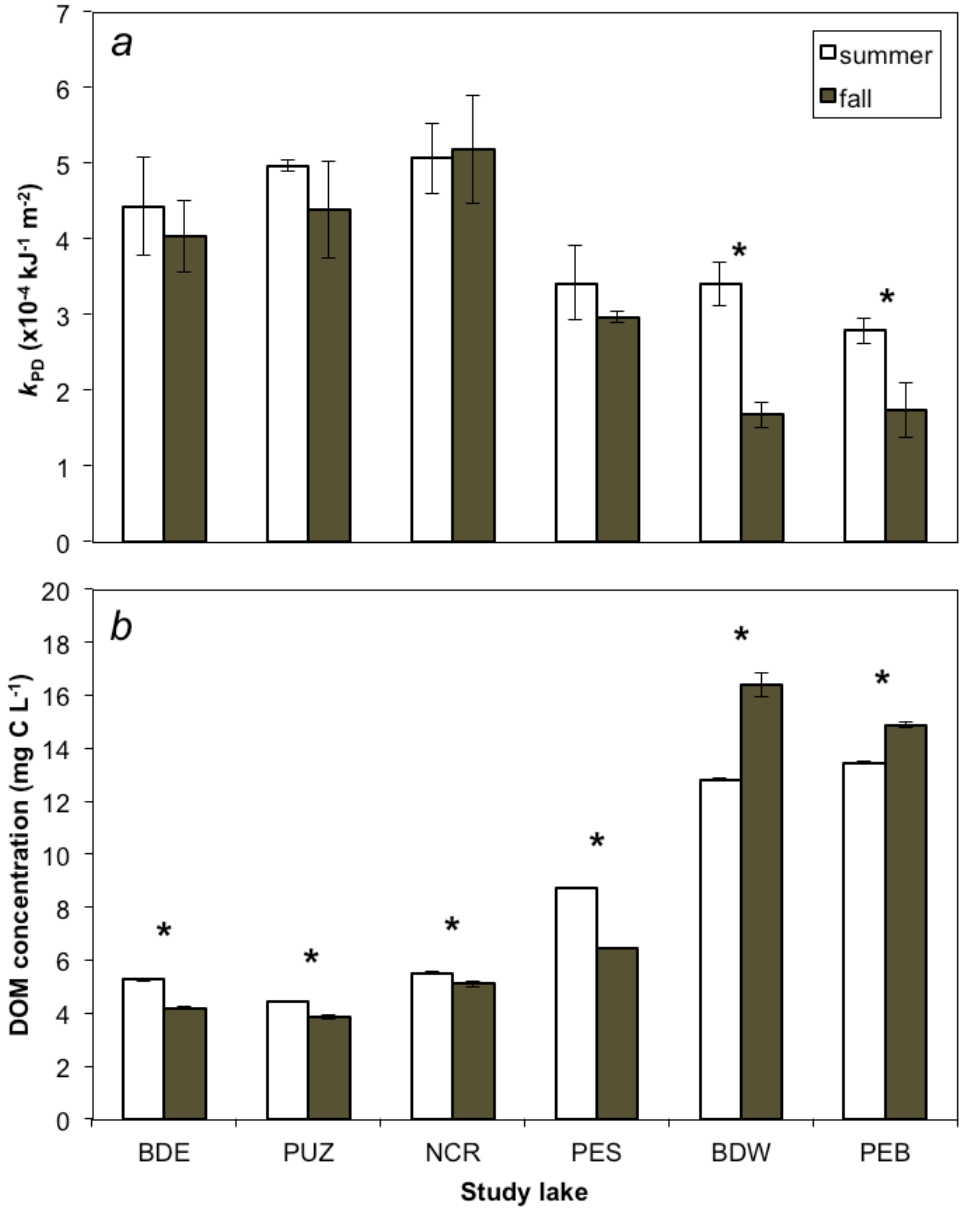

Figure 4.2 (a) Energy-normalized photodemethylation rate constants (k_{PD}) with 95% confidence intervals as error bars and (b) average dissolved organic matter (DOM) concentration with error bars as one standard deviation as a function of season for the 6 study lakes. *denote lakes for which (a) k_{PD} do not overlap with 95% confidence and (b) DOM is significantly different (p<0.05).

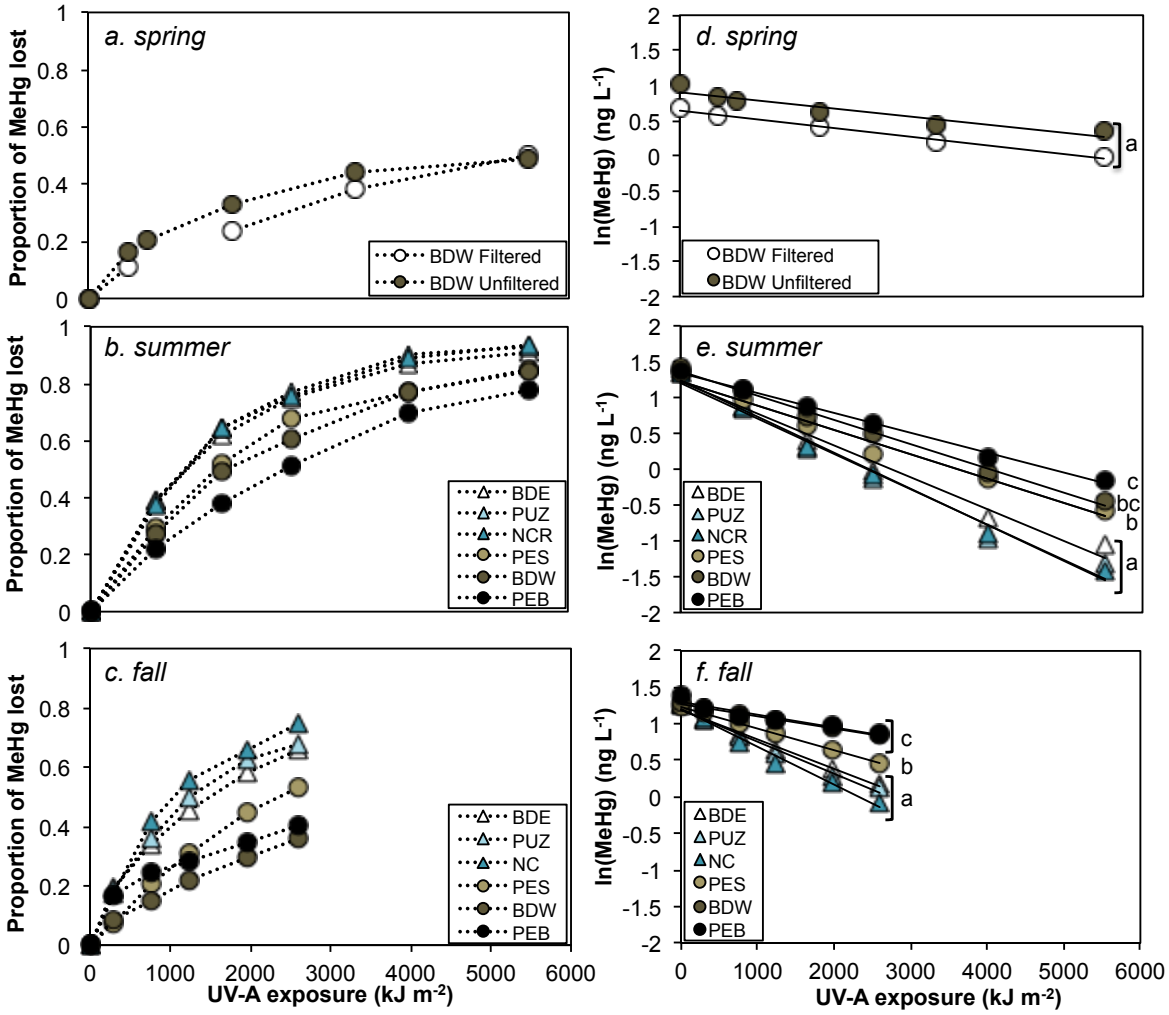

Figure 4.3 Proportion of methylmercury (MeHg) lost over 1-week irradiation experiments in (*a*) spring Big Dam West (BDW) filtered lake water and unfiltered lake water, (*b*) summer Big Dam East (BDE), Puzzle (PUZ), North Cranberry (NCR), Peskawa (PES), BDW, and Pebbleloggitch (PEB) filtered lake water, and (*c*) fall filtered lake water for the same 6 lakes and the corresponding natural log transformed MeHg concentration losses over the same 1-week irradiation experiments in (*d*) spring, (*e*) summer, and (*f*) fall. Different letters in *d*, *e*, and *f* represent photodemethylation rate constants (k_{PD}s that are significantly different at 95% confidence).

Table 4.1 Initial methylmercury (MeHg), dissolved organic matter (DOM), iron (Fe) concentrations and the resultant MeHg photodemethylation rate constants (k_{PD}), DOM photomineralization rates (k_{PM}), and DOM photobleaching rates (k_{PB}) determined from 1-week irradiation experiments in spring, summer, and fall for the study lakes Big Dam West (BDW), Big Dam East (BDE), Puzzle (PUZ), North Cranberry (NCR), Peskawa (PES), and Pebbleloggitch (PEB). All reaction rates are significant (p<0.05) and expressed with corresponding standard error on slope values.

Season	Lake	MeHg (ng L^{-1})	DOM (mg C L^{-1})	Fe (µg L^{-1})	$SUVA_{254}$ (L mg C^{-1} m^{-1})	k_{PD} x10^{-4} (kJ m^{-2})	k_{PM} x10^{-4} (mg C L^{-1} m^2 kJ^{-1})	k_{PB} x10^{-6} (A_{350} m^2 kJ^{-1})
spring								
	BDW	1.98 ± 0.27	7.0 ± 0.0	86.5 ± 5.7	n.a.	1.24 ± 0.00	n.a.	n.a.
summer								
	BDE	3.89 ± 0.07	5.3 ± 0.0	39.4 ± 3.1	3.10	4.42 ± 0.33	2.69 ± 0.12	4.97 ± 1.07
	PUZ	3.81 ± 0.14	4.4 ± 0.0	70.5 ± 1.8	2.90	4.96 ± 0.04	2.47 ± 0.34	4.43 ± 0.59
	NCR	3.80 ± 0.07	5.5 ± 0.0	92.0 ± 1.8	3.27	5.06 ± 0.23	4.15 ± 0.16	0.73 ± 0.85
	PES	3.81 ± 0.10	8.7 ± 0.0	126.6 ± 7.9	2.77	3.42 ± 0.25	4.67 ± 0.45	12.96 ± 0.85
	BDW	4.18 ± 0.10	12.8 ± 0.0	178.3 ± 8.0	5.85	3.41 ± 0.14	6.63 ± 0.23	9.25 ± 1.28
	PEB	3.90 ± 0.07	13.4 ± 0.0	140.1 ± 1.7	4.09	2.79 ± 0.08	6.47 ± 0.17	15.37 ± 1.05
fall								
	BDE	3.54 ± 0.11	4.2 ± 0.0	48.1 ± 0.6	2.10	4.03 ± 0.24	0.96 ± 0.14	2.80 ± 0.63
	PUZ	3.57 ± 0.20	3.9 ± 0.0	57.8 ± 5.3	2.12	4.38 ± 0.32	0.94 ± 0.16	3.04 ± 0.76
	NCR	3.59 ± 0.20	5.1 ± 0.1	92.0 ± 2.0	2.48	5.18 ± 0.36	1.06 ± 0.17	3.39 ± 0.47
	PES	3.43 ± 0.09	6.4 ± 0.0	119.6 ± 9.4	3.71	2.96 ± 0.04	2.45 ± 0.17	6.26 ± 1.11
	BDW	4.18 ± 0.10	16.4 ± 0.4	290.1 ± 4.2	3.79	1.67 ± 0.08	7.57 ± 0.59	14.15 ± 0.95
	PEB	3.90 ± 0.07	14.9 ± 0.1	203.6 ± 4.7	3.89	1.74 ± 0.18	4.50 ± 0.47	12.12 ± 0.95

3.2 Effects of lake water chemistry on MeHg photodemethylation

Initial DOM concentrations ranged from 3.9 to 16.4 mg C L^{-1} across all lakes and collection months and this measurement was a very strong predictor of photodemethylation rate constants (R^2=0.76; Figure 4.4). Photodemethylation decreased by 50% over a DOM concentration change of less than 9 mg C L^{-1} in the experimental treatments. Filtering had no effect on the photodemethylation rate constants in BDW lake (p=0.08) during the spring experiment (Figure 4.3a & 4.3d). Between-lake differences in photodemethylation rate constants were significant in both summer and fall experiment sets (Figure 4.3e & 4.3f). In summer, the proportion of MeHg lost was very similar in the 3 lower carbon lakes (91-94%), whereas the 3 higher carbon lakes lost less MeHg (78-85%; Figure 4.3b). In fall, low carbon lakes again lost more MeHg (66-75%) than higher carbon lakes (36-53%; Figure 4.3c) for the same cumulative irradiation received. The photodemethylation rate constants for the lake waters also consistently grouped together based on the DOM concentration. Low DOM lakes had significantly higher photodemethylation rate constants than the lakes with more DOM in both summer (Figure 4.3e; p<0.05) and fall experiments (Figure 4.3; p<0.05).

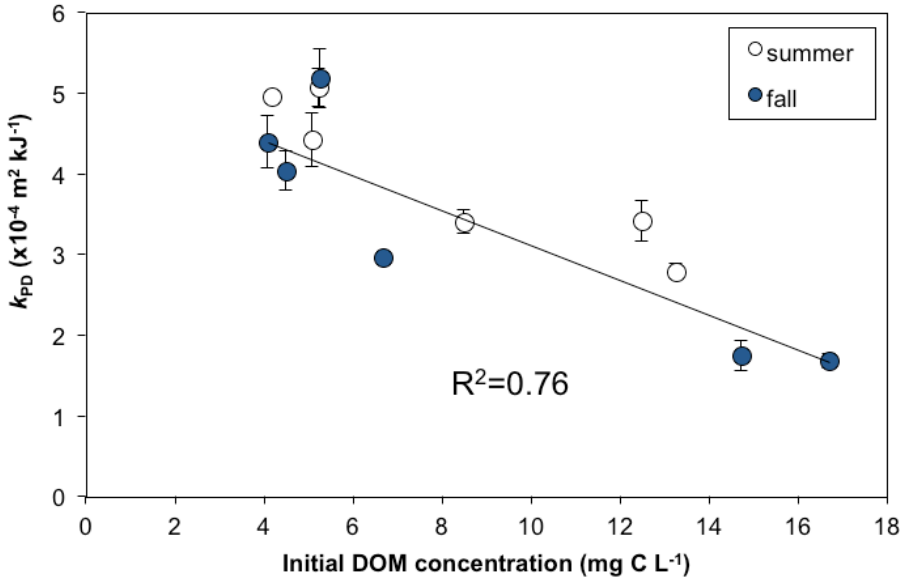

Figure 4.4 Energy-normalized photodemethylation rate constants (k_{PD}) as a function of initial dissolved organic matter (DOM) concentration. Data are plotted as rates with standard error for both summer and fall experiments with the relationship for pooled data (k_{PD} = -0.232[DOM] + 5.35, R^2=0.76, p=0.01).

Significant DOM photomineralization, measured as DOM concentration loss (in mg C L^{-1}) over cumulative radiation received, and DOM photobleaching, measured as A_{350} loss over cumulative radiation received, occurred within all lakes in both seasons when water was exposed to natural solar radiation (all R^2s>0.66, p's<0.05; Table 4.1; Figure A3.5 & A3.6). Photodemethylation rate constants were inversely related to DOM photoreactions through both photomineralization (r=-0.66, p=0.02) and photobleaching (r=-0.83, p<0.01). Negative linear regressions for photodemethylation and photomineralization (summer: R^2=0.58, p<0.05, fall: R^2=0.72, p=0.02; Figure 4.5a) and photodemethylation and photobleaching (summer: R^2=0.90, p=0.003; fall: R^2=0.83; p<0.01; Figure 4.5b) were compared between seasons. The relationship between photoreactions involving DOM (photomineralization & photobleaching) and

photoreactions involving MeHg (photodemethylation) had similar slopes between seasons (photomineralization: p=0.823; photobleaching: p=0.092) however the intercepts were significantly different (photomineralization: p<0.01; photobleaching: p=0.02).

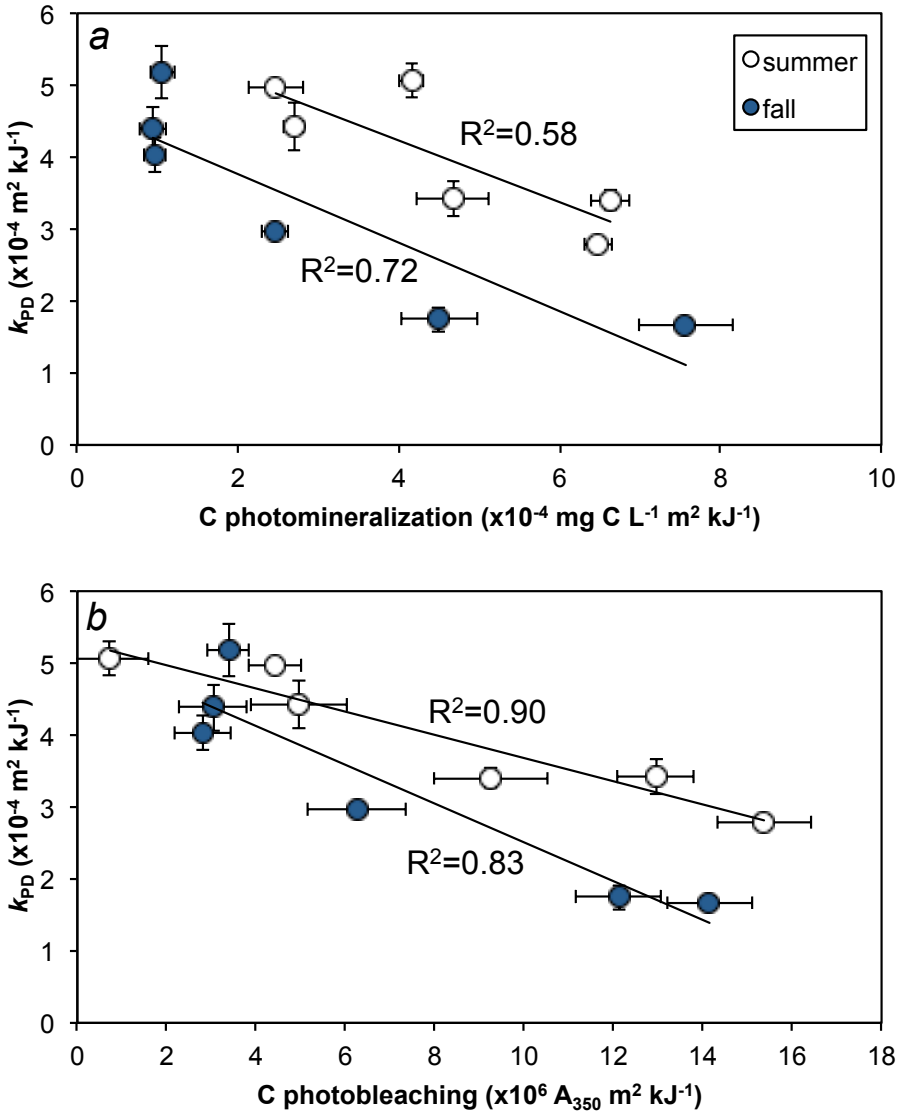

Figure 4.5 Energy-normalized photodemethylation rate constants (k_{PD}) and dissolved organic matter (DOM) photoreactions (*a*) photomineralization calculated as DOM loss (mgC L^{-1} m^2 kJ^{-1}; summer: R^2=0.58, y=-0.43x+5.94, p<0.05; fall: R^2=0.72, y=-0.48x+4.96, p=0.02), and (*b*) photobleaching measured as absorbance at 350 nm loss (A_{350} m^2 kJ^{-1}; summer: R^2=0.90, y=-0.16x+5.29, p=0.003; fall: R^2=0.83, y=-0.27x+5.20, p<0.01). Error bars are standard error on the corresponding reaction rate constants.

4. DISCUSSION

4.1 DOM concentration largely explains photodemethylation

Six lakes were sampled and used in experiments to represent spatial heterogeneity of water chemistry (DOM particularly) across Kejimkujik National Park. The lakes span across a 400 km^2 region and have different water sources. DOM source with some lakes were dominated by groundwater recharge and some dominated by surface water inputs via wetlands and catchment runoff (O'Driscoll et al. 2005). Study lakes with low DOM concentrations (<6 mg C L^{-1}; all within 2 mg C L^{-1}) all exhibited similar photodemethylation rate constants (e.g. BDE, PUZ, and NCR). The three higher carbon lakes had a greater range of DOM concentration (~10 mg C L^{-1}) and consequently, photodemethylation rate constants. Furthermore, 76% of the variation in photodemethylation rate constants between study lakes (Figure 4.3b,c,e,f) could be explained by the DOM concentration at the beginning of each experimental treatment (Figure 4.4). Lakes with higher DOM concentrations had lower photodemethylation rate constants and this pattern held across all lakes in both collection seasons, which was surprising given that the lakes encompassed a large range of DOM concentration and absorbance properties (i.e. A_{350}). This result suggests that the effects of catchment size, wetland representation in catchments, and surface water versus groundwater-fed lakes in our study system are important in controlling DOM and therefore photodemethylation.

Photodemethylation rate constants in the literature are typically reported in units of cumulative PAR photons per area (E m^{-2}) and therefore photodemethylation rate constants were also calculated using these units for simple comparison. Photodemethylation rate constants in our study ranged from 4.1 – 13.3 E m^{-2} and

corresponded well with the range of previously published rates for photodemethylation across many locations and water sources (2.6 – 13.7 E m^{-2}; Table A3.3). However, the effect of DOM on photodemethylation rate constants does not hold constant across ecosystem types; some studies have shown the impacts of DOM are significant (Li et al. 2010) while others have observed that the effects of DOM are less influential on photodemethylation than predicted (Black et al. 2012). Increases in DOM concentration from 3.9 to 16.4 mg C L^{-1} in our study lakes correspond with a 2-fold decrease in photodemethylation rate constants. In contrast, previous field-based studies found no statistical differences in photodemethylation rate constants between collection sites including different freshwater DOM sources such as natural wetlands (Black et al. 2012; Fleck et al. 2014) and domestic and wild rice fields that included a DOM concentration range of 8.5 – 36.3 mg C L^{-1} (Fleck et al. 2014). In a controlled study, Black et al. (2012) isolated DOM from wetlands using reverse osmosis to produce DOM ranges of 1.5 to 11.3 mg C L^{-1} in freshwaters, but again found that photodemethylation rate constants predicted based entirely on the attenuation of solar radiation by DOM concentration had less effect (6% reduction) on photodemethylation than predicted (~30% reduction). This result was surprising because photodemethylation is primarily driven by photon flux (Sellers et al. 1996; Hammerschmidt and Fitzgerald 2006; Lehnherr and St Louis 2009; Zhang and Hsu-Kim 2010; Li et al. 2010; Qian et al. 2014), which is to some degree controlled by DOM (Scully and Lean 1994; Morris et al. 1995). This finding further signifies the role, particularly in lakes, of DOM concentration and composition to MeHg photoreactions. Wetland DOM is often elevated in carbohydrates (Sulzberger and Durisch-Kaiser 2009), it is possible that the lower chromophoric content may result in the

lack of effects on photodemethylation observed by Black et al. (2012) compared to our findings and those by Lehnherr and St Louis (2009) in oligotrophic lakes.

The relative photoreactive DOM, as measured by the absorptivity and aromaticity of the DOM (e.g. A_{350}; SUVA), varies greatly among studies and likely plays a role in regulating the impact of DOM on photodemethylation of MeHg. Wetlands of varying DOM concentration can have $SUVA_{254}$ values of 1.5 – 2.58 L mg^{-1} m^{-1} (Fleck et al. 2014), whereas our study lakes had $SUVA_{254}$ values of 2.10 – 5.85 L mg^{-1} m^{-1}. This much higher $SUVA_{254}$ indicates a greater aromaticity (Weishaar et al. 2003) in our lake waters compared to Californian wetland waters. Optical measurements also highlight that DOM from different water sources may interact differently with MeHg photoreactions. Californian wetlands had a greater DOM concentration range than our study lakes (8.5 – 36.3 mg C L^{-1}), however there was no obvious reduction in photodemethylation due to DOM concentration (Fleck et al. 2014) and this further highlights the complexity of DOM effects on MeHg photochemistry. Coupled with results from this study, the variation in DOM effects on photodemethylation indicates the potential competition of photoreactive DOM with DOM-MeHg complexes in regulating photodemethylation rate constants in natural high carbon freshwaters.

4.2 Indirect seasonal effects on photodemethylation

The relationship between initial DOM concentration and photoreactions involving MeHg (i.e. photodemethylation rate constants) was not directly affected by sampling season; there were some differences in DOM concentration between seasons in each lake but photodemethylation rate constants did not group significantly by season across lakes

(Figure 4.4). Additionally, lakes with lower MeHg photodemethylation rate constants had higher rates of both DOM photomineralization (loss of DOM concentration; p=0.823) and DOM photobleaching (loss of A_{350}; p=0.092) regardless of season. However, the y-intercepts for k_{PD} versus both DOM phototransformations (photomineralization and photobleaching) were different between seasons (p=0.007 and p=0.019 respectively; Figure 4.5a & 4.5b). Temperature differences between seasons could explain these differences in intercepts if higher temperatures in summer result in a greater available pool of photoreactive DOM. The timing of water collection (summer versus fall) could also influence the DOM phototransformations we saw between the seasons tested in our experiments due to *in situ* processing and biological activity in the lake prior to water collection.

Factors that likely did not affect photodemethylation in our experimental framework include particle bound MeHg and biological activity during the experiments. The filtered versus unfiltered treatments of BDW water in spring showed that there was no effect of filtering on photodemethylation rate constants, however, for MeHg analyses samples are commonly filtered and therefore we chose to continue filtering (0.45 μm) for all the further experimental treatments. The water treatments were also not sterilized and, therefore, bacterial activity could have played a role influencing the DOM in the bottles in summer versus fall. No visible flocculation of organic matter or photosynthetic organism growth (algae) occurred over the 1-week experiments and samples were not re-filtered prior to chemical analysis, however, biological or photo-biological activity could have been present (Siciliano et al. 2005). Therefore, these experiments measured the combination of net abiotic and biologic photo-processes similar to those occurring in

actual lake surfaces confirming photodemethylation is driven primarily by abiotic processes in lake water columns (Sellers et al. 1996; Lehnherr and St Louis 2009; Tai et al. 2014; Jeremiason et al. 2015).

The photoreactivity of DOM will be determined by hydrology (precipitation and residence time) and temperature (Kellerman et al. 2014). Losses of terrestrial photoreactive DOM in lakes via photobleaching have been observed on a whole lake scale in Sweden's third largest lake (Köhler et al. 2013). That Swedish lake is a natural ecosystem scale experiment that highlights the impact of fresh inputs of photoreactive DOM and the resultant phototransformations, and the importance of hydrology and time scale. The majority of photodemethylation studies take place in summer or summer into fall (Table A3.3), which makes sense, given this is the most photochemically active period, has the most favourable field conditions, and that most water bodies in temperate to high latitudes will be covered in ice during winter periods, which eliminates the potential for photodemethylation in waters at those times (Poste et al. 2015). Depending on the time of year the DOM composition will likely differ and therefore this seasonal aspect to DOM will affect the photoreactivity of the DOM.

4.3 Competition between DOM photoreactions and DOM-MeHg photoreactions

Freshwaters with more DOM will intuitively support more photoreactions in near surface waters. However, in high carbon systems, higher concentrations of DOM which will increase the overall photoreactivity of the water (Garcia et al. 2005; Haverstock et al. 2012) may reduce the efficiency of secondary photoreactions, like photodemethylation, if more energetically favoured reaction pathways exist. Our data support the concept that

increased DOM concentration inhibits photodemethylation, because there is competition between photoreactions involving MeHg associated with DOM and photoreactions that involved DOM not associated with MeHg. The experimental treatments with lower MeHg photodemethylation rate constants also exhibited higher rates of both DOM photomineralization (loss of DOM concentration) and DOM photobleaching (loss of A_{350}) with k_{PD} versus both DOM phototransformations (photomineralization and photobleaching) exhibiting significant correlation (Figure 4.5a & 4.5b). A direct ratio calculation between DOM concentration and MeHg loss is not sensitive enough to explain photodemethylation rate constants (Black et al. 2012) because MeHg is typically present in freshwaters at concentrations of ng L^{-1} whereas DOM is typically present in freshwaters at concentrations of mg C L^{-1}. Black et al. (2012) hypothesized that there could be a limitation of strong DOM binding sites that could be saturated by MeHg at which point the MeHg could be associated with weaker binding sites (similar to photoreduction of Hg(II) (Vost et al. 2011)) and be more vulnerable to photodemethylation (Zhang and Hsu-Kim 2010). Methylmercury can be associated with both weak and strong sites at the same time (Hintelmann et al. 1995; O'Driscoll and Evans 2000). However, under ambient MeHg concentrations there is not likely to be a limitation of thiol binding sites (Haitzer et al. 2002; Zhang and Hsu-Kim 2010) and MeHg association with DOM occurs quite rapidly (Hintelmann et al. 1997). As the DOM:MeHg ratio increases, the DOM molecules that are not associated with MeHg are outnumbering and essentially outcompeting the DOM-MeHg complexes in the proportion of photoreactions that are occurring (Figure 4.4).

Dissolved organic matter is derived from many sources and the structural composition of the DOM can affect the ability of the DOM to both absorb solar radiation but also react and undergo internal transformations (Zepp et al. 1985; Fleck et al. 2014). Methylmercury loss through photodemethylation has been shown to be most correlated with a simultaneous reduction in absorbance from 280-350 nm and the loss of humic and fulvic portions of fluorescence excitation and emission matrices (Fleck et al. 2014). These optical measures highlight the relative abundance of photoreactive DOM and the importance of the phototransformation of DOM to MeHg loss. We propose thinking about photodemethylation in a more opportunist framework as this competition or limitation of energy available for different photoreactions involving DOM represents an indirect control on photodemethylation of MeHg (see Figure 4.1). The combinations of conditions that facilitate or inhibit MeHg photodemethylation are complex but linked to DOM in two ways: (i) MeHg is primarily associated with DOM complexes in natural freshwater systems (Hintelmann et al. 1997; Hill et al. 2009; Black et al. 2012) and, (ii) measurable photodemethylation will only occur in association with specific DOM-MeHg complexation sites (Qian et al. 2014; Jeremiason et al. 2015) but that this process will be quickly inhibited by competition for photons photoreactive DOM.

Dissolved organic matter across ecosystems, and thereby water sources, may not consistently display the tradeoff effect we have discovered in these lakes. Nevertheless, it is reasonable to suggest that if we quantify the extent to which rates of phototransformations of DOM vary across a wider range of sample types it could be a means to predict this DOM competition with MeHg photoreactions across ecosystems. It is important to better understand potential inhibition of MeHg removal through

photodemethylation particularly given that transport of DOM (and likely MeHg) is predicted to increase with increased rainfall in many boreal ecosystems (de Wit et al. 2016) including the Northeastern US (Strock et al. 2016) (and likely Nova Scotia and other boreal areas of Canada). This is the first study to test and quantify a consistent competitive interaction between MeHg photodemethylation and photoreactions involving DOM phototransformations (both photomineralization and photobleaching) support the conceptual idea that higher carbon systems will have slower rates of photodemethylation. Ultimately this research is key to developing more accurate predictions of photodemethylation and MeHg losses from freshwater aquatic ecosystems.

Acknowledgments

Funding for this research was provided from the National Science and Engineering Council (NSERC) of Canada in the form of a Discovery (#341960-2013), CREATE, and Canada Research Chair (#950-203477) grant to N.J.O. and an NSERC-PGS-D scholarship to S.J.K. Logistical field and laboratory support provided by Parks Canada (B. Mailman & M. Smith), Environment Canada (R. Tordon & R. Keenan), E. Mann, T. Christensen, L. Klapstein, and Acadia University C.A.R.E. labs.

References

Black, F. J., B. A. Poulin, and A. R. Flegal. 2012. Factors controlling the abiotic photo-degradation of monomethylmercury in surface waters. Geochim. Cosmochim. Acta **84**: 492–507. doi:10.1016/j.gca.2012.01.019

Evers, D. C., Y.-J. Han, C. T. Driscoll, and others. 2007. Biological mercury hotspots in the Northeastern United States and Southeastern Canada. BioScience **57**: 29–43. doi:10.1641/B570107

Fleck, J. A., G. Gill, B. A. Bergamaschi, T. E. C. Kraus, B. D. Downing, and C. N. Alpers. 2014. Concurrent photolytic degradation of aqueous methylmercury and dissolved organic matter. Sci. Total Environ. **484**: 263–275. doi:10.1016/j.scitotenv.2013.03.107

Garcia, E., M. Amyot, and P. A. Ariya. 2005. Relationship between DOC photochemistry and mercury redox transformations in temperate lakes and wetlands. Geochim. Cosmochim. Acta **69**: 1917–1924. doi:10.1016/j.gca.2004.10.026

Haitzer, M., G. R. Aiken, and J. N. Ryan. 2002. Binding of mercury(II) to dissolved organic matter: the role of the mercury-to-DOM concentration ratio. Environ. Sci. Technol. **36**: 3564–3570.

Hammerschmidt, C. R., and W. F. Fitzgerald. 2006. Photodecomposition of methylmercury in an Arctic Alaskan lake. Environ. Sci. Technol. **40**: 1212–1216. doi:10.1021/es0513234

Haverstock, S., T. Sizmur, J. Murimboh, and N. J. O'Driscoll. 2012. Modeling the photo-oxidation of dissolved organic matter by ultraviolet radiation in freshwater lakes: Implications for mercury bioavailability. Chemosphere **88**: 1220–1226. doi:10.1016/j.chemosphere.2012.03.073

Hill, J. R., N. J. O'Driscoll, and D. R. S. Lean. 2009. Size distribution of methylmercury associated with particulate and dissolved organic matter in freshwaters. Sci. Total Environ. **408**: 408–414. doi:10.1016/j.scitotenv.2009.09.030

Hintelmann, H., P. M. Welbourn, and R. D. Evans. 1995. Binding of methylmercury compounds by humic and fulvic acids. Water. Air. Soil Pollut. **80**: 1031–1034. doi:10.1007/BF01189760

Hintelmann, H., P. M. Welbourn, and R. D. Evans. 1997. Measurement of complexation of methylmercury(II) compounds by freshwater humic substances using equilibrium dialysis. Environ. Sci. Technol. **31**: 489–495. doi:10.1021/es960318k

Jeremiason, J., J. C. Portner, G. Aiken, K. T. Tran, M. T. Dvorak, A. Hiranaka, and D. Latch. 2015. Photoreduction of Hg(II) and photodemethylation of methylmercury: The key role of thiol sites on dissolved organic matter. Environ. Sci. Process. Impacts. doi:10.1039/C5EM00305A

Kellerman, A. M., T. Dittmar, D. N. Kothawala, and L. J. Tranvik. 2014. Chemodiversity of dissolved organic matter in lakes driven by climate and hydrology. Nat. Commun. **5**: 3804. doi:10.1038/ncomms4804

Kidd, K., M. Clayden, and T. Jardine. 2011. Bioaccumulation and biomagnification of mercury through food webs, p. 453–499. *In* G. Liu, Y. Cai, and N. O'Driscoll [eds.], Environmental Chemistry and Toxicology of Mercury. John Wiley & Sons, Inc.

Köhler, S. J., D. Kothawala, M. N. Futter, O. Liungman, and L. Tranvik. 2013. In-lake processes offset increased terrestrial inputs of dissolved organic carbon and color to lakes. PLoS ONE **8**: e70598. doi:10.1371/journal.pone.0070598

Krabbenhoft, D. P., M. L. Olson, J. F. Dewild, D. W. Clow, R. G. Striegl, M. M. Dornblaser, and P. VanMetre. 2002. Mercury loading and methylmercury production and cycling in high-altitude lakes from the Western United States. Water Air Soil Pollut. Focus **2**: 233–249. doi:10.1023/A:1020162811104

Lehnherr, I. 2014. Methylmercury biogeochemistry: a review with special reference to Arctic aquatic ecosystems. Environ. Rev. 1–15. doi:10.1139/er-2013-0059

Lehnherr, I., and V. L. St Louis. 2009. Importance of ultraviolet radiation in the photodemethylation of methylmercury in freshwater ecosystems. Environ. Sci. Technol. **43**: 5692–5698.

Lehnherr, I., V. L. St. Louis, C. A. Emmerton, J. D. Barker, and J. L. Kirk. 2012. Methylmercury cycling in high Arctic wetland ponds: Sources and sinks. Environ. Sci. Technol. **46**: 10514–10522. doi:10.1021/es300576p

Li, Y., Y. Mao, G. Liu, G. Tachiev, D. Roelant, X. Feng, and Y. Cai. 2010. Degradation of methylmercury and its effects on mercury distribution and cycling in the Florida Everglades. Environ. Sci. Technol. **44**: 6661–6666. doi:10.1021/es1010434

Little, M. E., N. M. Burgess, H. G. Broders, and L. M. Campbell. 2015. Distribution of mercury in archived fur from little brown bats across Atlantic Canada. Environ. Pollut. **207**: 52–58. doi:10.1016/j.envpol.2015.07.049

Mansfield, C. R., and F. J. Black. 2015. Quantification of monomethylmercury in natural waters by direct ethylation: Interference characterization and method optimization. Limnol Ocean. Methods **13**: 81–91.

Morris, D. P., H. Zagarese, C. E. Williamson, E. G. Balseiro, B. R. Hargreaves, B. Modenutti, R. Moeller, and C. Queimalinos. 1995. The attenuation of solar UV

radiation in lakes and the role of dissolved organic carbon. Limnol. Oceanogr. **40**: 1381–1391.

O'Driscoll, N. J., and R. D. Evans. 2000. Analysis of methyl mercury binding to freshwater humic and fulvic acids by gel permeation chromatography/hydride generation ICP-MS. Environ. Sci. Technol. **34**: 4039–4043. doi:10.1021/es0009626

O'Driscoll, N. J., A. N. Rencz, and D. R. S. Lean. 2005. Review of factors affecting mercury fate in Kejimkujik Park, Nova Scotia, p. 7–20. *In* Mercury cycling in a wetland-dominated ecosystem: a multidisciplinary study. SETAC.

Poste, A. E., H. F. V. Braaten, H. A. de Wit, K. Sørensen, and T. Larssen. 2015. Effects of photodemethylation on the methylmercury budget of boreal Norwegian lakes. Environ. Toxicol. Chem. n/a-n/a. doi:10.1002/etc.2923

Qian, Y., X. Yin, H. Lin, B. Rao, S. C. Brooks, L. Liang, and B. Gu. 2014. Why dissolved organic matter enhances photodegradation of methylmercury. Environ. Sci. Technol. Lett. **1**: 426–431. doi:10.1021/ez500254z

Scully, N. M., and D. R. S. Lean. 1994. The attenuation of ultraviolet radiation in temperate lakes. Erg Limnol **43**: 135–144.

Sellers, P., C. A. Kelly, J. W. M. Rudd, and A. R. MacHutchon. 1996. Photodegradation of methylmercury in lakes. Nature **380**: 694–697. doi:10.1038/380694a0

Siciliano, S. D., N. J. O'Driscoll, R. Tordon, J. Hill, S. Beauchamp, and D. R. S. Lean. 2005. Abiotic production of methylmercury by solar radiation. Environ. Sci. Technol. **39**: 1071–1077. doi:10.1021/es048707z

Strock, K. E., J. E. Saros, S. J. Nelson, S. D. Birkel, J. S. Kahl, and W. H. McDowell. 2016. Extreme weather years drive episodic changes in lake chemistry: implications for recovery from sulfate deposition and long-term trends in dissolved organic carbon. Biogeochemistry **127**: 353–365. doi:10.1007/s10533-016-0185-9

Sulzberger, B., and E. Durisch-Kaiser. 2009. Chemical characterization of dissolved organic matter (DOM): A prerequisite for understanding UV-induced changes of DOM absorption properties and bioavailability. Aquat. Sci. **71**: 104–126. doi:10.1007/s00027-008-8082-5

Tai, C., Y. Li, Y. Yin, L. J. Scinto, G. Jiang, and Y. Cai. 2014. Methylmercury photodegradation in surface water of the Florida Everglades: Importance of dissolved organic matter-methylmercury complexation. Environ. Sci. Technol. **48**: 7333–7340. doi:10.1021/es500316d

Vost, E. E., M. Amyot, and N. J. O'Driscoll. 2011. Photoreactions of mercury in aquatic systems, p. 193–218. *In* G. Liu, Y. Cai, and N. O'Driscoll [eds.], Environmental Chemistry and Toxicology of Mercury. John Wiley & Sons, Inc.

Weishaar, J. L., G. R. Aiken, B. A. Bergamaschi, M. S. Fram, R. Fujii, and K. Mopper. 2003. Evaluation of specific ultraviolet absorbance as an indicator of the chemical composition and reactivity of dissolved organic carbon. Environ. Sci. Technol. **37**: 4702–4708. doi:10.1021/es030360x

de Wit, H. A., S. Valinia, G. A. Weyhenmeyer, and others. 2016. Current browning of surface waters will Be further promoted by wetter climate. Environ. Sci. Technol. Lett. doi:10.1021/acs.estlett.6b00396

Wyn, B., K. A. Kidd, N. M. Burgess, R. A. Curry, and K. R. Munkittrick. 2010. Increasing mercury in yellow perch at a hotspot in Atlantic Canada, Kejimkujik National Park. Environ. Sci. Technol. **44**: 9176–9181.

Zepp, R. G., P. F. Schlotzhauer, and R. M. Sink. 1985. Photosensitized transformations involving electronic energy transfer in natural waters: role of humic substances. Environ. Sci. Technol. **19**: 74–81. doi:10.1021/es00131a008

Zhang, T., and H. Hsu-Kim. 2010. Photolytic degradation of methylmercury enhanced by binding to natural organic ligands. Nat. Geosci. **3**: 473–476. doi:10.1038/ngeo892

Chapter 5 : SUMMARY

1 General conclusions

The overall objective of this thesis was to examine the relationship between photoreactive dissolved organic matter (DOM) and methylmercury (MeHg) photodemethylation in lake waters. This relationship is of central importance, as this thesis shows, because increases in photoreactive DOM leads to decreased photodemethylation by outcompeting photoreaction pathways that involve MeHg. This competition effect needs to be carefully considered in systems that show elevated (and variable) DOM concentrations and DOM photoreactivity. Removal of MeHg from freshwater lakes through photodemethylation can be a significant sink for toxic MeHg (up to 80% of total MeHg sink) and the photoreactive DOM also present in the water dictates the strength of this sink. Laboratory studies have shown that a minimum amount of natural DOM is required to facilitate photodemethylation (Qian et al. 2014; Jeremiason et al. 2015) and this thesis in combination with other studies (Li et al. 2010; Kim et al. 2017) shows that this process is quickly inhibited in natural waters by a surplus of photoreactive DOM. Dissolved organic matter will react through various phototransformations and these pathways of photomineralization and photobleaching will essentially outcompete the photodemethylation pathway. Photodemethylation potential also therefore changes with depth in water columns, as the attenuation of solar radiation reduces available photons. Data presented in this thesis demonstrate how these processes act naturally in surface waters. Conclusions from this study consider processing from a macroscopic

whole-lake perspective, but of course small-scale variability will also be present, owing to spatiotemporal changes in hydrology, circulation, and stratification.

The concentration and photoreactivity of DOM changes significantly throughout an annual growing season, where a 2-fold seasonal change was characteristic within most of the chosen study lakes. Photoreactive DOM was defined in Chapter 2 as the loss of absorbance A_{350} in a water sample following ultraviolet-A (UV-A; 320-400 nm) exposure over a given time period (24 hours). In Chapter 2, six lakes were sampled in three different months and photobleached within the lab, in order to quantify the photoreactive DOM throughout the growing season. Lake waters with greater concentrations of DOM had greater losses of A_{350} and therefore photoreactive DOM (R^2=0.94). Lakes were subsequently re-sampled at the same times of year in two additional years, to show that there was a positive correlation between DOM and iron (Fe) concentration (r=0.91) and DOM and MeHg concentration (r=0.51) across summer and fall seasons in three years. These studies illustrate that (1) MeHg concentrations in the lakes over three years of sampling are more highly related to DOM transport into lakes than to photochemical processes, and (2) MeHg concentrations in high carbon lakes are less impacted by photochemical processing than initially predicted.

Experiments in Chapter 3 quantified the effect of photoreactive DOM on MeHg photodemethylation rate constants. A bulk water sample was collected from one of the high DOM lakes (BDW Lake) in June, August, and October. Direct photochemical manipulation of the natural DOM in the sample (through preconditioning in photoreactors) reduced the absorbance of the waters to 30% of the original absorbance (reduction of 70%). The purpose of this treatment was to mimic natural photochemical

processing that would occur at the surface of a lake that was no longer mixing or receiving lateral inputs of water (containing DOM and MeHg) from external sources (i.e. wetlands, runoff, precipitation). The experimental treatment (with reduced photoreactive DOM) did not have any effect on photodemethylation rate constants within sampling month. However, June water consistently had greater photodemethylation rate constants than the other two sampling periods (August and October). Photodemethylation efficiencies were also ten times higher in June than the other two sampling periods and declined with increasing DOM concentration (both natural and photochemically removed). Overall, the results from Chapter 3 highlighted that there is a greater potential for photodemethylation to occur in lower carbon waters with less photoreactive (more photobleached) DOM.

Building on outcomes from Chapter 3, the objective of the simulation experiments discussed in Chapter 4 was to quantify the DOM phototransformation and MeHg photodemethylation rate constants. Bulk water samples from one lake in spring (May), and six lakes in summer (July) and fall (October), were filtered, bottled, and placed in full sun to measure photochemical transformations of DOM and MeHg over one week in each season. Up to 90% of the MeHg (initial concentration ~3 ng L^{-1}) was lost in the lower DOM lake waters and photodemethylation rate constants were negatively related to DOM concentration (R^2=0.76). Interestingly, this relationship did not change across sampling and exposure seasons and photodemethylation rate constants were negatively related to rates of DOM phototransformation. Separately, photomineralization and photobleaching rates of DOM could explain 58-72% and 83-90% of the change in MeHg photodemethylation rate constants, respectively. Results in Chapter 4 suggest that the

competition between DOM and DOM-MeHg for available photons is higher in high-DOM waters. These results are similar to those in Chapter 3 when comparing the efficiency for photodemethylation between waters with different DOM. However, in Chapter 4 the actual photodemethylation rate constants were different between treatments. There are a few reasons for the difference between chapters: 1) Chapter 3 used water from the same lake but was manipulated in the lab and 2) the fixed wavebands of constant irradiation exposure in Chapter 3 may have reduced the potential for variation in photodemethylation due to an excess supply of UV-A photons compared to diurnal cycles exhibited in the natural radiation experiments of Chapter 4. These results and conclusions provide further evidence that DOM is a primary control on photodemethylation.

2 Specific significance and applications

Photodemethylation has been identified as the primary pathway for removing MeHg from freshwater lakes (Sellers et al. 2001; Hammerschmidt and Fitzgerald 2006; Lehnherr and St Louis 2009; Poste et al. 2015), Arctic ponds (Lehnherr et al. 2012), and wetlands (Black et al. 2012; Fleck et al. 2014) and the importance of DOM to this pathway is certain (Li et al. 2010; Fleck et al. 2014; Tai et al. 2014; Qian et al. 2014; Jeremiason et al. 2015). Predicting photodemethylation rate constants, however, is less straightforward (Black et al. 2012) and universal wavelength-specific rate constants (Fernández-Gómez et al. 2013) may apply only for the very surface of the water body. Photodemethylation rate constants at depth in the water column will be greatly influenced by prior attenuation of radiation within the aquatic environment with shorter wavelengths

(UV-B) being attenuated rapidly in surface waters (Sellers et al. 1996; Lehnherr and St Louis 2009; Poste et al. 2015) and this effect is strongly influenced by DOM (Scully and Lean 1994; Lehnherr and St Louis 2009; Haverstock et al. 2012). The results presented in this thesis from controlled experiments provide a rational and a well-quantified foundation for predicting the relationships between DOM and photodemethylation. This thesis also provides a conceptual framework to explain how and why more photoreactive DOM will likely inhibit photodemethylation in a variety of freshwaters. Quantifying the photoreactive nature of DOM in mercury sensitive environments is key to predicting the potential for photodemethylation to occur.

The effect of DOM on photodemethylation is dynamic and is influenced by the photoreactivity of DOM. Increased DOM (browning of waters) is predicted in many temperate and boreal lakes with future increases in precipitation and primary productivity (Isidorova et al. 2016; Strock et al. 2016; de Wit et al. 2016). As such, quantifying MeHg interactions with DOM are critical in these aquatic systems (Strock et al. 2016; de Wit et al. 2016). Observed as well as predicted increases in DOM flux from the landscape will likely also lead to increased mercury mobility and flux into freshwaters. Large-scale processes such as clearcutting and forestry activity not only greatly impact the magnitude of DOM transport from watersheds but can also affect DOM structure (Carignan et al. 2000; O'Driscoll et al. 2004, 2006). Based upon this research, browning of freshwaters will likely decrease or completely inhibit photodemethylation in these systems, particularly in mercury sensitive dystrophic systems like Kejimkujik National Park.

Outcomes of this thesis are important for management and mitigation. This work may influence mercury policy and awareness within Nova Scotia in regards to public

health and risk management strategies for these mercury sensitive ecosystems. Elevated MeHg concentrations in Kejimkujik National Park (Wyn et al. 2010; Little et al. 2015) and surrounding areas, despite reductions in atmospheric acid deposition (Whitfield et al. 2006) and mercury deposition (Cole et al. 2014), may be further explained from a source-sink perspective using photodemethylation rate constants presented in this thesis. Results from this research will facilitate the refinement of process-based freshwater mercury models predicting mercury accumulation in food webs such as the Dynamic Mercury Cycling Model (D-MCM; developed by R. Harris). Further work has focused primarily on the methylation potential from sediments as a primary indicator of MeHg risk to organisms following ecosystem disturbance, namely hydroelectric dam formation (Schartup et al. 2015; Calder et al. 2016). Refined models will help to predict changes in MeHg availability in high carbon lakes like those in Kejimkujik National Park, which are sensitive to mercury retention and subsequent risk to organisms in these ecosystems. Particularly, the application of these results in other freshwaters that are high in carbon and low in pH is key to determine the transferability of the relationship between DOM and MeHg photodemethylation identified in our study system. Results from this thesis also provide another framework in which mercury contamination needs to be addressed, by using water chemistry characteristics that target mercury speciation in susceptible freshwaters.

3 Future work

This thesis is the first study on MeHg photodemethylation in a temperate sub-boreal ecosystem with poor buffering capacity that has had chronic sulfate and mercury

deposition. The most comparable studies of DOM and MeHg photochemistry took place in California wetlands (both natural and constructed) (Black et al. 2012; Fleck et al. 2014) and Florida Everglades (Li et al. 2010), both of which have very different climates than our study site in Kejimkujik National Park but also suggest a definable relationship between DOM photochemistry and MeHg photodemethylation. More studies going forward need to focus on comparability in order to determine the application of these relationships across different ecosystems based on a DOM metric that addresses both concentration but also photoreactivity and thereby reactivity for MeHg species that are bound to the DOM.

The relationships found here between DOM concentration and both UV-A attenuation (K_d) and photodemethylation rate constants (k_{PD}) validate their application to lakes in Kejimkujik National Park to predict the strength of photodemethylation as a sink across lake types and seasons. A photodemethylation potential model should be constructed using DOM (concentration and absorbance properties) and MeHg (concentration) monitoring data from multi-year datasets and then tested using monitoring water quality data from Parks Canada and mercury fate data from lakes across Canada from Environment and Climate Change Canada. Additionally, aerial fluorescence light detection and ranging (LiDAR) has been shown to be a good surrogate for DOM concentration in estuarine samples (Rogers et al. 2012) and this optical application may be useful for characterizing variations in photoreactive DOM in remote freshwaters.

Both DOM and MeHg concentrations are controlled by hydrology, climate, and seasonality, which will help predict spatially and temporally when photodemethylation potential is weakest and therefore MeHg concentrations may be highest. These periods of

low photodemethylation potential will then need to be compared with biologically relevant risks. For example, there is very little to no photodemethylation predicted to occur in winter when lake surfaces are frozen and covered in ice and snow (Poste et al. 2015). Methylation will likely be very slow at this time and MeHg uptake to organisms may also be limited. Therefore, future studies should focus on spring melt or storm events when transport of solutes is increased and hot moments will likely exist along transitional boundaries (McClain et al. 2003; Mitchell et al. 2008; Singer et al. 2016).

The effect of both photosynthesizing and heterotrophic bacteria in the lakes of Kejimkujik National Park should also be explored. These organisms may provide a critical link in the persistent mercury story of this area by changing food web structure (microbial loops; see Sherr and Sherr (1988)) and mercury speciation and concentrations in the food web (water column speciation see Siciliano et al. (2005) and Eckley and Hintelmann (2006)). Recently, the use of divalent mercury (Hg(II)) by photosynthesizing microbes was identified in lab-based studies (Schaefer 2016; Grégoire and Poulain 2016) and these findings highlight the need for combining photochemistry with photobiology to address mercury cycling in natural waters. Even so, oligotrophic and dystrophic lakes receive the majority of organic matter from allochtonous sources, and therefore microbial studies that characterize detritus-based microbial loops within food webs may also help explain the high mercury concentrations in biota in Kejimkujik National Park.

Better optical characterization of DOM in mercury sensitive ecosystems is also needed to better predict photodemethylation potential. Measuring absorbance is fairly robust and quick and should be included immediately in monitoring programs that are not already measuring this simple parameter. Characterizing photoreactive DOM in different

ecosystems in combination with MeHg photodemethylation will better elucidate interactive relationships and provide a framework for addressing this MeHg sink in freshwater ecosystems globally. Predicted increases of fluxes of organic matter into freshwaters and browning of waters will result in an increase in the competitive effect between DOM and MeHg photoreactions. Specifically, the flux of DOM and mercury into lakes is crucial for constraining risks of MeHg production and exposure to food webs. A better understanding of the inputs and fate of MeHg depends upon DOM flux and photoreactions with DOM.

References

Black, F. J., B. A. Poulin, and A. R. Flegal. 2012. Factors controlling the abiotic photo-degradation of monomethylmercury in surface waters. Geochim. Cosmochim. Acta **84**: 492–507. doi:10.1016/j.gca.2012.01.019

Calder, R. S. D., A. T. Schartup, M. Li, A. P. Valberg, P. H. Balcom, and E. M. Sunderland. 2016. Future impacts of hydroelectric power development on methylmercury exposures of Canadian indigenous communities. Environ. Sci. Technol. **50**: 13115–13122. doi:10.1021/acs.est.6b04447

Carignan, R., P. D'Arcy, and S. Lamontagne. 2000. Comparative impacts of fire and forest harvesting on water quality in Boreal Shield lakes. Can. J. Fish. Aquat. Sci. **57**: 105–117. doi:10.1139/f00-125

Cole, A. S., A. Steffen, C. S. Eckley, and others. 2014. A survey of mercury in air and precipitation across Canada: Patterns and trends. Atmosphere **5**: 635–668. doi:10.3390/atmos5030635

Eckley, C. S., and H. Hintelmann. 2006. Determination of mercury methylation potentials in the water column of lakes across Canada. Sci. Total Environ. **368**: 111–125.

Fernández-Gómez, C., A. Drott, E. Björn, S. Díez, J. M. Bayona, S. Tesfalidet, A. Lindfors, and U. Skyllberg. 2013. Towards universal wavelength-specific photodegradation rate constants for methyl mercury in humic waters, exemplified

by a boreal lake-wetland gradient. Environ. Sci. Technol. 130529101435009. doi:10.1021/es400373s

Fleck, J. A., G. Gill, B. A. Bergamaschi, T. E. C. Kraus, B. D. Downing, and C. N. Alpers. 2014. Concurrent photolytic degradation of aqueous methylmercury and dissolved organic matter. Sci. Total Environ. **484**: 263–275. doi:10.1016/j.scitotenv.2013.03.107

Grégoire, D. S., and A. J. Poulain. 2016. A physiological role for HgII during phototrophic growth. Nat. Geosci. **9**: 121–125. doi:10.1038/ngeo2629

Hammerschmidt, C. R., and W. F. Fitzgerald. 2006. Photodecomposition of methylmercury in an Arctic Alaskan lake. Environ. Sci. Technol. **40**: 1212–1216. doi:10.1021/es0513234

Haverstock, S., T. Sizmur, J. Murimboh, and N. J. O'Driscoll. 2012. Modeling the photo-oxidation of dissolved organic matter by ultraviolet radiation in freshwater lakes: Implications for mercury bioavailability. Chemosphere **88**: 1220–1226. doi:10.1016/j.chemosphere.2012.03.073

Isidorova, A., A. G. Bravo, G. Riise, S. Bouchet, E. Björn, and S. Sobek. 2016. The effect of lake browning and respiration mode on the burial and fate of carbon and mercury in the sediment of two boreal lakes: Carbon and mercury burial. J. Geophys. Res. Biogeosciences **121**: 233–245. doi:10.1002/2015JG003086

Jeremiason, J., J. C. Portner, G. Aiken, K. T. Tran, M. T. Dvorak, A. Hiranaka, and D. Latch. 2015. Photoreduction of Hg(II) and photodemethylation of methylmercury: The key role of thiol sites on dissolved organic matter. Environ. Sci. Process. Impacts. doi:10.1039/C5EM00305A

Kim, M.-K., A.-Y. Won, and K.-D. Zoh. 2017. Effects of Molecular Size Fraction of DOM on Photodegradation of Aqueous Methylmercury. Chemosphere. doi:10.1016/j.chemosphere.2017.02.033

Lehnherr, I., and V. L. St Louis. 2009. Importance of ultraviolet radiation in the photodemethylation of methylmercury in freshwater ecosystems. Environ. Sci. Technol. **43**: 5692–5698.

Lehnherr, I., V. L. St. Louis, C. A. Emmerton, J. D. Barker, and J. L. Kirk. 2012. Methylmercury cycling in high Arctic wetland ponds: Sources and sinks. Environ. Sci. Technol. **46**: 10514–10522. doi:10.1021/es300576p

Li, Y., Y. Mao, G. Liu, G. Tachiev, D. Roelant, X. Feng, and Y. Cai. 2010. Degradation of methylmercury and its effects on mercury distribution and cycling in the

Florida Everglades. Environ. Sci. Technol. **44**: 6661–6666. doi:10.1021/es1010434

Little, M. E., N. M. Burgess, H. G. Broders, and L. M. Campbell. 2015. Distribution of mercury in archived fur from little brown bats across Atlantic Canada. Environ. Pollut. **207**: 52–58. doi:10.1016/j.envpol.2015.07.049

McClain, M. E., E. W. Boyer, C. L. Dent, and others. 2003. Biogeochemical hot spots and hot moments at the interface of terrestrial and aquatic ecosystems. Ecosystems **6**: 301–312.

Mitchell, C. P. J., B. A. Branfireun, and R. K. Kolka. 2008. Spatial characteristics of net methylmercury production hot spots in peatlands. Environ. Sci. Technol. **42**: 1010–1016. doi:10.1021/es0704986

O'Driscoll, N. J., D. R. S. Lean, L. L. Loseto, R. Carignan, and S. D. Siciliano. 2004. Effect of dissolved organic carbon on the photoproduction of dissolved gaseous mercury in lakes: potential impacts of forestry. Environ. Sci. Technol. **38**: 2664–2672.

O'Driscoll, N. J., A. N. Rencz, and D. R. S. Lean. 2005. Review of factors affecting mercury fate in Kejimkujik Park, Nova Scotia, p. 7–20. *In* Mercury cycling in a wetland-dominated ecosystem: a multidisciplinary study. SETAC.

O'Driscoll, N. J., S. D. Siciliano, D. Peak, R. Carignan, and D. R. S. Lean. 2006. The influence of forestry activity on the structure of dissolved organic matter in lakes: Implications for mercury photoreactions. Sci. Total Environ. **366**: 880–893. doi:10.1016/j.scitotenv.2005.09.067

Poste, A. E., H. F. V. Braaten, H. A. de Wit, K. Sørensen, and T. Larssen. 2015. Effects of photodemethylation on the methylmercury budget of boreal Norwegian lakes. Environ. Toxicol. Chem. n/a-n/a. doi:10.1002/etc.2923

Poulin, B. A., J. N. Ryan, and G. R. Aiken. 2014. Effects of iron on optical properties of dissolved organic matter. Environ. Sci. Technol. **48**: 10098–10106. doi:10.1021/es502670r

Qian, Y., X. Yin, H. Lin, B. Rao, S. C. Brooks, L. Liang, and B. Gu. 2014. Why dissolved organic matter enhances photodegradation of methylmercury. Environ. Sci. Technol. Lett. **1**: 426–431. doi:10.1021/ez500254z

Rogers, S. R., T. Webster, W. Livingstone, and N. J. O'Driscoll. 2012. Airborne laser-induced fluorescence (LIF) light detection and ranging (LiDAR) for the quantification of dissolved organic matter concentration in natural waters. Estuaries Coasts **35**: 959–975. doi:10.1007/s12237-012-9509-8

Schaefer, J. K. 2016. Biogeochemistry: Better living through mercury. Nat. Geosci. advance online publication. doi:10.1038/ngeo2638

Schartup, A. T., P. H. Balcom, A. L. Soerensen, K. J. Gosnell, R. S. D. Calder, R. P. Mason, and E. M. Sunderland. 2015. Freshwater discharges drive high levels of methylmercury in Arctic marine biota. Proc. Natl. Acad. Sci. **112**: 11789–11794. doi:10.1073/pnas.1505541112

Scully, N. M., and D. R. S. Lean. 1994. The attenuation of ultraviolet radiation in temperate lakes. Erg Limnol **43**: 135–144.

Sellers, P., C. A. Kelly, and J. W. M. Rudd. 2001. Fluxes of methylmercury to the water column of a drainage lake: The relative importance of internal and external sources. Limnol. Oceanogr. **46**: 623–631. doi:10.4319/lo.2001.46.3.0623

Sellers, P., C. A. Kelly, J. W. M. Rudd, and A. R. MacHutchon. 1996. Photodegradation of methylmercury in lakes. Nature **380**: 694–697. doi:10.1038/380694a0

Sherr, E., and B. Sherr. 1988. Role of microbes in pelagic food webs: A revised concept. Limnol. Oceanogr. **33**: 1225–1227. doi:10.4319/lo.1988.33.5.1225

Siciliano, S. D., N. J. O'Driscoll, R. Tordon, J. Hill, S. Beauchamp, and D. R. S. Lean. 2005. Abiotic production of methylmercury by solar radiation. Environ. Sci. Technol. **39**: 1071–1077. doi:10.1021/es048707z

Singer, M. B., L. R. Harrison, P. M. Donovan, J. D. Blum, and M. Marvin-DiPasquale. 2016. Hydrologic indicators of hot spots and hot moments of mercury methylation potential along river corridors. Sci. Total Environ. **568**: 697–711. doi:10.1016/j.scitotenv.2016.03.005

Strock, K. E., J. E. Saros, S. J. Nelson, S. D. Birkel, J. S. Kahl, and W. H. McDowell. 2016. Extreme weather years drive episodic changes in lake chemistry: implications for recovery from sulfate deposition and long-term trends in dissolved organic carbon. Biogeochemistry **127**: 353–365. doi:10.1007/s10533-016-0185-9

Tai, C., Y. Li, Y. Yin, L. J. Scinto, G. Jiang, and Y. Cai. 2014. Methylmercury photodegradation in surface water of the Florida Everglades: Importance of dissolved organic matter-methylmercury complexation. Environ. Sci. Technol. **48**: 7333–7340. doi:10.1021/es500316d

Whitfield, C. J., J. Aherne, S. A. Watmough, P. J. Dillon, and T. A. Clair. 2006. Recovery from acidification in Nova Scotia: temporal trends and critical loads for 20 headwater lakes. Can. J. Fish. Aquat. Sci. **63**: 1504–1514. doi:10.1139/f06-053

de Wit, H. A., S. Valinia, G. A. Weyhenmeyer, and others. 2016. Current browning of surface waters will Be further promoted by wetter climate. Environ. Sci. Technol. Lett. doi:10.1021/acs.estlett.6b00396

Wyn, B., K. A. Kidd, N. M. Burgess, R. A. Curry, and K. R. Munkittrick. 2010. Increasing mercury in yellow perch at a hotspot in Atlantic Canada, Kejimkujik National Park. Environ. Sci. Technol. **44**: 9176–9181.

APPENDICES

Appendix 1: Supplementary information for Chapter 2: Photoreactivity of dissolved organic matter in the lakes of Kejimkujik National Park Nova Scotia: Implications for methylmercury photochemistry

Table A1.1 Catchment area, volume, flushing rate, dissolved organic carbon (DOM) concentration, and methylmercury (MeHg) concentration for each sampling lake. Physical lake characteristics presented in O'Driscoll et al. (2005). DOM and MeHg concentrations are presented as 2013 means ± 1 standard deviation (n=3).

Lake	Catchment Area (km^2)	Volume ($x10^3$ m^3)	Flushing Rate (y^{-1})	Wetland in Watershed (%)	[DOM] ($mg\ L^{-1}$)	[MeHg] ($ng\ L^{-1}$)
BDE	2.0	1055	1.6	0	5.86 ± 1.06	0.09 ± 0.05
PUZ	2.1	911	2.0	26.06	5.71 ± 1.33	0.09 ± 0.02
NC	3.6	498	6.1	13.52	7.29 ± 1.15	0.62 ± 0.55
PES	66.0	12249	4.6	3.59	12.69 ± 3.19	0.16 ± 0.04
BDW	40.0	2593	13.1	5.04	17.06 ± 2.64	0.33 ± 0.20
PEB	1.6	474	2.9	14.99	19.55 ± 3.46	0.65 ± 0.78

Figure A1.1 Dissolved organic carbon (DOC) normalized results from irradiation experiments arranged in order of increasing average DOC concentration showing (A) DOC loss (B) and absorbance at 350nm loss over the 24 hour irradiation period for each sampling month.

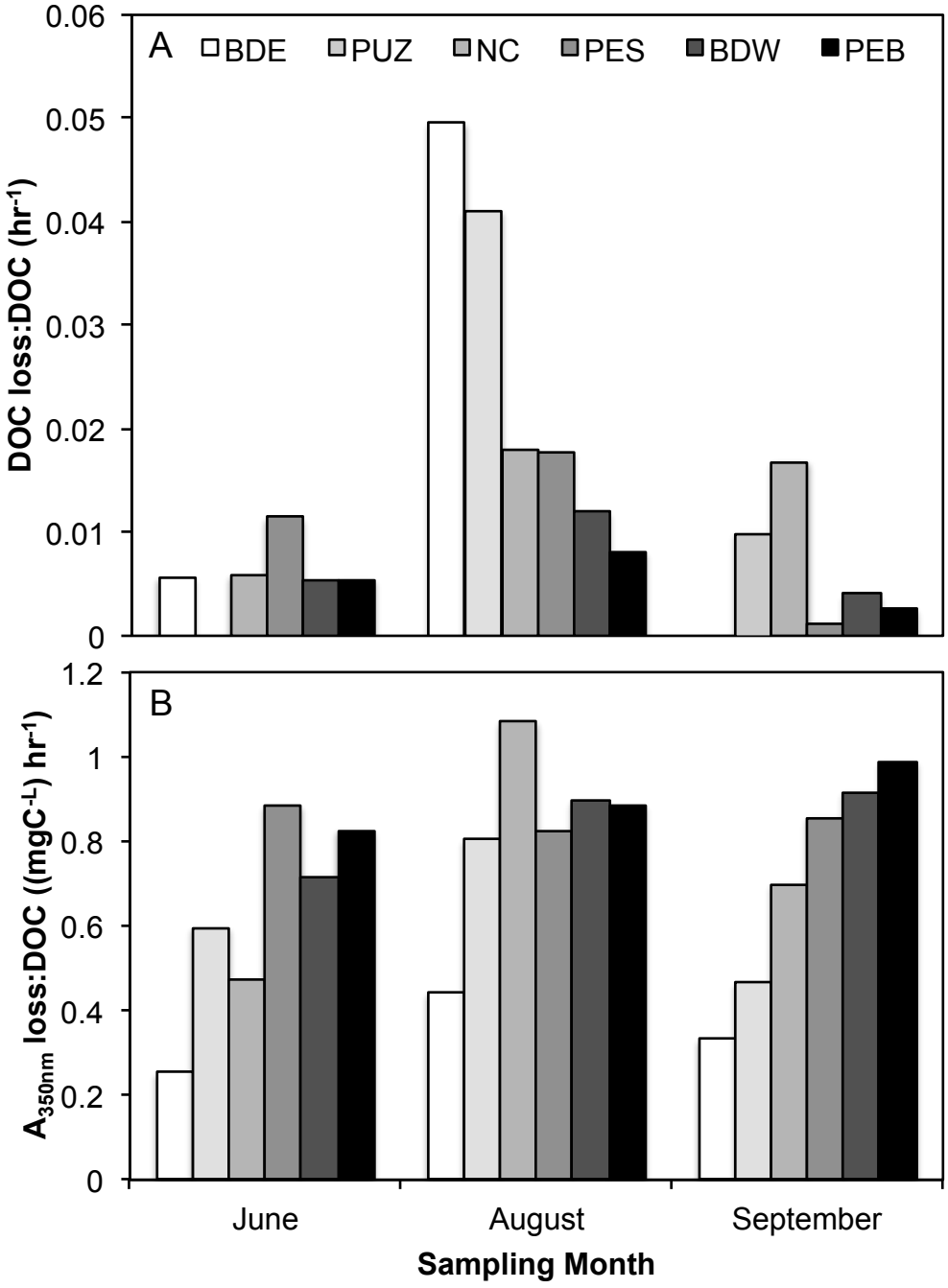

Figure A1.2 Complete UV-A attenuation depth (depth of non-detectable UV-A) for each study lake during sampling. Sampling depth is shown using a dashed line.

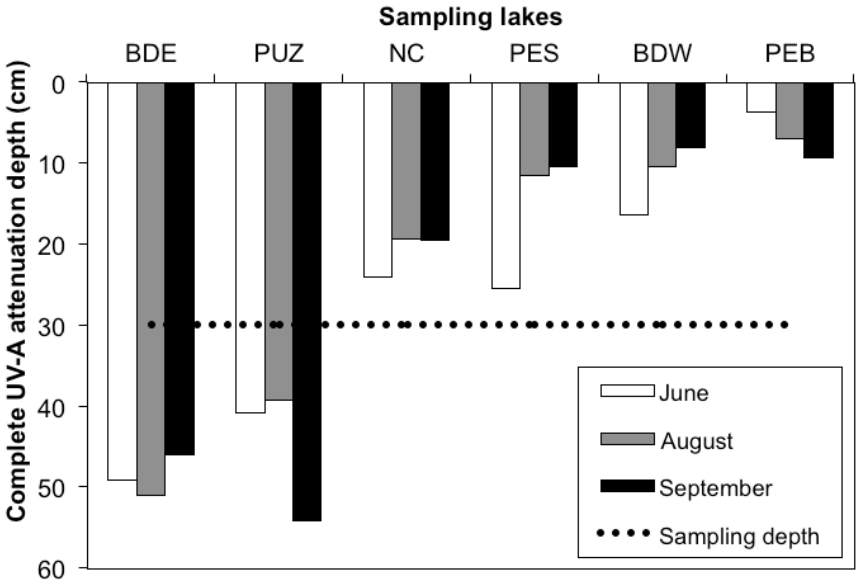

Figure A1.3 Example of absorbance coefficients at 350 nm (A_{350nm}) during one irradiation experiment for PEB lake (grey squares) in fall (September) with high concentrations of dissolved organic carbon (DOC; 24.9 ± 0.33 mg L^{-1}) and PUZ lake (white circles) in late-summer (August) with low DOC concentrations (4.8 ± 0.47 mg $^{-1}$). Data are means ± 1 standard deviation of experimental replicate measurements (n=3). Note the two y-axes are an order of magnitude apart to facilitate comparison.

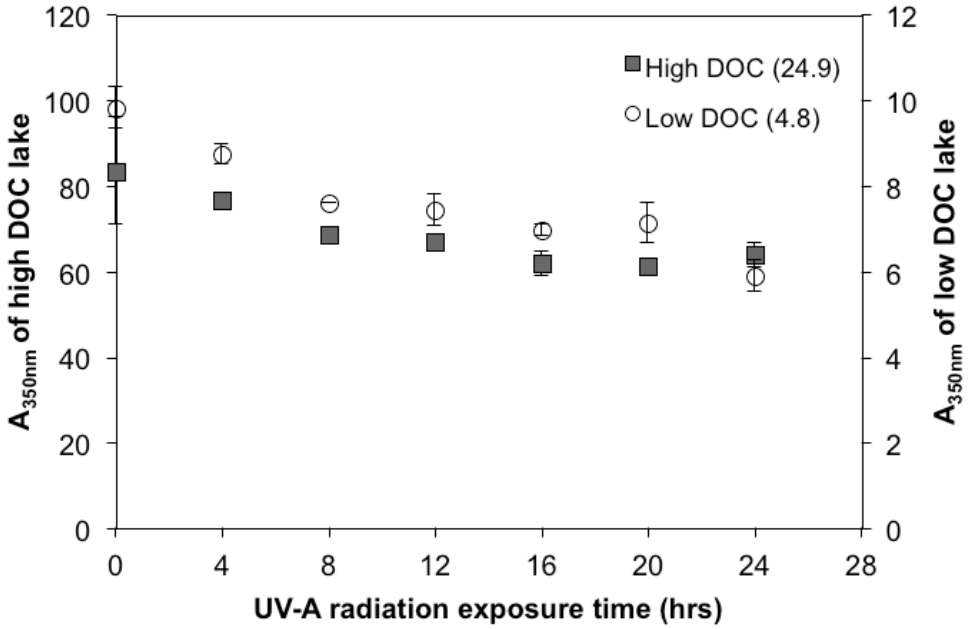

Figure A1.4 Change in spectral slope ratio (S_R: $S_{275\text{-}295nm}/S_{350\text{-}400nm}$) over each 24-hour irradiation experiment in each sampling month: summer (June), late-summer (August), and fall (September).

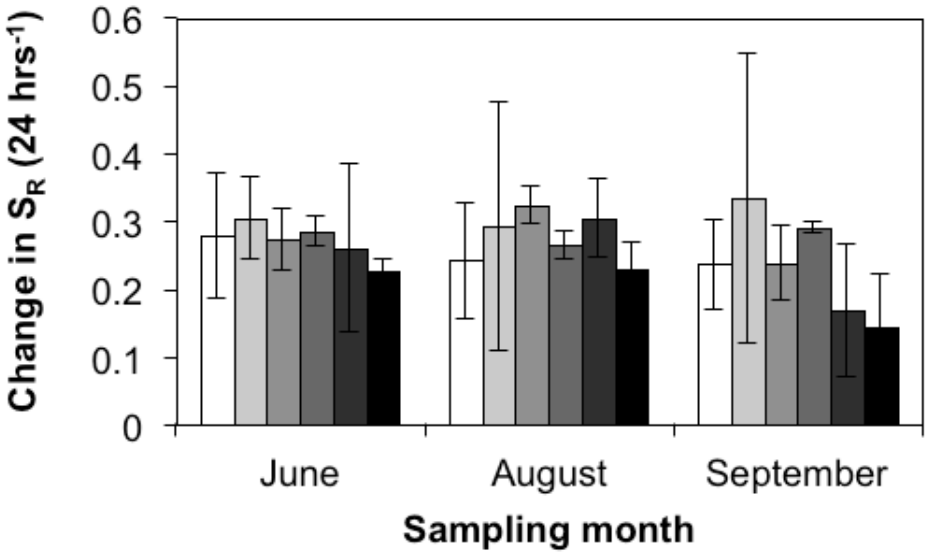

Figure A1.5 Contributions of iron (Fe) to the total absorbance in each lake water sample expressed in percentage absorbance using calculations from Poulin et al. (2014).

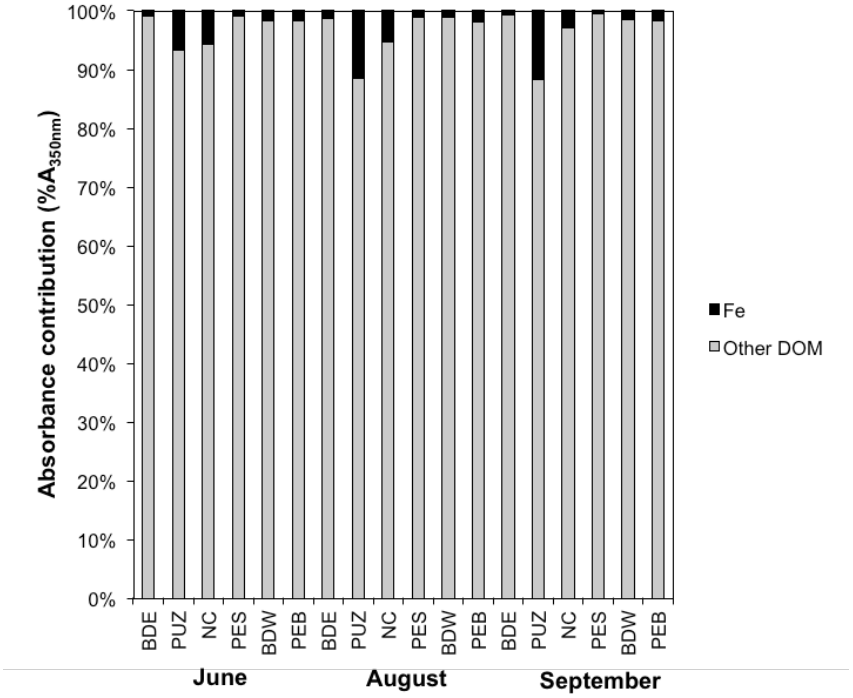

Appendix 2: Supplementary information for Chapter 3: Quantifying the effects of photoreactive dissolved organic matter on methylmercury photodemethylation rate constants in freshwaters

Table A2.1 Water characteristics measured in each experimental sample for each UV-A exposure. Dissolved organic carbon (DOC) concentration, absorbance at 350 nm (A_{350}), specific ultraviolet absorbance ($SUVA_{254}$), ultraviolet spectral slope ratio (UV S_R), ultraviolet-visible spectral slope ratio (UV-vis S_R), and methylmercury (MeHg) concentration.

Month	Treatment	UV-A (kJ)	DOC (mg C L^{-1})	A_{350} (AU cm^{-1})	$SUVA_{254}$ (m^{-1} mg C L^{-1})	UV S_R	MeHg (ng L^{-1})
June	(1) 100% DOM_p + 1 ng L^{-1} MeHg spike	0	10.26	0.113	8.97	0.93	1.674
		35.17	9.46	0.098	8.89	1.03	1.203
		42.49	9.40	0.100	8.96	1.04	0.961
		49.37	9.43	0.103	8.86	1.01	1.022
		68.39	8.99	0.087	8.63	1.08	0.705
		81.84	8.95	0.092	8.64	1.12	0.468
		91.16	8.85	0.089	8.72	1.10	0.702
		control	10.05	0.115	9.03	0.92	1.136
	(2) <30% DOM_p + 1 ng L^{-1} MeHg spike	0.00	3.80	0.017	3.17	1.25	0.816
		35.17	3.90	0.014	2.78	1.39	0.547
		42.49	4.22	0.016	2.84	1.16	0.439
		49.37	3.89	0.015	2.66	1.59	0.655
		68.39	3.95	0.014	2.16	1.06	0.511
		81.84	3.64	0.011	2.34	0.81	0.258
		91.16	3.23	0.007	1.50	0.61	0.368
		control	4.23	0.020	3.43	1.32	0.853
	(3) 100% DOM_p	0.00	10.14	0.117	8.91	0.91	0.288
		35.17	9.24	0.101	9.09	1.02	0.276

		42.49	9.19	0.098	8.92	1.03	0.198
		49.37	9.41	0.099	8.78	1.06	0.219
		68.39	8.67	0.088	8.52	1.06	0.138
		81.84	8.59	0.086	8.47	1.06	0.108
		91.16	8.51	0.086	8.47	1.05	0.124
		control	10.22	0.116	8.81	0.90	0.228
August	(1) 100% DOM_p + 1 ng L^{-1} MeHg spike	0.00	21.03	0.251	9.32	0.94	1.533
		35.17	19.66	0.222	9.35	1.02	1.086
		42.49	19.40	0.222	9.45	1.05	1.078
		49.37	19.56	0.226	9.43	1.04	1.163
		68.39	18.38	0.209	9.41	1.05	0.831
		81.84	18.50	0.206	9.35	1.05	0.830
		91.16	18.14	0.206	9.41	1.06	0.919
		control	20.87	0.252	9.42	0.94	1.517
	(2) <30% DOM_p + 1 ng L^{-1} MeHg spike	0.00	7.22	0.067	4.72	1.06	0.889
		35.17	6.36	0.025	1.95	0.63	n.a.
		42.49	7.32	0.086	6.48	1.34	0.694
		49.37	7.93	0.040	4.18	1.37	0.919
		68.39	5.77	0.026	1.96	0.64	n.a.
		81.84	5.86	0.094	6.92	1.35	0.299
		91.16	6.84	0.031	2.46	0.94	0.365
		control	6.85	0.074	5.72	1.14	0.868
	(3) 100% DOM_p	0.00	21.14	0.253	9.39	0.94	0.419
		35.17	20.41	0.221	9.02	1.01	0.327
		42.49	20.00	0.217	9.12	1.02	0.316
		49.37	20.09	0.219	9.14	1.02	0.328
		68.39	19.01	0.204	9.15	1.05	0.264

		81.84	19.25	0.204	8.96	1.06	0.240
		91.16	18.76	0.197	9.08	1.09	0.261
		control	21.14	0.252	9.31	0.94	0.414
October	(1) 100% DOM_p + 1 ng L^{-1} MeHg spike	0.00	19.08	0.225	9.28	0.95	1.426
		35.17	17.89	0.202	9.31	1.03	0.915
		42.49	17.65	0.197	9.39	1.03	1.134
		49.37	17.62	0.201	9.45	1.02	0.997
		68.39	17.01	0.184	9.31	1.05	0.677
		81.84	16.99	0.184	9.15	1.07	0.818
		91.16	16.77	0.182	9.24	1.08	0.828
		control	18.83	0.224	9.34	0.95	1.361
	(2) <30% DOM_p + 1 ng L^{-1} MeHg spike	0.00	6.20	0.027	3.43	1.47	0.621
		35.17	n.a.	0.025	n.a.	0.83	0.663
		42.49	7.01	0.052	4.57	1.03	0.437
		49.37	7.22	0.053	5.04	1.14	0.448
		68.39	7.92	0.049	5.64	1.34	0.311
		81.84	5.55	0.026	2.53	1.33	0.365
		91.16	6.37	0.091	8.07	0.91	0.296
		control	5.89	0.033	3.85	1.18	0.698
	(3) 100% DOM_p	0.00	19.08	0.153	6.62	0.98	0.328
		35.17	18.57	0.197	8.94	1.03	0.240
		42.49	18.31	0.195	9.06	1.00	0.253
		49.37	18.17	0.198	9.18	1.01	0.296
		68.39	17.33	0.188	9.12	1.04	0.192
		81.84	17.20	0.183	9.13	1.06	0.197
		91.16	17.19	0.183	9.11	1.07	0.220
		control	19.38	0.227	9.15	0.94	0.313

Figure A2.1 (A) Full spectrum (300-800nm) of photoreactor irradiance compared to ambient solar radiation on a cloudless June day for Nova Scotia, and (B) a photograph showing beaker placement within the photoreactor for irradiation experiments.

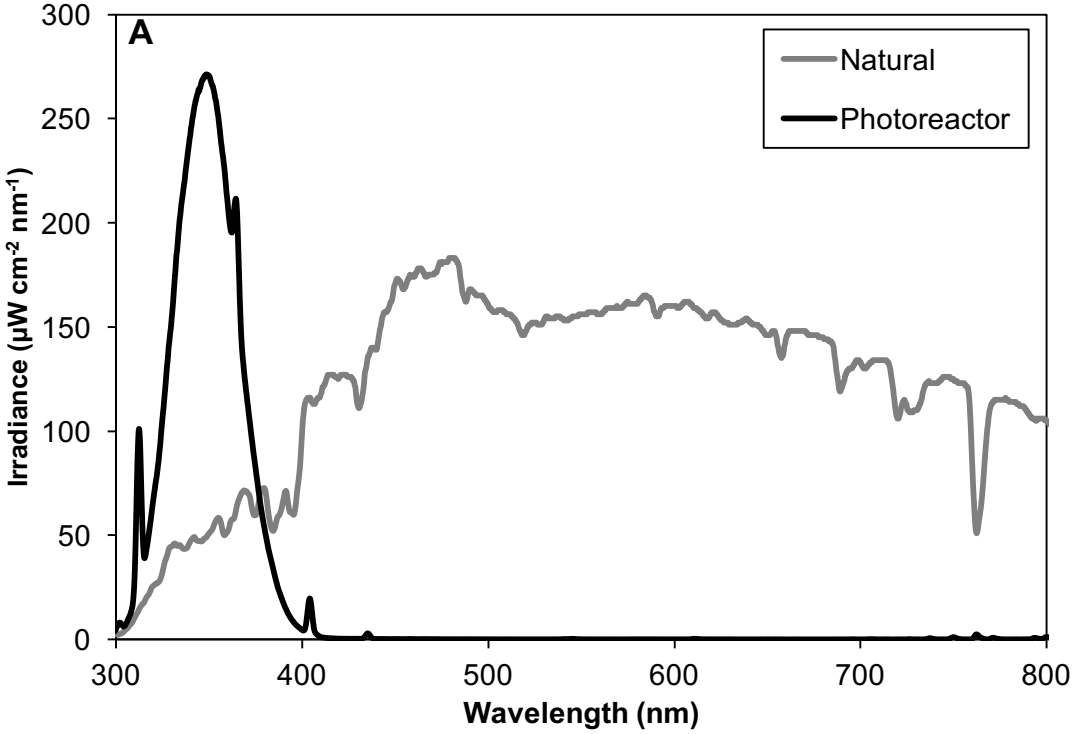

B

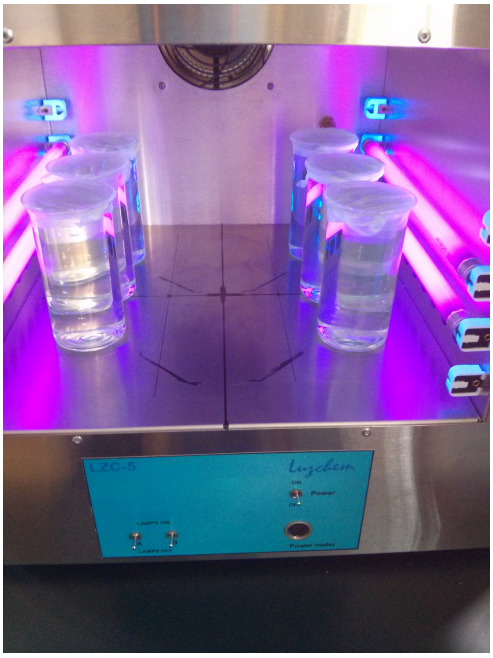

Figure A2.2 The natural log transformed data for methylmercury (MeHg) concentration for each of the three water quality treatments: Treatment 1: 100% photoreactive dissolved organic matter (DOM_p) plus a MeHg spike, Treatment 2: <30% DOM_p plus a MeHg spike, Treatment 3: 100% DOM_p with no MeHg spike, in each of the months (A): June, (B): August, and (C): October.

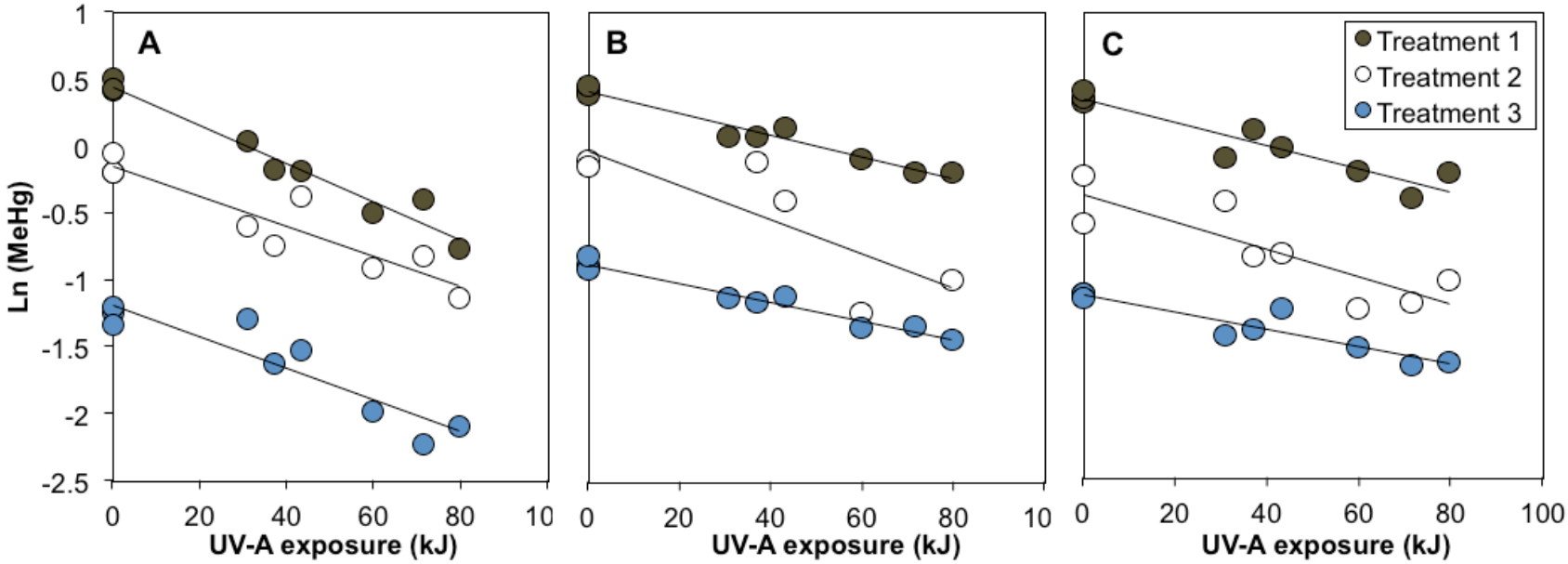

Figure A2.3 No correlation between initial MeHg concentration and photodemethylation rate constant (k_{PD}; Pearson's r=0.290, p=0.449).

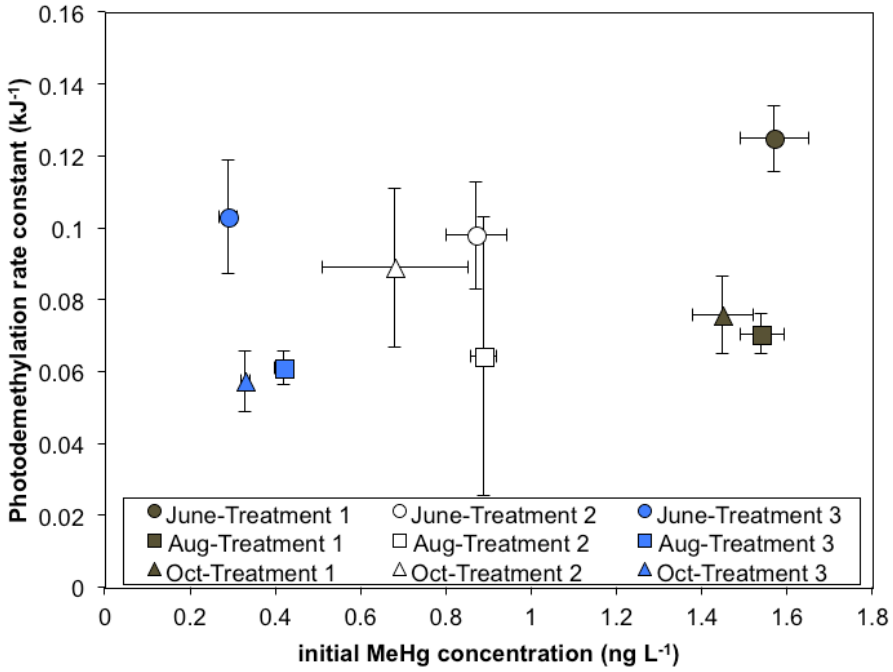

Figure A2.4 Correlation between initial dissolved organic carbon (DOC) concentration (mg C L^{-1}) and photodemethylation rate constant (k_{PD}; Pearson's r=-0.585, p=0.098).

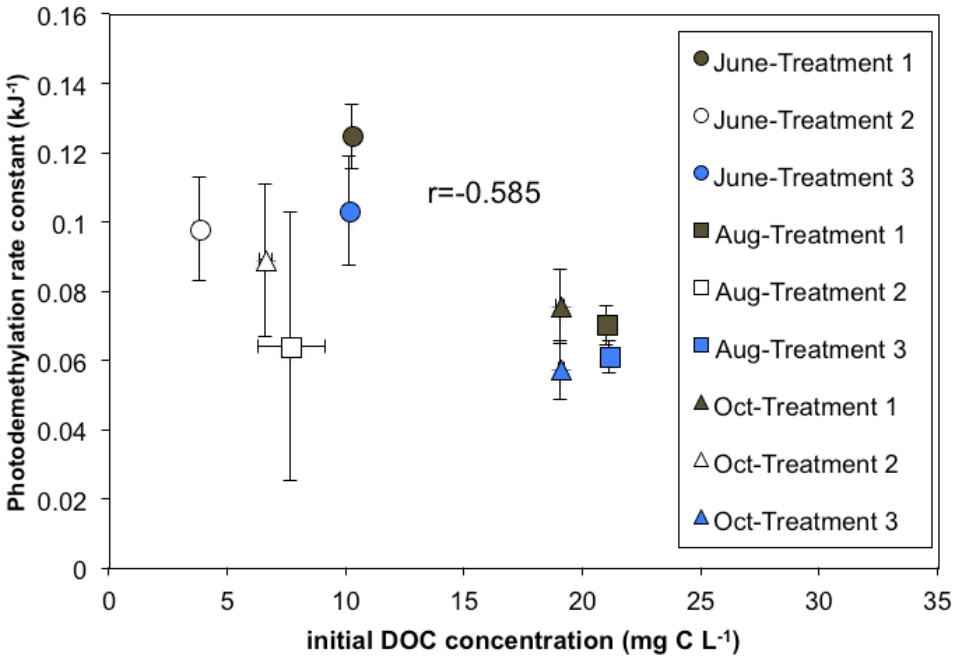

Figure A2.5 Correlation between significant change in ultraviolet spectral slope ratio (UV S_R) and photodemethylation rate constant (Pearson's r=0.841, *p*=0.036).

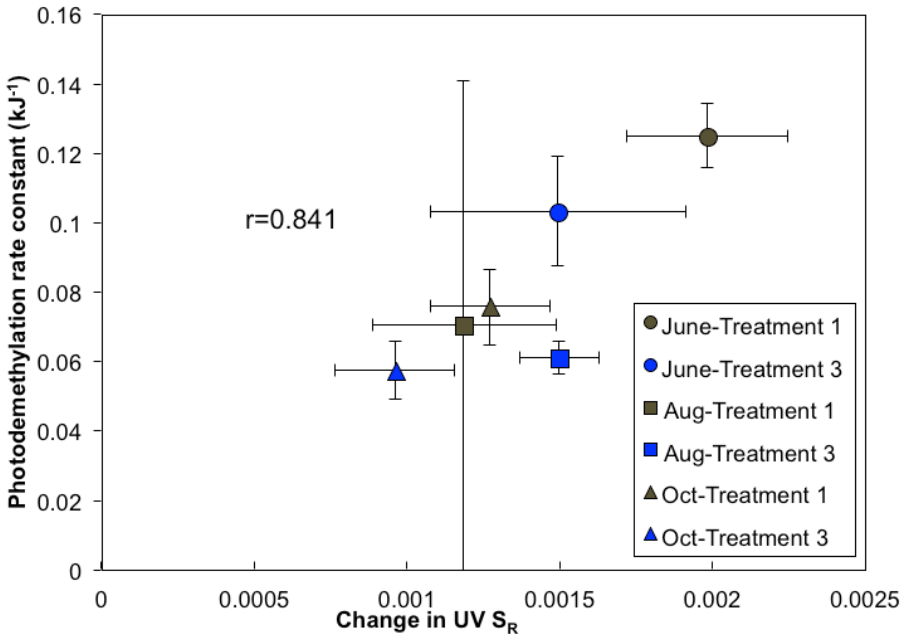

Figure A2.6 Correlation between initial dissolved organic carbon (DOC) concentration (mg C L^{-1}) and photodemethylation efficiency (Pearson's r=-0.78, *p*=0.012).

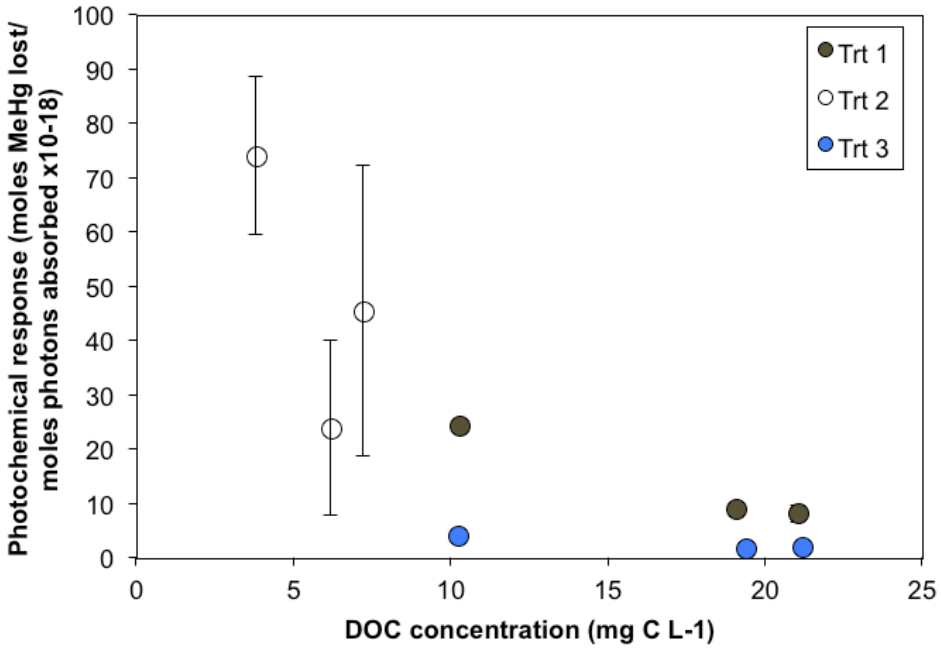

Appendix 3: Supplementary information for Chapter 4: Dissolved organic matter inhibits freshwater methylmercury photodemethylation

Table A3.1 Summary of cumulative UV-A exposure intensity, methylmercury concentration (MeHg), and dissolved organic matter (DOM) concentration for each experimental treatment in each of the seasons and lakes.

Season	Lake	Treatment	Day	UV-A (kJ m^{-2})	MeHg (ng L^{-1})	DOM (mgC L^{-1})	pH
Spring	BDW	Filtered	0	0	1.98 ± 0.27	6.92 ± 0.05	5.18
Spring	BDW	Filtered	1	502	1.75 ± 0.20	6.61 ± 0.05	n.a.
Spring	BDW	Filtered	2	735	n.a.	6.63 ± 0.00	n.a.
Spring	BDW	Filtered	3	1804	1.51 ± 0.05	6.37 ± 0.06	n.a.
Spring	BDW	Filtered	5	3317	1.22 ± 0.09	5.96 ± 0.03	n.a.
Spring	BDW	Filtered	7	5491	0.99	5.84 ± 0.01	n.a.
Spring	BDW	Filtered	control	0	2.32 ± 0.05	6.90 ± 0.02	n.a.
Spring	BDW	Unfiltered	0	0	2.78 ± 0.10	7.10 ± 0.03	5.29
Spring	BDW	Unfiltered	1	502	2.32 ± 0.06	6.73 ± 0.01	n.a.
Spring	BDW	Unfiltered	2	735	2.21	6.61 ± 0.02	n.a.
Spring	BDW	Unfiltered	3	1804	1.85 ± 0.09	6.37 ± 0.10	n.a.
Spring	BDW	Unfiltered	5	3317	1.54 ± 0.05	5.89 ± 0.12	n.a.
Spring	BDW	Unfiltered	7	5491	1.422	5.84 ± 0.01	n.a.
Spring	BDW	Unfiltered	control	0	2.68 ± 0.04	6.83 ± 0.03	n.a.
Summer	BDE	6 lakes	0	0	3.88 ± 0.07	5.10	n.a.
Summer	BDE	6 lakes	1	819	2.36 ± 0.05	4.89	5.24
Summer	BDE	6 lakes	2	1644	1.49 ± 0.04	4.73	5.14
Summer	BDE	6 lakes	3	2513	0.97 ± 0.01	4.34	5.04
Summer	BDE	6 lakes	5	3994	0.50 ± 0.01	4.03	n.a.
Summer	BDE	6 lakes	7	5515	0.35 ± 0.01	3.64	5.61
Summer	BDE	6 lakes	control	0	3.81 ± 0.09	5.04	5.32
Summer	PUZ	6 lakes	0	0	3.81 ± 0.13	4.17	n.a.
Summer	PUZ	6 lakes	1	819	2.34 ± 0.07	3.97	4.90
Summer	PUZ	6 lakes	2	1644	1.34 ± 0.06	3.76	4.91
Summer	PUZ	6 lakes	3	2513	0.87 ± 0.03	3.50	4.89
Summer	PUZ	6 lakes	5	3994	0.38 ± 0.01	2.90	n.a.
Summer	PUZ	6 lakes	7	5515	0.27 ± 0.01	2.96	4.88
Summer	PUZ	6 lakes	control	0	3.06 ± 0.30	4.24	4.88
Summer	NCR	6 lakes	0	0	3.80 ± 0.07	5.24	n.a.
Summer	NCR	6 lakes	1	819	2.37 ± 0.10	4.96	4.82

Summer	NCR	6 lakes	2	1644	1.36 ± 0.00	4.60	4.89
Summer	NCR	6 lakes	3	2513	0.93 ± 0.02	4.23	4.84
Summer	NCR	6 lakes	5	3994	0.41 ± 0.01	3.49	n.a.
Summer	NCR	6 lakes	7	5515	0.24 ± 0.00	3.04	5.03
Summer	NCR	6 lakes	control	0	3.51 ± 0.05	5.22	4.76
Summer	PES	6 lakes	0	0	3.81 ± 0.10	12.50	n.a.
Summer	PES	6 lakes	1	819	2.68 ± 0.11	12.03	4.44
Summer	PES	6 lakes	2	1644	1.84 ± 0.04	11.41	4.50
Summer	PES	6 lakes	3	2513	1.23 ± 0.03	11.01	4.53
Summer	PES	6 lakes	5	3994	0.88 ± 0.01	10.28	n.a.
Summer	PES	6 lakes	7	5515	0.57 ± 0.01	9.99	4.89
Summer	PES	6 lakes	control	0	3.79 ± 0.13	12.48	4.46
Summer	BDW	6 lakes	0	0	4.18 ± 0.10	8.50	n.a.
Summer	BDW	6 lakes	1	819	3.02 ± 0.09	8.05	4.72
Summer	BDW	6 lakes	2	1644	2.11 ± 0.06	7.34	4.81
Summer	BDW	6 lakes	3	2513	1.65 ± 0.04	6.99	4.91
Summer	BDW	6 lakes	5	3994	0.94 ± 0.02	6.00	n.a.
Summer	BDW	6 lakes	7	5515	0.65 ± 0.01	4.80	4.93
Summer	BDW	6 lakes	control	0	3.33 ± 0.05	8.46	4.70
Summer	PEB	6 lakes	0	0	3.90 ± 0.07	13.25	n.a.
Summer	PEB	6 lakes	1	819	3.05 ± 0.04	12.67	4.28
Summer	PEB	6 lakes	2	1644	2.43 ± 0.04	11.98	4.31
Summer	PEB	6 lakes	3	2513	1.91 ± 0.04	11.53	4.36
Summer	PEB	6 lakes	5	3994	1.19 ± 0.03	10.63	n.a.
Summer	PEB	6 lakes	7	5515	0.86 ± 0.03	9.63	4.44
Summer	PEB	6 lakes	control	0	3.91 ± 0.07	13.22	4.32
Fall	BDE	6 lakes	0	0	3.54 ± 0.11	4.50	5.22
Fall	BDE	6 lakes	1	294	2.86	4.39	5.14
Fall	BDE	6 lakes	2	764	2.33	4.39	5.22
Fall	BDE	6 lakes	3	1226	1.92	4.35	5.20
Fall	BDE	6 lakes	5	1965	1.47	4.26	5.16
Fall	BDE	6 lakes	7	2596	1.21	4.22	5.10
Fall	BDE	6 lakes	control	0	3.27 ± 0.09	4.46	5.23
Fall	PUZ	6 lakes	0	0	3.57 ± 0.20	4.08	3.98
Fall	PUZ	6 lakes	1	294	2.90	3.99	3.90
Fall	PUZ	6 lakes	2	764	2.28	3.94	3.88
Fall	PUZ	6 lakes	3	1226	1.79	3.89	3.87
Fall	PUZ	6 lakes	5	1965	1.34	3.82	3.84
Fall	PUZ	6 lakes	7	2596	1.15	3.82	3.81
Fall	PUZ	6 lakes	control	0	3.03 ± 0.30	4.02	3.94

Fall	NCR	6 lakes	0	0	3.59 ± 0.20	5.25	3.95
Fall	NCR	6 lakes	1	294	2.96	5.15	3.96
Fall	NCR	6 lakes	2	764	2.09	5.10	3.97
Fall	NCR	6 lakes	3	1226	1.59	5.04	3.96
Fall	NCR	6 lakes	5	1965	1.24	5.00	3.96
Fall	NCR	6 lakes	7	2596	0.91	4.95	3.91
Fall	NCR	6 lakes	control	0	3.04 ± 0.04	5.27	4.06
Fall	PES	6 lakes	0	0	3.43 ± 0.09	6.69	3.82
Fall	PES	6 lakes	1	294	3.17	6.52	3.81
Fall	PES	6 lakes	2	764	2.72	6.45	3.81
Fall	PES	6 lakes	3	1226	2.38	6.30	3.82
Fall	PES	6 lakes	5	1965	1.90	6.17	3.82
Fall	PES	6 lakes	7	2596	1.60	6.01	3.80
Fall	PES	6 lakes	control	0	2.90 ± 0.06	6.72	3.82
Fall	BDW	6 lakes	0	0	3.66 ± 0.07	16.71	4.12
Fall	BDW	6 lakes	1	294	3.35	16.49	4.23
Fall	BDW	6 lakes	2	764	3.12	16.06	4.26
Fall	BDW	6 lakes	3	1226	2.85	15.49	4.29
Fall	BDW	6 lakes	5	1965	2.57	15.18	4.30
Fall	BDW	6 lakes	7	2596	2.34	14.77	4.32
Fall	BDW	6 lakes	control	0	3.65 ± 0.05	16.53	4.20
Fall	PEB	6 lakes	0	0	4.02 ± 1.14	14.73	3.72
Fall	PEB	6 lakes	1	294	3.34	14.43	3.72
Fall	PEB	6 lakes	2	764	3.03	14.11	3.72
Fall	PEB	6 lakes	3	1226	2.88	14.09	3.71
Fall	PEB	6 lakes	5	1965	2.63	13.77	3.71
Fall	PEB	6 lakes	7	2596	2.41	13.44	3.69
Fall	PEB	6 lakes	control	0	3.34 ± 0.06	14.65	3.67

Table A3.2 Catchment area, volume, and flushing rate for each sampling lake. Physical lake characteristics presented in O'Driscoll et al. (2005).

Lake	Catchment Area (km^2)	Volume ($x10^3$ m^3)	Flushing Rate (y^{-1})	Wetland in Watershed (%)
BDE	2.0	1055	1.6	0
PUZ	2.1	911	2.0	26.06
NCR	3.6	498	6.1	13.52
PES	66.0	12249	4.6	3.59
BDW	40.0	2593	13.1	5.04
PEB	1.6	474	2.9	14.99

Table A3.3 Summary table of published photodemethylation rate constants (k_{PD}; that use cumulative PAR photons as the radiation exposure measurement) in freshwaters and corresponding location, water source, methylmercury (MeHg), source, MeHg concentration, dissolved organic matter (DOM) concentration, and reference from the literature. Summary table is adapted from Fleck et al. (2014) where k_{PD}s were converted into common units (E m^{-1}) and corrected for respective bottle wall attenuations.

Reference	Location	Water source	Season	DOM (mg C L^{-1})	Absorbance properties reported	k_{PD} corrected
Sellers et al. 1996	ELA, Ontario, CA	Lake	not reported	17	not reported	5.2-13
Sellers et al. 2001	ELA, Ontario, CA	Lake	May - October	17	not reported	2.6-5.2
Lehnherr and St Louis 2009	ELA, Ontario, CA	Lake	July	12.8	not reported	4.5
Hines and Brezonik 2004	Marcell, Minnesota, USA	Lake	May - September	11	not reported	10
Li et al. 2010	Everglades, Florida, USA	Freshwater wetland	July - September	6.0-22	not reported	13.67
Zhang and Hsu-Kim 2010	Laboratory experiments	Commercial Isolates	*October + December*	0-2	not reported	
Hammerschmidt and Fitzgerald (2010)	Alaska, USA	Lake	July	0.4-10	not reported	3.8
Black et al. 2012	San Francisco, California, USA	Coastal wetland	April	1.5-11.3	UV/Vis absorbance, Fluorescence	9.9 +/- 2.0
Fleck et al. 2014	Sacramento, California, USA	Freshwater wetland, rice fields	July	8.5-36.3	UV/Vis absorbance, SUVA254, spectral slopes, UV SR, UV-vis SR, fluorescence (FEEM plots)	7.5 +/- 3.5
Jeremiason et al. 2015	St. Louis River, TN, USA	isolates	August	3.0-30.0	UV/Vis absorbance	
This study	Kejimkujik National Park, Nova Scotia, CA	Lakes	May-October	3.0-16.0	UV/Vis absorbance SUVA254 spectral slopes UV SR	4.1-13.3

Figure A3.1. Methylmercury (MeHg) concentration over 1-week irradiation experiments compared to UV-A exposure (kJ m^{-2}) in (*a*) spring Big Dam West (BDW) filtered and unfiltered lake water, (*b*) summer Big Dam East (BDE), Puzzle (PUZ), North Cranberry (NCR), Peskawa (PES), BDW, and Pebbleloggitch (PEB) filtered lake water, and (*c*) fall filtered lake water for the same 6 lakes.

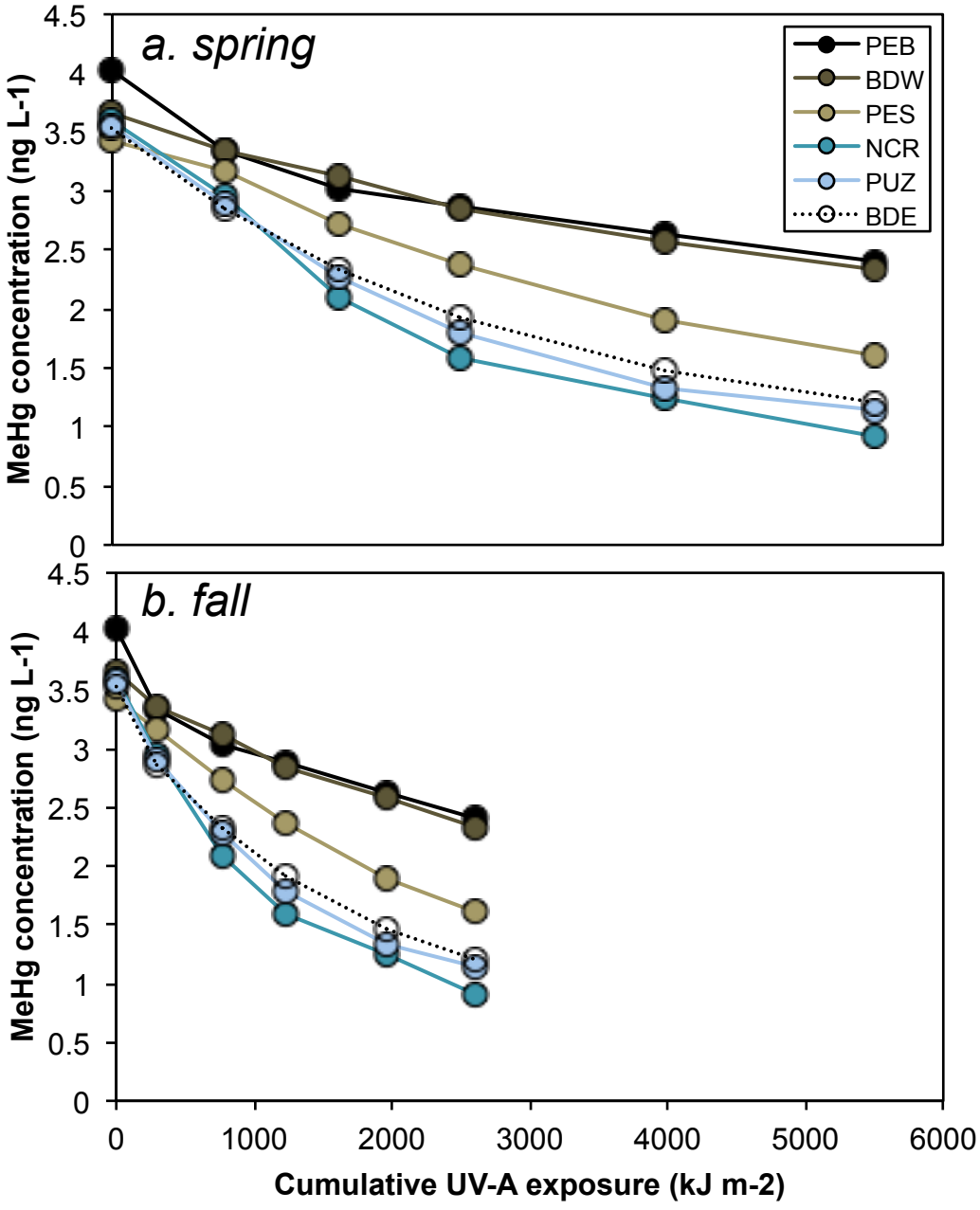

Figure A3.2 Methylmercury (MeHg) concentration over 1-week irradiation experiments compared to cumulative PAR photon flux (E m^{-2}) in (*a*) summer Big Dam East (BDE), Puzzle (PUZ), North Cranberry (NCR), Peskawa (PES), Big Dam West (BDW), and Pebbleloggitch (PEB) filtered lake water, and (*b*) fall filtered lake water for the same 6 lakes.

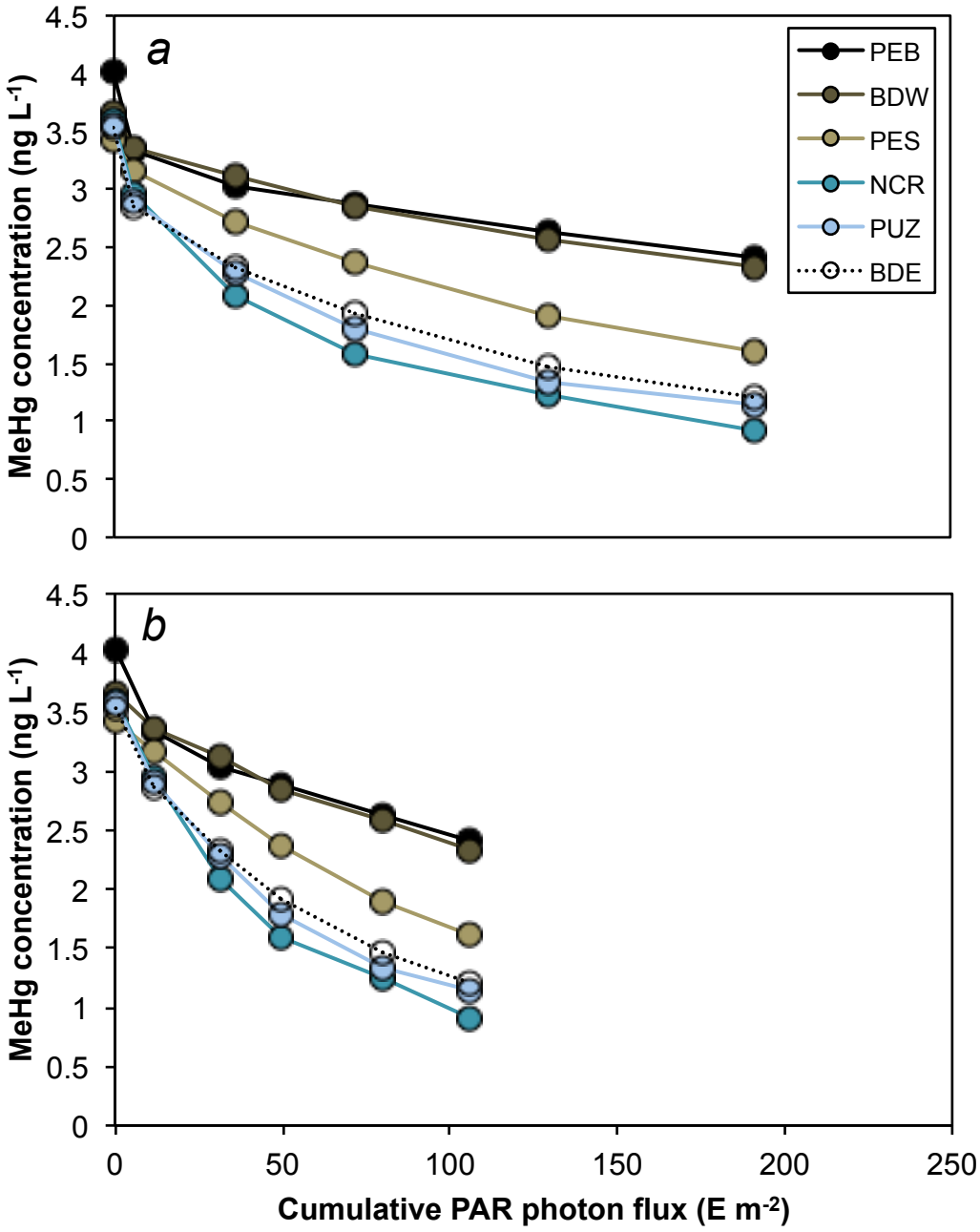

Figure A3.3 Natural log transformed methylmercury (MeHg) concentration over 1-week irradiation experiments compared to cumulative PAR photon flux (E m^{-2}) in (*a*) summer Big Dam East (bde), Puzzle (puz), North Cranberry (ncr), Peskawa (pes), Big Dam West (bdw), and Pebbleloggitch (peb) filtered lake water, and (*b*) fall filtered lake water for the same 6 lakes.

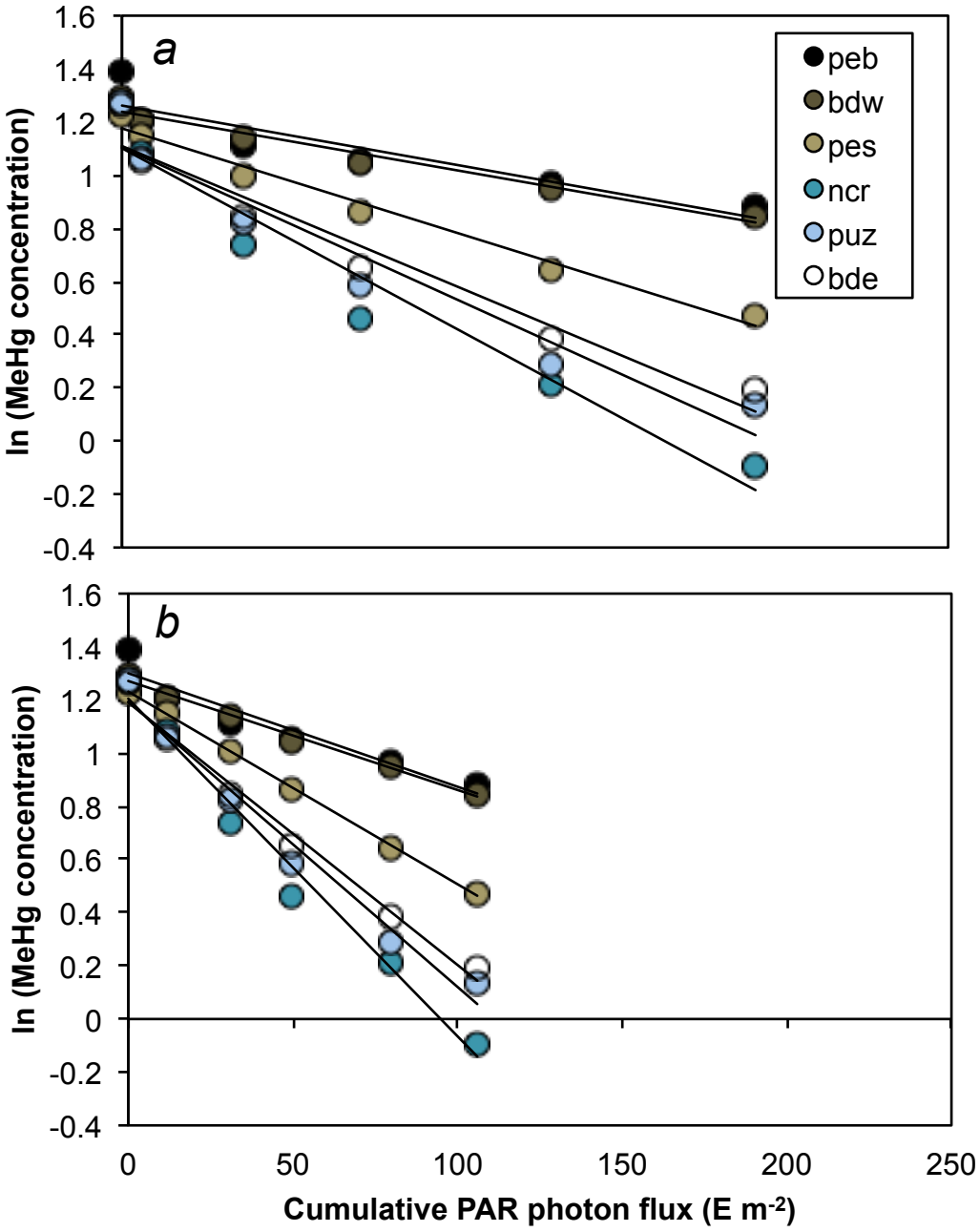

Figure A3.4 Average water temperature inside experimental bottles for 1-week irradiation experiments in summer and fall (n=6).

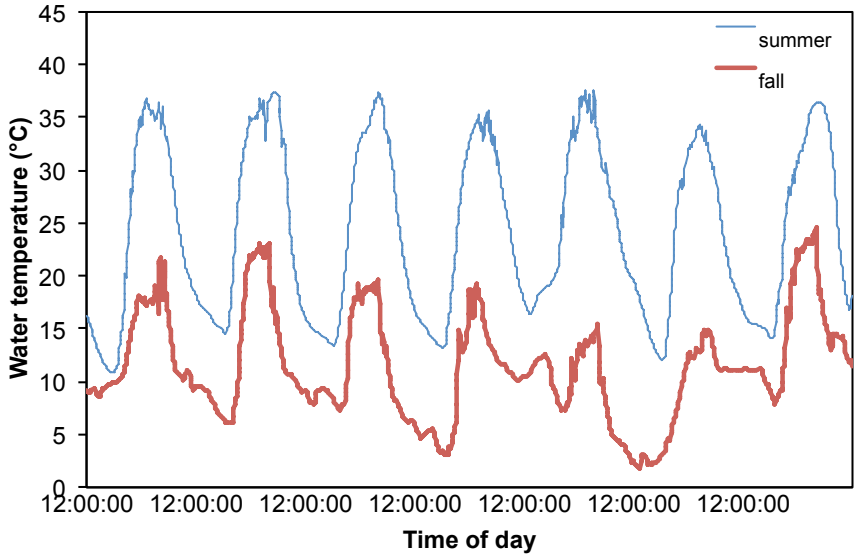

Figure A3.5 Dissolved organic matter (DOM) concentration with UV-A exposure in 1-week experiments in (*a*) summer and (*b*) fall. Slopes of regressions are photomineralization (k_{PM}; all R^2>0.86, p<0.001.

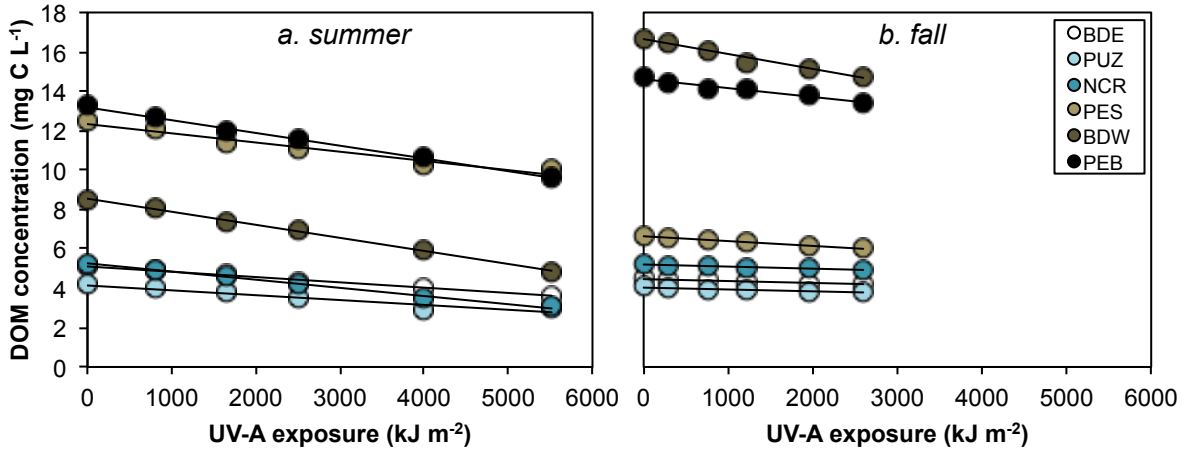

Figure A3.6 Absorbance at 350 nm (A_{350}) with UV-A exposure in 1-week experiments in (*a*) summer and (*b*) fall. Slopes of regressions are photobleaching (k_{PB}; all R^2>0.75, p<0.02).